Michael Traxler, BSc

Synthesis and Application of Organogermanium Compounds: From Small Metallorganic Precursors towards Functional Nano Sized Particles

MASTER'S THESIS

to achieve the university degree of

Diplom-Ingenieur

Master's degree programme: Technical Chemistry

submitted to

Graz University of Technology

Supervisor

Univ.-Prof. Dipl.-Chem. Dr.rer.nat., Frank Uhlig

Institute for Inorganic Chemistry

Co-supervisor
Ph.D Ana Torvisco

Graz, August 2019

AFFIDAVIT

I declare that I have authored this thesis independently, that I have not used other than the declared sources/resources, and that I have explicitly indicated all material which has been quoted either literally or by content from the sources used. The text document uploaded to TUGRAZonline is identical to the present master‘s thesis.

Date

Signature

Abstract

In contrast to organosilicon and organotin compounds, which have already found widespread use in industrial applications, organogermanium compounds are less explored mainly due to their challenging preparation and environmental scarcity. Recent developments in the field of organogermanium chemistry showed that these compounds display promising features for the use as precursors for functional materials in the field of macromolecules, optical applications and as anode material in lithium ion energy storage systems.

The objective of this work was to overcome literature known difficulties in order to open a direct, high yielding and selective reaction route towards organogermanium dihalides, trihalides, dihydrides and trihydrides. Furthermore, all synthesized compounds were fully characterized using various analysis techniques including ^{73}Ge NMR spectroscopy of organogermanium hydrides, which is only rarely found in literature. Moreover, organogermanium nanoparticles were prepared, using previously synthesized organogermanium trihydrides as precursors in a microwave assisted dehydrogenative coupling reaction. This formerly unknown material was characterized using various analysis techniques such as SEM, SAXS and MALDI-TOF mass spectrometry.

In addition, in cooperation with the University of Western Ontario (Canada), a selective reaction route for the preparation of organogermanium monochloride compounds with organic residues bearing no steric demand at *ortho*-position was developed, using a procedure *via* an aminophenol species as reaction intermediate.

Kurzfassung

Im Gegensatz zu Organosilizium- und Organozinnverbindungen, die häufig in industriellen Anwendungsgebieten Verwendung finden, sind Organogermaniumverbindungen vergleichsweise noch wenig erforscht. Dies ist vorwiegend auf die schwierige Herstellung solcher Verbindungen aber auch deshalb, da das Element rar in der Erdkruste zu finden ist. Jedoch zeigen jüngste Entwicklungen, dass Organogermaniumverbindungen vielversprechende Edukte für die Herstellung von Funktionsmaterialien als Makromoleküle, optischen Anwendungen und als Anodenmaterial für Lithiumakkus darstellen.

Das Ziel dieser Masterarbeit war es die Schwierigkeiten in der Synthese von Organogermaniumverbindungen zu überwinden und einen direkten, selektiven Reaktionsweg für die Darstellung von Organogermaniumdihalide, Organogermaniumtrihalide, Organogermaniumdihydride und Organogermaniumtrihydride zu entwickeln. Weiters wurden alle hergestellten Verbindungen vollständig characterisiert. Eine der Analysenmethoden für Organogermaniumhydride war ^{73}Ge NMR Spektroskopie, welche nur selten in der Literatur zu finden ist. Darüber hinaus wurden organogermanium Nanopartikel von zuvor hergestellten Organogermaniumtrihydriden in einer Mikrowellenreaktion dargestellt. Dieses zuvor unbekannte Material wurde mit verschiedenen Materialanalysentechniken wie zum Beispiel SEM, SAXS und MALDI-TOF Massenanalyse characterisiert.

In einer Kooperation mit der University of Western Ontario (Kanada) wurde eine Reaktionsroute für die selektive Darstellung von Organogermaniummonochloriden mit organischen Resten ohne sterischem Anspruch in *ortho*-Position erfolgreich geöffnet.

Danksagung

An dieser Stelle möchte ich mich bei allen lieben Menschen bedanken, die zur erfolgreichen Entstehung dieser Abschlussarbeit beigetragen haben.

Großer Dank gilt vor allem meinem Betreuer, Prof. Frank Uhlig, für die Möglichkeit meine Masterarbeit in seiner Arbeitsgruppe anfertigen zu dürfen. Danke für deine Ideen, deine Unterstützung, dein Vertrauen in mich und die Freiheit, dass ich mich auch auf der anderen Seite der Welt verwirklichen durfte.

Natürlich geht mein Dank auch an alle Mitglieder der Arbeitsgruppe Uhlig/Flock/Fischer und meine Labor- und Bürokollegen der letzten Jahre, für das angenehme Arbeitsklima, die Hilfsbereitschaft und die Unterstützung. Special thanks go to Ana Torvisco for her great ideas and her professional as well personal support. Ganz herzlich möchte ich mich auch bei Prof. Fischer und Prof. Flock bedanken, die immer ein offenes Ohr für Probleme hatten. Auch bei den „guten Seelen des Instituts“ - Babsi, Moni, Yaiza, Marit – möchte ich mich für alles was sie im Hintergrund tuen bedanken. Auch bei den ehemaligen Arbeitskollegen Melanie und Astrid möchte ich mich bedanken für all das Wissen, das ich durch eure Betreuung erlernt habe.

Weiters möchte ich mich bei Prof. Gudat für die Germanium NMR Messungen, bei Manfred Kriechbaum für die SAXS Analysen, bei Judith Biedermann für die SEM Analysen bedanken. Besonder Dank gilt Prof. Robert Saf. Nicht nur für deine GPC

und MALDI-TOF Messungen, sondern auch für unsere fruchtbaren Diskussionen und deine Unterstützung.

A special thank goes to Prof. Kim Baines and her group for hosting me in Canada. I will never forget this amazing time overseas and I am looking forward to meet all of you soon again.

Besonderer Dank gilt auch Bernhard, Jana, Lukas, Markus und Michael. Ohne dem „Rudel“ wäre das Studium nur halb so lustig gewesen. Auch möchte ich mich bei meinen „alten Freunden“ bedanken, die einerseits in der WG, aber auch immer, wenn man nach OÖ kommt für jeden Spaß zu haben sind.

Ebenso möchte ich mich bei meiner Freundin Susi von Herzen bedanken. Danke, für deine kompromisslose Unterstützung und den unglaublichen Rückhalt den du mir gibst. Aber natürlich auch für unsere unzähligen privaten chemischen Gespräche, die zum Gelingen dieser Arbeit auch sicher beigetragen haben.

Jedoch gilt der größte Dank meiner Familie, die mich seit Beginn meiner Ausbildung immer unterstützt haben und ohne die mein Studium nicht möglich gewesen wäre. Danke, dass ich mich immer auf euch verlassen kann und ihr mir bei allen meinen Entscheidungen zur Seite steht.

Danke!

Contents

1. Literature

1.1. General aspects of germanium

Germanium was first discovered in its elemental form by Clemens Winkler in 1886.[1] With a natural abundance of 5.6 ppm in the earth's crust, germanium is the least available element in Group 14 and is found in rare sulfidic minerals such as Argyrodite (Ag_8GeS_6) or Germanite ($Cu_6FeGe_2S_8$). Industrially, germanium is available by oxidizing the sulfides of Sphalerite (ZnS; accompanied with GeS_2) ores into the corresponding oxides by roasting. The oxides (ZnO and GeO_2) are treated with hydrochloric acid (HCl) or chlorine gas (Cl_2) to gain the volatile germanium tetrachloride ($GeCl_4$) which can subsequently be distilled. The purified $GeCl_4$ is then hydrolyzed to GeO_2 which can be reduced to elemental germanium with hydrogen or carbon. The metal can be further purified by zone melting processes.

In its compound form, germanium occurs in two different oxidation states (II and IV). Due to the instability of germanium(II) compounds, they are easily oxidized to germanium(IV) derivatives. Thus, only germanium(IV) compounds are found in nature.[2] The preparation of germanium(II) and germanium(IV) containing starting materials is shown in Figure 1.1.

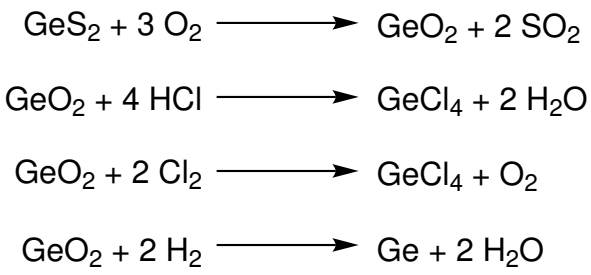

Figure 1.1.: Preparation of important germanium containing starting materials germanium dioxide, germanium tetrachloride and metallic germanium.

Organogermanium compounds define themselves as compounds containing at least one germanium−carbon bond. The first one of these compounds, Et_4Ge, was synthesized already by Winkler in 1887 by the reaction of diethylzinc and germanium tetrachloride.[3] Due to its low availability and high prices, no new organogermanium compounds were published for more than 30 years. In 1925, tetraphenylgermane was synthesized by Morgan *et al.*, which was the first compound containing a germanium−aryl bond and in this year also Dennis and coworkers prepared further tetra-substituted organogermanium compounds.[4, 5] In the following years, new sources for germanium were discovered which led to an increased number of new compounds up to the 1960s.

Potential applications for organogermanium compounds are, besides materials for electronics and energy storage, also medical applications as antibacterial agents, due to low toxicity against mammals but significant activity against bacteria.[6–8] Especially the synthesis of organometallic, oligo- and polymeric germanes grew as an important field due interesting properties such as conductivity, absorption of UV light or thermochroism.[9–11] With its increased band gap conductivity and hole, as well electron mobility compared to silicon, elemental germanium is considered a good candidate for electrical applications as well. These special characteristics and the demand for new functional materials make germanium based materials increasingly important in upcoming years.

In Group 14, germanium shows in its chemical behavior closer relations to its isostructural lighter homologue silicon than to tin and lead, making the chemistry of silicon representative for the one of germanium.[2] Systematic trends of compounds of Group 14 elements are increase of bond distances and covalent atomic radius, and decrease of bonding energy when going from the lighter to the heavier homologue (stability C−M: Si>Ge>Sn>Pb).[2, 12] Due to the similar electronegativity of Ge, C and H, the polarities are residue dependent in Ge−C and Ge−H bonds.[13] Generally, the thermal stability of organometallic hydrides decreases when going from Si to Pb downwards and with increasing number of hydrogen atoms attached to the metal center. The high affinity to hydrolysis of Si−H bonds is not found for other group 14 elements.

1.2. Tetraarylgermanes and organogermanium halides

Even though there is no direct use in industrial applications of the small number of so far known tetraarylgermanes, such compounds features a valuable starting materials for other organogermanium compounds. For the introduction of aromatic residues, typically Grignard reagents (Figure 1.2) or organolithium species (Figure 1.3) are reacted with germanium halides.[4, 14, 15]

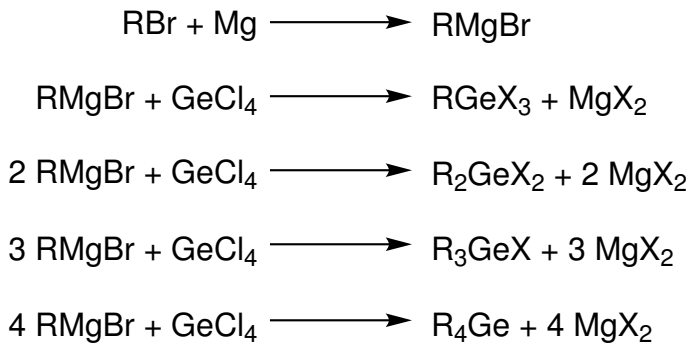

Figure 1.2.: Preparation of the Grignard reagent and reaction with $GeCl_4$ to prepare tetraorganogermanes and organogermanium halides.

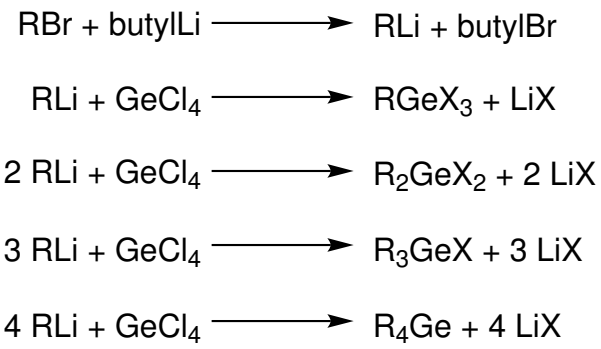

Figure 1.3.: Formation of the organolithium species using butyllithium and conversion towards organogermanium compounds.

Alternatively, tetra- and trisubstituted germanes can be prepared from GeO_2 with a hexacoordinated germanium complex as intermediate and subsequent conversion with Grignard reagents. This reaction procedure offers an alternative to $GeCl_4$ as key intermediate in the preparation of organogermanium compounds replacing Cl_2 and HCl as environmentally ploblematic reagents. It was first reported by the group of Reye in late 1980s with an anionic hexacoordinate germanium compound (Figure 1.4).[16, 17]

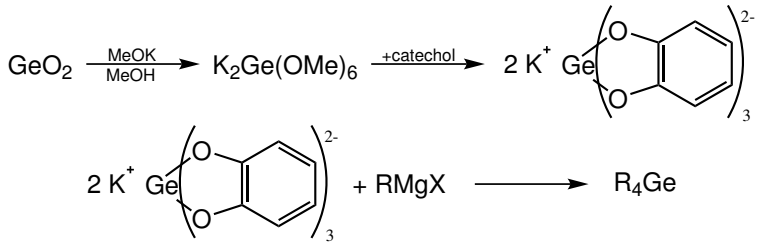

Figure 1.4.: Usage of anionic hexacoordinate germanium complexes in the synthesis of tetrasubstituted organogermanes.

Recently, Glavinovic *et al.* reported the mechanochemical synthesis of a hexacoordinate germanium species from germanium metal or GeO_2 using either quinone or catechol, stabilized by electron donors. Furthermore, they showed the conversion of those complexes with Grignard reagent to tetrasubstituted germanes (Figure 1.5).[18, 19] Unfortunately, this reaction route also shows a lack of selectivity in the synthesis of not fully

substituted germanes resulting in a product mixture of mainly di- and trifunctional germanes.

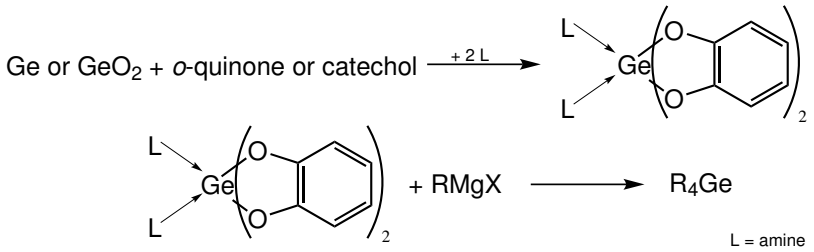

Figure 1.5.: Usage of amine donor stabilized germanium complexes in the synthesis of tetra substituted organogermanes.

In contrast to tetraorganogermanes, organogermanium halides show powerful features as starting materials for the preparation of other germanium compounds because of their stability at room temperature. Nevertheless, exclusion of water is important because of facile hydrolysis of the Ge−X bond by air moisture under the formation of hydroxides. Grignard and organolithium reagents can be used in the preparation of arylgermanium halides when changing the stoichiometry of the reaction. Nonetheless, these reactions usually result in a product mixture of mono-, di- and triarylgermanium halides present.[20–24] Isolation is even further complicated by halogen-metal exchange when different halogens are used. Thus, high yields are rare. Recently, Uhlig and coworkers published a selective synthesis of novel tetraarylgermanes and triarygermanium halides with respect to the substitution pattern of the aryl residue introduced.[25]

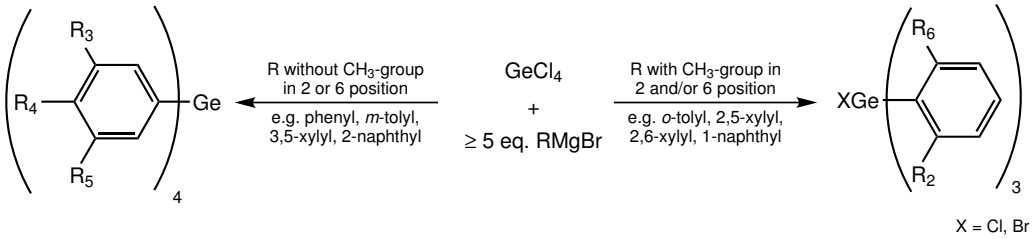

Figure 1.6.: Selective preparation of tetraorganogermanes and triorganogermanium halides depending on substitution pattern of the residue.[25]

Redistribution reactions are commonly used for Group 14 elements in literature to prepare Group 14 organometallic halides and widely applied for silicon and tin compounds (Figure 1.7).[26, 27] But when employing the reaction with germanium, it results in a difficult to separate product mixture, due to reaction equilibria, making the adjustment of reaction conditions challenging. Usually, elevated temperatures and catalytic amounts of $AlCl_3$ are needed. Comproportionation reactions have been employed between germanium halides and arylgermanes (Figure 1.8).[28–30]

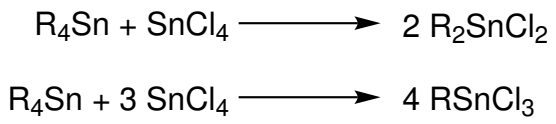

Figure 1.7.: Kocheshkov reaction between tetraorgano stannanes and tin tetrachloride.

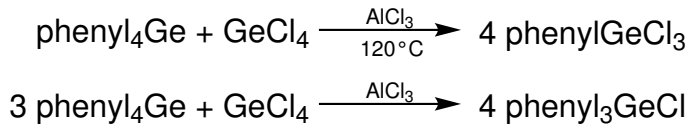

Figure 1.8.: Redistribution reactions for the preparation of phenylgermanium chlorides.

Aryl transfer reactions from organometallic silicon chlorides onto germanium tetrachloride catalyzed by $AlCl_3$ were closely investigated by Zhun *et al.*. Reactions of di- and triphenylsilicon chlorides and tetraphenylsilane with germanium tetrachloride gave di- and triphenylgermanium chlorides at low catalyst concentrations or phenylgermanium trichloride above 10 wt% of aluminum chloride. Furthermore, when using phenylsilicon trichloride with germanium tetrachloride, phenylgermanium trichloride is obtained in good yields independent of the catalyst concentration (Figure 1.9).[31, 32] In addition, transmetalation reactions from organotributylstannanes with germanium tetrachloride to form arylgermanium trichlorides were investigated by Kultyshev *et al.*.[33, 34]

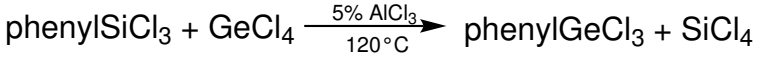

Figure 1.9.: $AlCl_3$ catalyzed aryl transfer from silicon to germanium.

Moreover, the halogenation of organogermanes is possible, using for bromides and iodides, elemental halogenides, and for chlorides, halogenated solvents as halogen source.[14, 35] As further halogenation agents, haloalkanes and hydrogen halides also find use in the synthesis of organogermanium halides, but the reaction results usually in a product mixture of mono-, di- and trihalides, that is hard to separate. If available, this can be circumvented by halogenation of organogermanium hydrides as starting materials, since the Ge−H bond shows higher affinity towards substitution than the Ge−C bond, leading to a controlled reaction with good yields. In literature, carbon tetrachloride with DBP (dibenzoyl peroxide) or *N*-halosuccinimides have been found as useful reagents for that reaction.[20, 23, 36, 37] Instead of DBP, palladium can also be used to catalyze the chlorination of organogermanium hydrides with CCl_4 (Figure 1.10).[38]

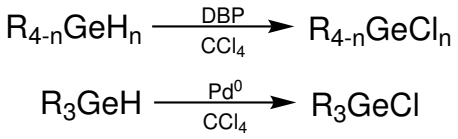

Figure 1.10.: Use of CCl_4 for the chlorination of organogermanium hydrides.

The catalytic insertion of $GeCl_2$·dioxane into the C−Br bond of arylbromides results in the formation of mixed arylgermanium trihalides.[39] Furthermore, arylgermanium trichloride can be formed in a two-step reaction from the reaction of elemental germanium and germanium tetrachloride followed by subsequent reaction of the dichlorogermylene with arylchloride as shown in Figure 1.11.[40]

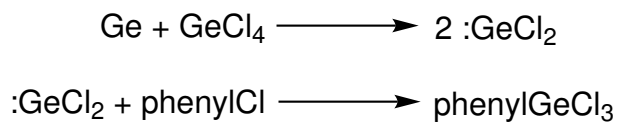

Figure 1.11.: Synthesis of phenylgermanium trichloride by the insertion reaction of germanium dichloride with phenylchloride.

Mixed organogermanium hydrochlorides were selectively obtained by Ohshita by replacement of a hydride moiety from organogermanium hydrides using $CuCl_2$. By adding

further equivalents, as well as catalytic amounts of CuI to the reaction mixture, the fully halogenated product is gained.[41] The reason why two equivalents of $CuCl_2$ are needed for the substitution of one hydride moiety is the reduction towards a copper (I) species and not to elemental copper. The hydrochlorides are interesting due to their possible application in dehydrohalogenative coupling reactions.

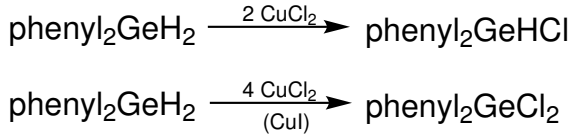

Figure 1.12.: Selective chlorination of phenylgermanium dihydride using $CuCl_2$ of $CuCl_2$(CuI).

Alternatively to $CuCl_2$, organogermanium chlorides hydrochlorides can be prepared by cleavage of an aromatic group with trifluorosulfonic acid (HOTf) and subsequent substitution of the OTf group using NH_4Cl or LiCl (Figure 1.13).[38, 42]

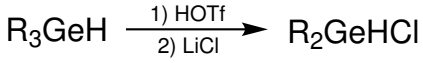

Figure 1.13.: Substitution of an aryl group by a Cl using triflation route as shown for the cleavage of a residue of a organogermanium monohydride.[38]

1.3. Organogermanium hydrides

Organogermanium hydrides have recently gained higher interest due to their applicability as precursors in the preparation of oligo- and polygermanes, or volatile compounds in the deposition of thin films in microelectronics. Organogermanium hydrides are less prone to decomposition under elimination of dihydrogen than the heavier Group 14 analogue tin, but more than silicon derivatives, which is in agreement with lower M−H bond dissociation energy when going from Si to Sn. Furthermore, the

reactivity increases with increasing hydride moieties when going from mono- towards trihydrides.[43]

The first group to report the synthesis of a compound bearing a Ge−H bond were Voegelen *et al.* in 1902, when they prepared GeH_4 by the reaction of zinc and germanium with sulfuric acid present.[44] Another possible way for the preparation or organogermanium hydrides was introduced by Gilman in 1955, with the reaction of tetraphenylgermane with metallic lithium under the formation of a lithiated species (Ph_3GeLi), which can be subsequently transformed into triphenylgermane.[45] A similar reaction was reported by Tamborsky in 1962, but he reduced triphenylgermanium chloride to get the same germyllithium intermediate as Gilman which can be reacted to the corresponding germane.[46]

Nevertheless, the most applied and straightforward route towards organogermanium hydrides is the reduction of organogermanium halides with lithium aluminum hydride ($LiAlH_4$) in polar solvents. This route is not only the most direct, but also highly effective and commonly used in literature.[20–23, 39, 47–54]

$$4\ R_{4-n}GeX_n + n\ LiAlH_4 \longrightarrow 4\ R_{4-n}GeH_n + LiX + AlX_3$$

Figure 1.14.: Preparation of organogermanium hydrides from respective halides by hydrogenation with lithium aluminum hydride.

1.4. Oligo- and polygermanes

In recent years, oligo- and polymeric materials with element−element bonds of Group 14 elements have gained attention, due to their applicability in the fields of molecular electronics and nanotechnology as well as anodic material in lithium ion batteries. Generally, the thermochemical dissociation energy of the formed Ge−Ge single bond is far

lower than in corresponding C−C and Si−Si.[55] Nevertheless, the bond can be further stabilized by electron donating groups such as halogens, whilst electron withdrawing groups destabilize the bond and compounds show tendency towards decomposition.[56] Contrary to oligo- and polysilanes and –stannanes which are well explored, applications of germanium derivatives have been limited due to cost intensive preparation and only few available building blocks and routes.[9, 57] Nonetheless, the drive for new functional materials in combination with superior properties of these materials promoted the research in that field over the years and different polymerization methods have been developed.

1.5. Linear oligo- and polygermanes

Linear polymers of Group 14 elements can be approximated as linear chains of a metal backbone built by M−M single bonds covered by an organic jacket (Figure 1.15).[58–61]

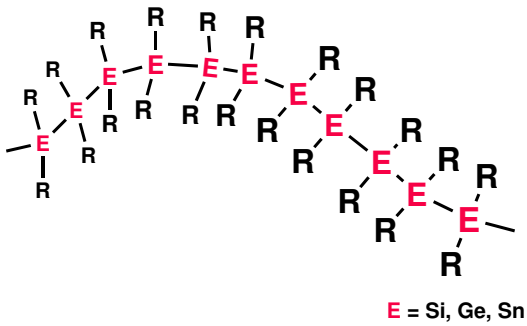

Figure 1.15.: Schematic representation of organometallic linear polymers.

Group 14 linear organometallic polymers feature a phenomenon of so called σ-conjugation. The concept of this effect was first described for oligosilanes and later expanded to higher homologues germanium and tin.[62–65] It shows that the effective overlap of hybridized atomic orbitals of neighboring elements leads to distribution of electron density over the metal backbone. This delocalization makes the $\sigma \rightarrow \sigma^*$ electronic transition possible which results in characteristic properties like absorption in the UV region,

thermochroism and further interesting electrochemical and optical behavior that make such materials interesting for application as photoresists in lithography, semiconductors and electronic devices working as quantum wires.[62, 66, 67]

Over the years various synthetic methods for Ge—Ge bonds have been developed (Figure 1.16). Among the commonly applied ones are the Wurtz-type coupling[4, 68–70], usage of Grignard and organolithium reagents[71–78], germylene insertion or electrochemical coupling[79–81], as well as lanthanide catalyzed coupling[82, 83]. In contrast to the field of tin containing polymers, where the synthesis of polystannanes using metal catalyzed dehydrocoupling reactions is commonly applied in literature, only one example has been reported for organogermanium dihydrides as precursors.[84] In most of these reactions organogermanium halides and hydrides make important precursors for the synthesis of germanium containing oligo- and polymers.

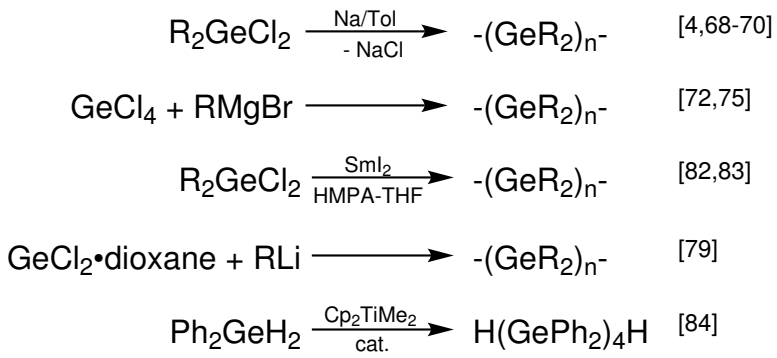

Figure 1.16.: Various methods to prepare linear organogermanium oligo- and polymers.

1.6. Organogermanium nanoparticles

With their size and shape dependence in electronic and optical behavior of semiconductor nanoparticles, as for instance visible photoluminescence by nano-sized silicon and germanium structures, a wide field for possible application opened. A special electronic feature is that Ge nanoparticles are expected to show function of a direct band gap material.[85–89] Despite these promising applications, the preparation of germanium

nanoparticles is limited due to high costs of the germanium precursors and limited synthetic preparation methods, which are for the most parts, physical methods such as chemical vapor or liquid deposition, plasma techniques or etching. The industrial applicability in germanium ion implantation, metal hydride reduction and sputtering techniques is so far still limited, due to problems in the control of implantation size and scale-up. Furthermore, often high temperatures, supercritical solvents or strong reducing agents have to be applied.[57, 90–101] An example for surface functionalized germanium nanoparticles is shown in Figure 1.17.

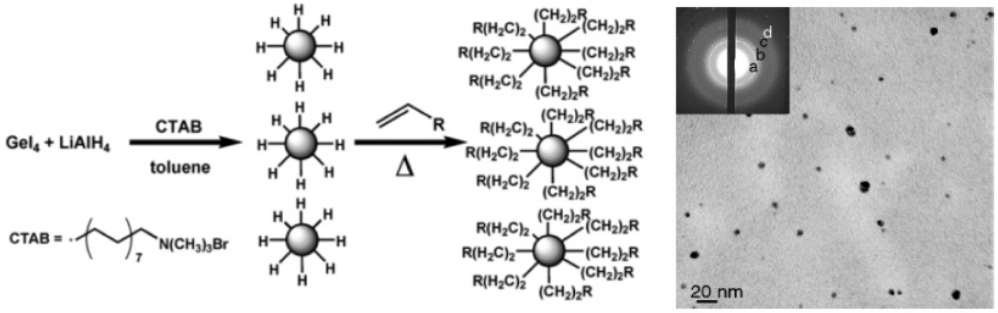

Figure 1.17.: Reaction scheme for the synthesis and surface functionalized Ge quantum dots (left); electron microscopy image, with electron diffraction pattern in inset (right).[92]

For the conversion of monoorgano trihydrides of group 14 elements (REH_3 with E = Ge,Sn) towards 3D polymers are, compared to respective linear polymers, only few preparation routes published (Figure 1.18). Interestingly, metal catalyzed dehydropolymerization was so far not applied to organotin trihydrides, but to organogermanium trihydrides as precursors. Choi and Tanaka applied zirconocene based catalysts for the conversion of phenylgermane towards high molecular weight partly cross-linked polygermanes at low temperatures.[102] Recently, Uhlig and coworkers prepared 3D metalorganic polymers for the higher group 14 homologue tin, using an amine catalyzed dehydrogenative coupling for the conversion of organotin trihydrides.[58, 103, 104]

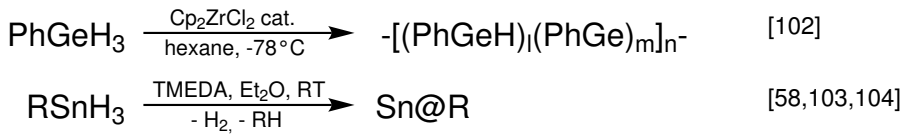

Figure 1.18.: Methods to prepare group 14 organometallic 3D polymers *via* dehydrogenative coupling.

A further field field of application for germanium based materials, which is gaining recently increasing interest, is the usage as Li-alloying electrode material in lithium ion batteries.[105–109] Since graphite has, with 372 mAh/g, a relatively low theoretical capacity, the usage of Ge, with 1623 mAh/g, as lithium alloying material would increase the capacity by a factor of four. Silicon would have an even higher capacity value, but compared to germanium it shows a 10^4 lower diffusion rate of lithium ions.[108] But the major problem is the rapid capacity loss when using germanium based materials. Currently, two major ways of of preventing this issue are under discussion. These are on the one hand the usage of nanomaterials with the higher surfaces and so shorter diffusion ways in combination with the prevention of agglomeration and *in-situ* growth of germanium nanoparticles within graphene (Figure 1.19).[110, 111]

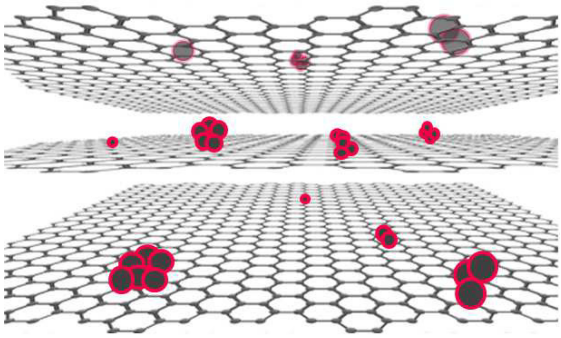

Figure 1.19.: Schematic representation of organogermanium nanoparticles within graphene.

2. Results and discussion

2.1. Synthesis of organogermanium halides and hydrides

This work expands the synthetic efforts towards organogermanium halide and hydride compounds in the Uhlig group, which were investigated by Wolf within her PhD thesis.[38] In the process of her work, she developed a selective route towards organogermanium monohydrides for ligands bearing steric demand in *ortho*-position.[25] Furthermore, the reaction route towards organogermanium di- and trihydrides was developed using sequential cleavage of organic ligands with triflic acid. During her work various novel organogermanium compounds were synthesized and characterized, such as organogermanium monohydrides (e.g. 2,5 $-$xylyl$_3$GeH, 2,6 $-$xylyl$_3$GeH, 3,5 $-$xylyl$_3$GeH) which are here investigated using ^{73}Ge NMR spectroscopy, organogermanium dihydrides (2,5 $-$xylyl$_2$GeH$_2$, 2,6 $-$xylyl$_2$GeH$_2$, 1 $-$naphthyl$_2$GeH$_2$) which are within this work prepared *via* a high yielding reaction route or organogermanium trihydrides (2,5 $-$xylyl$_2$GeH$_2$, 2,6 $-$xylyl$_2$GeH$_2$) which are here synthesized *via* a high yielding route and in addition fully characterized since essential analysis techniques are neglected there. The synthesis of organogermanium di- and trichlorides done within this work was prepared *via* the reaction procedure used by Wolf for the synthesis of 2,5$-$xylyl$_3$GeCl.

In contrast to the reaction procedure developed by Wolf *via* the triflation route, this work focuses on the high yielding synthesis of germanes by optimizing the conditions for the Grignard route and the separation of the different hydride species. Moreover, the newly optimized reaction route was used in order to prepare on the one hand known compounds to show the advantages of this reaction route and on the other hand to prepare novel organogermanium compounds.

Within the work of this thesis, oranogermanium hydrides and halides were prepared and characterized by NMR, IR, GCMS, HRMS, EA and, for solids, single X-ray diffraction analysis. As residues for the synthesis of the organometallic compounds were different aromatic residues chosen. Three different xylyl isomers with differences in their steric demand in *ortho*-position were applied. 1−naphthyl, which shows a larger aromatic system, and *p*−^{n}butylphenyl, which should increase solubility in the particle preparation, were used as well. Furthermore, organogermanium di- and trihydride compounds with the 2−((dimethylamino)methyl)phenyl (L^{CN}) residue were synthesized, which were prepared by hydrogenation of respective halides that were prepared at the University of Pardubice. The phenyl residue was used to prove the selective reaction towards trioganogermanium compounds with germanium aminopheonlates as intermediates. (Figure 2.1)

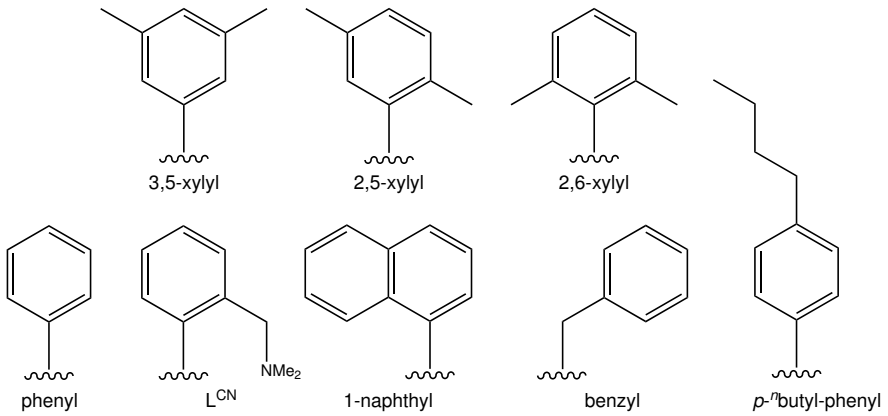

Figure 2.1.: Residues used within this work for the synthesis of organogermanium compounds.

2.1.1. Organogermanium halides

2.1.1.1. Organogermanium monohalides from aminophenolate complexes

In literature, organogermanium halides are most commonly prepared *via* either conversion of Grignard or organolithium reagents with $GeCl_4$ (Section 1.2). For the synthesis of organogermanium monohalides Wolf showed recently the selective preparation of this product class, if the aromatic residue used shows steric demand in *ortho*-position. Nevertheless, for residues without this steric demand the reaction only proceeds selectively towards tetraorganogermanes.[25] In order to gain the desired organogermanium monohalides for those residues an aromatic residue has to be cleaved using for instance triflic acid, which increases reaction time and decreases isolated yields, since such reactions display various side reactions (Figure 2.2).[38]

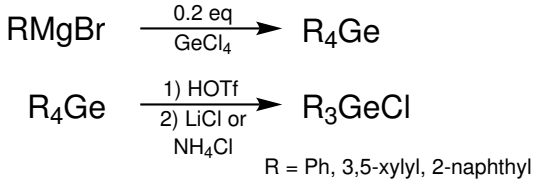

Figure 2.2.: Synthesis of triorganogermanium chlorides with ligands showing steric demand in *ortho*-position using triflation route.[25, 38]

Thus, a more direct route for the synthesis of organogermanium monohalides bearing no steric demand in *ortho*-position was highly desired. In 2017, Glavinovic *et al.* reported the synthesis of various tetraorganogermanes *via* the conversion of a hexacoordinated germanium quinolate complex with Grignard reagents.[18] Based on this reaction procedure the usage of an aminophenolate compared to the quinolate complex is supposed to hinder the reaction to the formation of tetrasubstituted germanes, which can be explained by the additional steric demand which is introduced by the secondary amine functionality.[112] This lower reactivity is able to decrease the reactivity to yield lower substituted organogermanium halides (Figure 2.3).

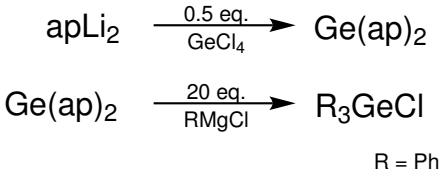

Figure 2.3.: Synthesis of triorganogermanium chlorides with ligands showing steric demand in *ortho*-position using $Ge(ap)_2$ as intermediate.

The reaction procedure towards the germanium aminophenolate ($Ge(ap)_2$) involves the synthesis of the aminophenol from catechol and subsequent activation with a lithiation agent before conversion with $GeCl_4$. Important feature of this reaction is that after the conversion with Grignard reagents the starting aminophenol can be collected as the hydrochloride species and potentially reused. Since the aminophenol residue is prone to radical formation, all synthetic steps were performed under argon atmosphere using Schlenk and glove box technique. Furthermore, because the N−C bond is prone to hydrolysis, reactions were performed under exclusion of water when possible.

Synthesis of 2,4–di–$tert$–butyl–6–($tert$–butylamino)phenol (apH_2)

The synthesis of the apH_2 was derived from the literature known synthesis routes of Blackmore *et al.* and Chegerev *et al.*. [113, 114] Initial use of the unmodified synthetic route of Blackmore did not yield in desired conversion rates. Even though the reaction was refluxed for several days a conversion of about 50% was obtained and only 20% could be isolated as pure, recrystallized product. In the modified reaction procedure, when I_2 was used in catalytical amounts as promotor, 80% conversion was reached after one hour of reflux and about 60% was gained as purified, isolated yield.

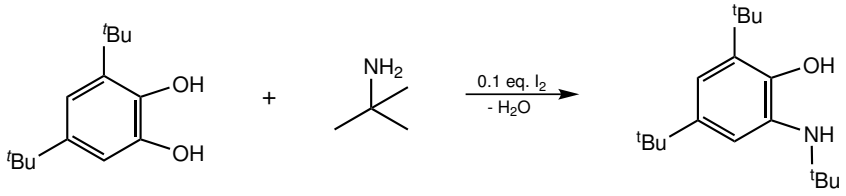

Figure 2.4.: Synthesis of 2,4–di–*tert*–butyl–6–(*tert*–butylamino)phenol (apH_2).

Synthesis of $Ge(ap)_2$

Compared to germanium catechol complexes which have been prepared already in 1988, the synthesis of respective aminophenol complexes was first reported in 2008 by the group of Abakumov with 2,6 −diisopropylphenyl substituted nitrogen atom on the aminophenol being the only known compound of this compound class up to this point.[112] They used a synthetic route *via* an exchange reaction between germanium tetrachloride and lithium *o*-amidophenolate. Furthermore, the Baines group attempted the synthesis of aminophenol substituted germanium complexes *via* the mechanochemical procedure. However, no complex formation was observed mostly because the reactions were performed under ambient conditions with the aminophenol susceptible to radical formation.

Based on the successful synthesis of aminophenol substituted germanium complexes in the group of Abakumov, using lithium *o*-amidophenolate, we assessed various literature procedures towards this reagent. Two main routes are found for the preparation of different lithium *o*-amidophenolates, which are used in subsequent conversion with metal halogenides. On the one hand, the reaction of metallic lithium with a iminoquinone[112, 115], and on the other hand metallation of a aminophenol using organolithium species, like BuLi[113, 114] or $LiN(TMS)_2$[116].

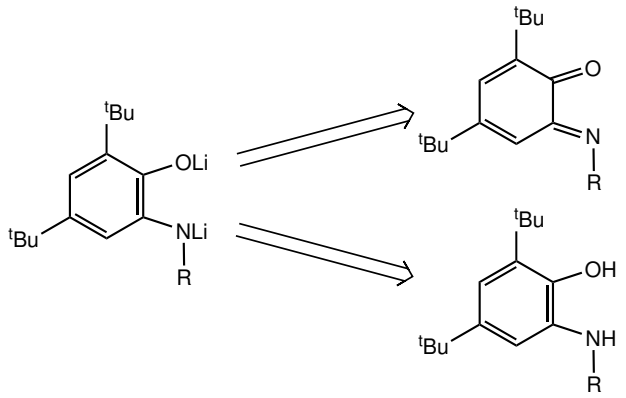

Figure 2.5.: Retrosynthesis of lithium–2,4–di–*tert*–butyl–6–(organo)phenolate ($apLi_2$) R = *tert*–butyl, (2,6–di–*iso*–propyl)phenyl.

Synthesis *via* both reaction pathways was attempted with *in situ* conversion with $GeCl_4$. No product was gained when using the redox reaction, which always led towards a dark green solution prior to conversion, which suggests radical species formation. For the metallation reaction, best results were gained with $LiN(TMS)_2$ as lithiation reagent. The reason for that is the easy purification of this solid reagent by recrystallization from hexanes and thus better reaction control, which is to our experience crucial for the reaction to proceed without radical formation. Furthermore, reactions can be easily performed in the glove-box. For the reaction, a THF solution of $LiN(TMS)_2$ is added dropwise to a solution of apH_2 and the reaction mixture turns into a light blue. The reaction is stirred for one hour, at which point $GeCl_4$ is added dropwise and the color is changed to a deep dark blue and the reaction is also accompanied with heat formation. The addition of $GeCl_4$ is continued until the deep blue color dissipates and a slight yellow-green solution is gained, which was stirred for 30 minutes. At this point, the solvent was evaporated and hexanes or pentane was added to the remaining off white slurry. The alkane phase is collected and DCM is added to the solids. From the collected DCM phase, pure $Ge(ap)_2$ is gained when evaporating the solvent. Furthermore, upon cooling the alkane phase, further product can be isolated. The formation of the novel $Ge(ap)_2$, with the *tert*-butyl group at the nitrogen, was confirmed by ESI-MS and NMR.

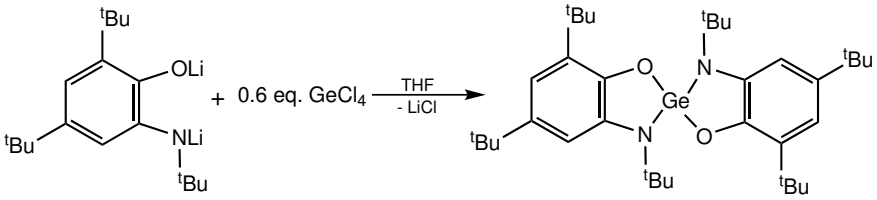

Figure 2.6.: Synthesis of germanium–bis–2,4–di–*tert*–butyl–6–(*tert*–butylamino)phenolate ($Ge(ap)_2$).

Attempts to prepare the hexacoordinated species of this compound by stirring or refluxing $Ge(ap)_2$ in pyridine like shown for tin complexes in literature was not successful.[114] These findings show that the decrease of the size of the metal center from Sn to Ge results in hindered synthesis of the hexacoordinated complex. Compared to the catechol complexes, where hexacoordination is commonly found, the steric bulk of the aminophenol residue is higher, resulting in the prevention of the addition of pyridine to the molecule.

Conversion of $Ge(ap)_2$ towards organogermanium monohalides

The reaction was tested for the phenyl residue as reference for residues without steric demand in *ortho*-position. For the conversion of $Ge(ap)_2$ using Grignard reagents, the complex was dissolved in THF and 20 equivalents of a PhMgCl solution in THF was added. The reaction was refluxed for 24 hours. Hexanes and water were added, but no phase separation was visible. Thus, 1 M HCl was added to get phase separation. Furthermore, in between the two layers a white precipitate was suspended. The interphase, as well as the oragnic phase were collected. The interphase, a white solid, was identified as $apH_2{\cdot}HCl$. The solvent of the organic phase was removed using a rotary evaporator. The crude mixture was investigated by NMR and GC-MS. The mixture was dissolved in a small amount of DCM and purified using preparatory TLC with hexanes as eluens. The bands were identified and the solid phase was extracted with chloroform.

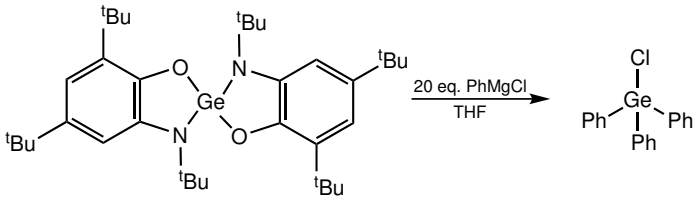

Figure 2.7.: Conversion of $Ge(ap)_2$ towards phenylgermanium monochloride.

The NMR of the crude mixture suggested product formation, due to peaks in the aromatic region. Furthermore, the GC-MS shows signals for biphenyl, which is a common side product from quenching, aminophenol and triphenylgermanium chloride as well as small amounts of tetraphenylgermane. The majority of the product is however triphenylgermanium chloride with a ratio of 19:1 to tetraphenylgermane. Pure triphenylgermanium chloride was gained by separation using preparatory TLC. Increasing the reaction time towards 48 hours reflux did not change this ratio. This proves that the reaction towards the tetraphenyl derivative is hindered. Furthermore, it proves that using aminophenolate compared to catecholate complexes decreases the reactivity in the conversion with Grignard reagents due to steric bulk and facilitates the selective synthesis of organogermanium monohalides bearing a residue without steric demand in *ortho*-position.

2.1.1.2. Organogermanium di- and trihalides via direct Grignard conversion

Organogermanium di and trihalides display, since they bear more functionalizable groups, a high potential as starting materials for various other germanium compounds and they are additionally stable at room temperature. Literature lacks up to this point in high-yielding and upscaleable reactions procedures towards organogermanium di- and trihalides.

As previously mentioned are Grignard reactions and lithiations the most common reactions in the synthesis of organogermanium compounds. (Section 1.2) However, both

preparation methods show various disadvantages in the synthesis of di- or trigermanium halides. For instance they always result in inseparable product mixtures, long reaction and work-up procedures and low yields leading to cost intensive reaction.[38, 117] Nevertheless, the Grignard route showed fewer problems and was, despite the problems mentioned, applied for the synthesis within this thesis. Careful adjustment of parameters and reaction procedures allowed for control over the product mixtures and shift of the main product. Especially choosing the correct stoichiometry between $GeCl_4$ and the Grignard reagent enables the preferential formation of R_4Ge, R_3GeX, R_2GeX_2 or $RGeX_3$ respectively. Wolf *et al.* showed that when using 5-fold excess of Grignard reagent, the reaction proceeds selectively towards R_4Ge or R_3GeX dependent on the steric bulk in the *ortho*-position.[25] Due to that, the main goal of this work was the preferential synthesis of R_2GeX_2 and $RGeX_3$ (Figure 2.8).

$$\mathrm{RBr + Mg \xrightarrow[THF\ or\ Et_2O]{} RMgBr}$$

$$\mathrm{RMgBr + GeCl_4 \xrightarrow[-MgX_2]{THF} \mathbf{RGeX_3} + R_2GeX_2 + R_3GeX}$$

$$\mathrm{2\ RMgBr + GeCl_4 \xrightarrow[-MgX_2]{Et_2O} RGeX_3 + \mathbf{R_2GeX_2} + R_3GeX}$$

Figure 2.8.: Formation and conversion of the Grignard reagent with $GeCl_4$ towards $RGeX_3$ and R_2GeX_2. The main product is indicated in boldface.

No selective preparation was possible because of the inevitable formation of product mixtures, but we were able to control the reaction that we could influence the product distribution dependent on the stoichiometry of the Grignard reagent towards $GeCl_4$. Yields higher than 70% of monoorganogermanium species could be isolated for all the different residues used within the synthesis. The focus of this work lies particularly on the preparation of the organogermanium trihalides species. Thus, the optimization towards diorganogermanium dihalides is only exemplary shown for $2,5-xylyl_2GeX_2$ (**11**), but not extended to other residues. In the case of the monoorganogermanium

trihalide synthesis, a molar ratio of 1.11:1.00 between arylbromide and $GeCl_4$ was used. When diorganogermanium dihalides were desired, the ratio was increased to 1.67:1.00, respectively. The significantly lower ratio of 2:1 was used, because while screening the reaction, we discovered that the Grignard reaction route tends towards overarylation. Moreover, the higher stoichiometry between arylbromide and $GeCl_4$ in the formation of $RGeX_3$ can be explained by the incomplete reaction of the Grignard reagent formation, which was indicated by unreacted arylbromide after the Grignard reagent conversion. As solvent for Griganrd reagent preparation and subsequent conversion with $GeCl_4$, THF was used for the preparation of $RGeX_3$ and Et_2O for the preparation of R_2GeX_2. Within the reaction procedure, the removal of the excess magnesium (Mg:RBr = 1.1:1) before the reaction with $GeCl_4$ was very important in order to prevent the formation of digermanes as side products, as was shown by Glockling *et. al.*.[75] Therefore, the Grignard solution was filtered using a cannula or Celite®. Another procedure to prevent overarylation was the dropwise addition of the Grignard reagent at 0°C to the solution of $GeCl_4$ in corresponding ether.

Furthermore, reaction times and temperatures were optimized. Best results were found under rather mild conditions (stirring for 12-16 hours while letting the reaction warm from 0°C to room temperature). Reaction at higher temperatures led immediately towards higher substituted compounds, while when keeping the reaction at low temperature the reaction progress was hindered. The reaction conversion was monitored for the preparation of 2,5 −xylylGeX_3 and 2,5 −xylyl$_2GeX_2$ which showed good conversion at a moderate amount of other arylated species after 12-16 hours stirring for both compounds. Thus, this procedure was performed for all Grignard reactions (compounds **1**-**5**,**11**). To quench the reaction, 10% HCl was added to the stirring reaction mixture at 0°C. The organic layer was separated using a cannula and the water layer was washed twice with the ethereal solvent used for the reaction. Subsequently, the combined organic layers were dried over Na_2SO_4. The dried solution was filtered using a filter cannula and the remaining Na_2SO_4 was washed twice with ethereal solvent.

The THF or Et_2O was removed under *vacuo* to receive the crude product as mixture of R_nGeX_{4-n} with $RGeX_3$ or R_2GeX_2 as main product as desired.

Typical side products were aryl−H and diaryl obtained from quenching the Grignard conversion with 10% HCl, unreacted arylbromide was also detected (Figure 2.9). It is of highest importance to eliminate these side products before subsequent hydrogenation of the halides, because the organogermanium trihydrides have similar properties to these side products and are not separable from those. Thus, these side products were evaporated under *vacuo* at elevated temperatures, because of the high boiling points of the arylbromides.

$$RMgBr + HCl \longrightarrow RH + MgX_2$$

$$2\ RMgBr + 2\ HCl \longrightarrow R\text{-}R + 2\ MgX_2 + H_2$$

Figure 2.9.: Side products which occur from quenching unreacted Grignard reagent with 10% HCl.

The purified reaction product was gained as a wax-like, off white solid, which was analyzed by GCMS. The GCMS spectra showed a mixture of $RGeX_3$, R_2GeX_2 and R_3GeX for all compounds (Table 2.1). Due to the fact that arylbromide and $GeCl_4$ were used, halide exchange between bromide and chloride occurred. Thus all possible halide species were present in the product ($RGeX_3$ = $RGeCl_3$, $RGeCl_2Br$, $RGeClBr_2$, $RGeBr_3$; R_2GeX_2 = R_2GeCl_2, $R_2GeClBr$, R_2GeBr_2; R_3GeX = R_3GeCl, R_3GeBr). The two possibilities to avoid the halogen exchange would be either the usage of arylchlorides with $GeCl_4$ or the usage of arylbromides with $GeBr_4$. Earlier results showed that both reaction pathways showed problems in starting the Grignard reaction and lowered conversion when using the arylchlorides, and also no improvement in the separation of the different organogermanium species.[38] Thus, the reaction employing arylbromide and $GeCl_4$ was used due to higher yields obtained for using arylbromide and lower cost of $GeCl_4$ as compared to $GeBr_4$, despite the halogen exchange as a consequence. Furthermore, the subsequent hydrogenation of the R_nGeX_{4-n} product mixture, shows indifferent reaction behavior independent of which bromide or chloride species

are present. The only limitation is that the stoichiometry cannot be adjusted correctly, which did not matter since excess of reducing agent was used for all reactions.

Table 2.1.: Optimized product mixtures gained by the conversion of $GeCl_4$ with Grignard reagent; semi-quantitative determination using GCMS.

Compound	$RGeX_3$ [%]	R_2GeX_2 [%]	R_3GeX [%]
p−^{n}butylphenylGeX$_3$ (1)	62	26	6
3,5 −xylylGeX$_3$ (2)	74	23	3
2,5 −xylylGeX$_3$ (3)	92	8	traces
2,6 −xylylGeX$_3$ (4)	76	23	traces
1 −naphthylGeX$_3$ (5)	93	7	traces
2,5 −xylyl$_2$GeX$_2$ (11)	3	85	11

Since the direct reaction using the Grignard reaction always led to product mixtures, the only way to prepare pure R_2GeCl_2 and $RGeCl_3$ compounds was by chlorination of hydride derivatives (Figure 2.10). This well known literature reaction is applied to compounds **15**-**19** and **24**-**26** by refluxing it in freshly distilled CCl_4 in the presence of elemental Pd as catalyst for more than 16 hours to yield pure colorless solids or oils as compounds **6**-**10** and **12**-**14** after filtration and evaporation of the CCl_4 under reduced pressure. Moreover, this reaction was a further way to characterize the liquid organogermanium trihydrides by derivatization into the trichloro compound, which led to single crystal X-ray diffraction quality crystals for compounds **8**, **9** and **10**. Other compounds characterized with single crystal X-ray diffraction were **12**, **13** and **14**.

$$RGeH_3 \xrightarrow[CCl_4]{Pd^0} RGeCl_3$$

$$R'_2GeH_2 \xrightarrow[CCl_4]{Pd^0} R'_2GeCl_2$$

Figure 2.10.: Chlorination of organogermanium hydride compounds in order to prepare $RGeCl_3$ and R_2GeCl_2 compounds in a pure way (R = $p-^n$butylphenyl, 3,5 −xylyl, 2,5 −xylylGe, 2,6 −xylyl, 1 −naphthyl; R' = 2,5 −xylylGe, 2,6 −xylyl, 1 −naphthyl).

2.1.2. Organogermanium hydrides

The main goal of this thesis was the preparation of organogermanium hydride compounds as precursors for subsequent polymerization reactions to organogermanium nanoparticles. After the successful synthesis of diorganogermanium dihalides and monoorganogermanium trihalides in good yields, the hydrogenation and especially subsequent selective separation of the prepared hydride compounds was the main challenge in the high yield preparation of mono- and diarylated germanium compounds. In order to achieve this, the corresponding arylgermanium halide mixtures prepared *via* the Grignard route were hydrogenated using excess $LiAlH_4$ (Figure 2.11).

$$RGeX_3 + R_2GeX_2 + R_3GeX \xrightarrow[Et_2O]{LiAlH_4} RGeH_3 + R_2GeH_2 + R_3GeH + LiX + AlX_3$$

Figure 2.11.: Hydrogenation of the organogermanium halide mixtures using reduction with $LiAlH_4$.

The reaction was performed in various different aprotic, non halogenated solvents, such as 2-methylnaphthalene, mesitylene, toluene, THF and Et_2O. Although working with Et_2O is tricky for the exothermic reaction because its low boiling point and for its lower solubility of the organogermanium halides, it is of highest importance to use Et_2O in this reaction, because the formed $RGeH_3$ can otherwise not be separated from the solvent. Furthermore, it is advisable to use freshly ground $LiAlH_4$ for the reaction to enhance reactivity. For this reaction, usually the starting organogermanium halide mixtures were, depending on the residue used, solved or suspended in Et_2O, cooled to 0°C and the solid powder of $LiAlH_4$ was added in portions. Gas formation confirmed immediate reaction. After stirring the reaction for 2 hours at 0°C and further 30 minutes at room temperature, the reaction was complete. Subsequently, the reaction was quenched with 3% H_2SO_4 and a saturated tartrate solution was added. The organic phases were dried over Na_2SO_4 and the Et_2O was evaporated under *vacuo*. When mixtures of organogermanium halides were used as starting materials, the reaction resulted in a

mixture of usually mono-, di- and trihydrides. This mixture can be separated due to the solubility of the different hydrides in pentane and their boiling point. $RGeH_3$ is a liquid and can be distillative separated from R_2GeH_2 and R_3GeH. The remaining mixture can be separated by washing it with pentane. The organogermanium dihydrides are soluble. The remaining solids yield after filtration and drying pure organogermanium monohydride. The solvent of the filtrate is removed under removed pressure to give pure R_2GeH_2.

In addition to that, the side products ($RGeH_3$ and R_3GeH in the preparation of R_2GeH_2; R_2GeH_2 and R_3GeH in the preparation of $RGeH_3$) could be used as starting materials in other reactions (e.g. Wurtz type coupling) or even transferred into the desired products by cleavage of a Ge−C bond using triflic acid with subsequent hydrogenation to introduce more hydrogen moieties, or chlorination of hydrides and subsequent addition of a Grignard reagent to introduce an additional aryl group.[38]

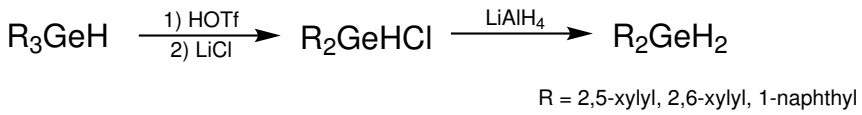

Figure 2.12.: Preparation of organogermanium dihydrides from organogermanium monohydrides as example for the further usage of isolated side products.

The benzylGeH_3 was used to compare the conversion of the organogermanium trihydrides towards organometallic nanoparticles, to investigate on the differences between a direct π system at the germanium vs. a benzylic π system. It was not synthesized *via* the Grignard route. Instead the benzyl$GeCl_3$, which was acquired commercially was used as starting material for the hydrogenation reaction. Nevertheless, the same reaction protocol as mentioned above was used for the preparation of benzylGeH_3, which proceeded straightforward to the desired product.

Intra-amine functionality in organogermanium hydrides

In 2011, Lechner *et. al.* reported the formation of Sn−Sn bonds from organotin hydrides in an amine catalyzed dehydrogenative coupling reaction.[118] Subsequently, this reaction was not only applied to organotin dihydrides, but also expanded towards even more labile organotin trihydrides.[58, 103, 104] Initial results from Reischauer show that the polymerization of organotin trihydrides are similarly catalyzed when using an intramolecular amine (2-((dimethylamino)methyl)phenyl residue (L^{CN})) base rather than adding an external amine base (e.g. TMEDA). Since with tin derivatives too fast uncontrollable reaction occurred as soon as the hydride was formed, the focus was also expanded to the preparation of organogermanium hydrides with an intra amine base. This is supposed to prevent that behavior by using the less labile germanium as central atom compared to tin. The corresponding monohydride ($L^{CN}{}_3GeH$) was prepared before by Royo and coworkers *via* lithiation route in order to prepare $L^{CN}{}_3GeCl$ and subsequent hydrogenation with $LiAlH_4$ (Figure 2.13).[119] Mono- and trihydrides bearing the L^{CN}-residue have not been prepared yet.

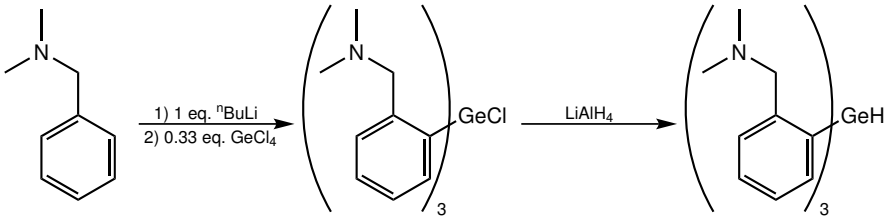

Figure 2.13.: Synthesis of $L^{CN}{}_3GeH$ *via* lithiation, conversion with $GeCl_4$ and subsequent hydrogenation with $LiAlH_4$.[119]

Both $L^{CN}GeCl_3$ and $L^{CN}{}_2GeCl_2$, were prepared in the working group of Prof. Ruzicka from the University of Pardubice *via* lithiation of the residue and conversion with $GeCl_4$. The hydrogenation reaction the chlorides showed initially two rather tricky features. On the one hand, detection of the starting material in GCMS was not possible, because it would decompose at that conditions, due to that usual reaction control with GCMS was not possible. Furthermore, the chlorides showed low solubility in standard solvents

used for hydrogenation, like Et_2O, THF or toluene. Good solubility was only obtained in standard halogenated solvents, which cannot be used for hydrogenation reactions with $LiAlH_4$. In addition, organogermanium trihydrides can only be isolated from Et_2O, as shown before. With the electron donation to the germanium central atom and the poor solubility, it was found, that the reactivity within the hydrogenation reaction is vastly decreased. Product formation was only detected at increased temperatures for several hours using reaction control with ^1H NMR. Due to these initial results, various reaction solvents (Et_2O, THF, 1,2-dichlorobenzene) were tested at different reaction temperatures and times. For the hydrogenation of both $L^{CN}GeCl_3$ and $L^{CN}{}_2GeCl_2$, the reaction procedure needed reflux in Et_2O for several hours over several days. Furthermore, the hydrogenated products showed dependence on the quenching reagent used. In all other reactions shown before, the reaction was quenched with 3% H_2SO_4, to maintain an acidic solution, to which saturated tartrate solution was added. Nevertheless, when using this procedure on the one hand, and diluted, degassed water on the other hand, two different germanium di- or trihydride shifts were found in the ^1H NMR, which indicates two different products formed. This is presumably due to interaction between aluminum salts, formed while quenching, and the $-N(CH_3)_2$ intra-amine arm. This was investigated by quenching parts of a reaction mixture with distilled degassed water, 3% H_2SO_4 or 3% H_2SO_4 and saturated tartrate solution. Product could only be isolated when the reaction was quenched with distilled degassed water. To investigate if the yielded product shows a dative adduct, elemental analysis was performed which proved that the gained product is pure $L^{CN}GeH_3$ or $L^{CN}{}_2GeH_2$ without further adducts.

2.2. NMR spectroscopy

Within this work, ^{1}H, ^{13}C and ^{73}Ge NMR spectroscopy was performed. All ^{1}H, ^{13}C and ^{73}Ge shifts are presented in the Experimental part of this work. ^{13}C NMR spectroscopy was only used for the characterization of pure compounds because it is impractical for reaction control because it shows little indication if desired compounds were formed. ^{13}C spectra show expected number and position for the signals measured, thus no further interpretation of signals is done here.

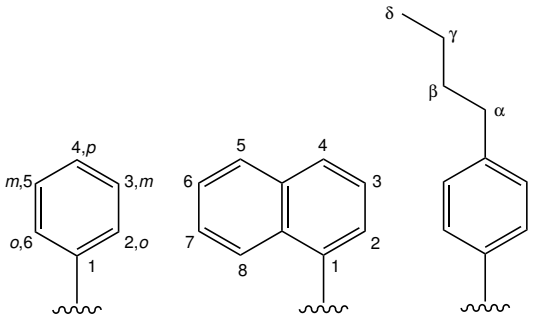

Figure 2.14.: Numbering of carbon positions of residues. For the numbering of phenyl also *o,m,p*-nomenclature is used. Carbons of aliphatic sidechains are numbered with greek letters.

2.2.1. ^{1}H NMR spectroscopy

^{1}H NMR is of limited use to determine reaction progress and product formation in the synthesis of organogermanium halide mixtures (R_nGeX_{4-n}), due to their nearly identical chemical shifts and furthermore, vast overlapping of different signals. For $RGeCl_3$ and R_2GeCl_2 compounds, ^{1}H NMR is of limited use, due to only little indication if clean products or product mixtures are present due to the aromatic region being too crowded. Only methyl groups of xylyl residues could be used to determine the purity of products due to formation of shoulders in the signal if another species is present. For the $RGeCl_3$, R_2GeCl_2, $RGeH_3$ and R_2GeH_2 compounds, the aliphatic and aromatic

protons show a distinct pattern for each residue, which are only slightly shifted due to the change from chloride to hydride moiety on the germanium central atom or changing a hydride/chloride to a residue moiety. $p-^t$butylphenyl-compounds (**6**, **15**, **22** and **40**) show two doublets in the aromatic region and a triplet, quintet, sextet and another triplet in the aliphatic region corresponding to the hydrogen at C_α, C_β, C_γ and C_δ position. Those signals show an upfield shift with increasing distance to the aromatic ring. The NMR-spectra with the 3,5 −xylyl residue show a very simple pattern consisting of a singlet, for the 2,6 −H, and another singlet, for the 4 −H in the aromatic region. Also, a further singlet shift is found in the aliphatic region corresponding to the 6 protons of the two methyl groups. The ^{1}H NMR spectrum of 2,5 −xylyl compounds show a singlet for the 6 −H and a doublet for the 3,4 −H in the aromatics, while two singlets are found in the aliphatic region for the protons of the methyl groups in 2 and 5 position. 2,6 −xylyl compounds show a triplet corresponding to the 4 −H and a doublet for the 3,5 −H of the aromatic residue. Furthermore, a singlet for the protons of the methyl groups in 2,6-position can be found in the aliphatic region. The proton spectra of 1-naphthyl compounds show, as expected, signals only in the aromatic region, although it is worth mentioning that the signals are shifted more downfield than for all other residues. Single signals are often not resolved completely for compounds bearing that residue, leading usually to multiplets, or doublets of doublets. Compounds with the intramolecular base residue 2 −((dimethylamino)methyl)phenyl (L^{CN}) show a doublet for the 6 −H and a multiplet for 3,4,5 −H in the aromatic region, as well as a singlet for the CH_2 protons around 3.20 ppm and a singlet for the protons of the CH_3 protons in the aliphatic region. The NMR signals of the benzylgermanium trihydride show two multiplets in the aromatic region and a quadruplet of the CH_2 group, which gets split due to *J*-coupling with the three germane protons next to the group.

^{1}H (Ge)−H NMR shifts

^{1}H NMR spectroscopy is an especially valuable tool for the investigation for organogermanium hydrides. The detection of hydride protons within the spectra enables the indication if the desired compounds are formed and also if product mixtures are present. These signals show characteristic chemical shifts between the aromatic and aliphatic region and the shift is also corresponding to the number of hydride protons in the molecule. Furthermore, within this region a upfield shift can be detected when exchanging a residue with a hydride. In all cases for the germanes with aromatic residues, the peak shows no multiplicity due to lack of neighboring protons. Whereas, the benzyl germane shows splitting of the signal to a triplet due to the CH_2 protons next to the germane hydrides. Table 2.2 shows the comparison of the (Ge)−H shifts of literature known arylgermanium hydride compounds with compounds prepared within this work.

Table 2.2.: ^{1}H (Ge)−H NMR shifts of arylgermanium hydrides prepared within this thesis and similar compounds in literature.

Compound	**δ^1H (Ge)−H** [ppm]	**Solvent**
GeH_4[120]	3.27	CCl_4
R_3GeH		
phenyl$_3$GeH[121]	5.61	$CDCl_3$
o−tolyl$_3$GeH[122]	5.95	$CDCl_3$
o−(MeOCH$_2$)phenyl$_3$GeH[122]	5.99	$CDCl_3$
o−(EtOCH$_2$)phenyl$_3$GeH[122]	6.01	$CDCl_3$
o−(^{t}butylOCH$_2$)phenyl$_3$GeH[122]	6.05	$CDCl_3$
o−(MeSCH$_2$)phenyl$_3$GeH[122]	6.37	$CDCl_3$
o−(MeOCH$_2$)phenyl$_2$*o*−(HOCH$_2$)phenylGeH[122]	6.04	$CDCl_3$
L$^{CN}{}_3$GeH^a [119]	6.05	$CDCl_3$
2,4,6 −mesityl$_3$GeH[123]	5.83	CCl_4

2,4 −xylyl$_3$GeH[38]	5.84	$CDCl_3$
2,5 −xylyl$_3$GeH[38]	5.82	$CDCl_3$
2,6 −xylyl$_3$GeH[38]	5.90	$CDCl_3$
3,5 −xylyl$_3$GeH[38]	5.52	$CDCl_3$
1 −naphthyl$_3$GeH[38]	6.48	$CDCl_3$
R_2GeH_2		
phenyl$_2$GeH$_2$[124]	5.00	THF−d_8/pentane
p−(MeO)phenyl$_2$GeH$_2$[39]	5.20	C_6D_6
2,4,6 −mesityl$_2$GeH$_2$[123]	5.05	CCl_4
2,5 −xylyl$_2$GeH$_2$[38] (**26**)	5.03	$CDCl_3$
2,6 −xylyl$_2$GeH$_2$[38] (**24**)	5.13	$CDCl_3$
1 −naphthyl$_2$GeH$_2$[38] (**25**)	5.64	$CDCl_3$
3,5 −xylyl$_2$GeH$_2$ (**23**)	5.02	$CDCl_3$
p−^{n}butylphenyl$_2$GeH$_2$ (**22**)	5.04	$CDCl_3$
$L^{CN}{}_2$GeH$_2$ (**27**)[a]	5.44	C_6D_6
$RGeH_3$		
phenylGeH$_3$[125]	4.12	CCl_4
p−(MeO)phenylGeH$_3$[39]	4.27	C_6D_6
p−tolylGeH$_3$[39]	4.77	C_6D_6
2,4,6 −mesitylGeH$_3$[123]	4.13	CCl_4
2,4,6 −tri^{i}propylphenylGeH$_3$[23]	4.28	$CDCl_3$
2,4,6 −tri^{t}butylphenylGeH$_3$[126]	4.79	C_6D_6
2,6 −di(2,6−di^{i}propylphenyl)phenylGeH$_3$[54]	3.58	C_6D_6
2,5 −xylylGeH$_3$[38] (**17**)	4.14	$CDCl_3$
2,6 −xylylGeH$_3$[38] (**18**)	4.12	$CDCl_3$
1 −naphthylGeH$_3$ (**19**)	4.52	$CDCl_3$
3,5 −xylylGeH$_3$ (**16**)	4.24	$CDCl_3$
p−^{n}butylphenylGeH$_3$ (**15**)	4.25	$CDCl_3$
L^{CN}GeH$_3$ (**21**)[a]	4.52	C_6D_6
other compounds within this thesis		
benzylGeH$_3$[127] (**20**)	3.74 (t)	$CDCl_3$

[a] 2 −((dimethylamino)methyl)phenyl = L^{CN}

It can be seen that all compounds prepared within this work show signals in the expected region for (Ge)−H shifts. All signals reported here were all measured in nonpolar solvents including $CDCl_3$, CCl_4 or C_6D_6. Chemical shifts show with less than 0.2 ppm only little dependence of which nonpolar solvent was used. A qualitative comparison, categorizing the values for the proton shifts of arylgermanium hydrides listed in Table 2.2, is shown in Figure 2.15.

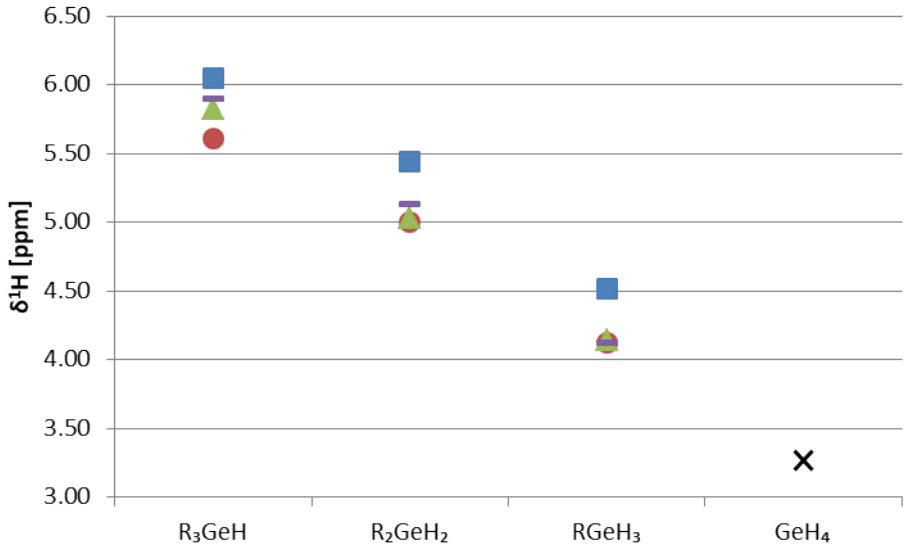

Figure 2.15.: ^{1}H (Ge)−H NMR shifts for selected novel and literature known aromatic germanium hydrides (red circles = phenyl; blue squares = L^{CN}; green triangles = 2,5 −xylyl; purple dashes = 2,6 −xylyl).

For the various compounds a nearly linear trend can be found with a downfield shift of about 0.9 ppm when exchanging an aryl group with a hydride functionality. Especially interesting is the downfield shift of hydrides bearing the 1-naphthyl residue compared to other residues, which was reported before, for mono- and dihydrides, by Wolf.[38] This deshielding is also found for the 1 −naphthylGeH_3 compound. Furthermore, the shift of L^{CN} compounds show distinct sensibility to the number of residues on the germanium center. With the shift is found only slightly downfield for $L^{CN}{}_3$GeH compared to other monohydrides, this difference is more pronounced for dihydrides and trihydrides, with

the same deshielding for $L^{CN}GeH_3$ as for $1-naphthylGeH_3$. This effect is hypothesized, due to increased probability of donation of electron density to the germanium center *via* the amine functionality in less sterically crowded germanium central atoms.

2.2.2. ^{73}Ge NMR spectroscopy

In the use of NMR spectroscopy as analysis technique for characterization and reaction control of group 14 element compounds, germanium shows a distinct exception (see Table 2.3). While ^{13}C is extensively used for characterization in organic synthesis, ^{29}Si and $^{117}Sn/^{119}Sn$ NMR spectroscopy is also widely used in the analysis of main group metal organics, with the advantage of gaining direct information of the central atom and its environment. For germanium, with its only NMR active isotope being ^{73}Ge[128], a spin $9/2$ nucleus with a large quadrupole moment, characterization by NMR is only rarely found in literature. Its high quadrupole moment also results in peak broadening if the germanium nucleus investigated is not symmetrically surrounded.

Despite the relative isotope abundance of ^{73}Ge is greater than respective ^{13}C or ^{29}Si, it lacks sensitivity due to is low gyromagnetic ratio, which is among the lowest in the periodic table of NMR active nuclei. This requires advanced instrumentation, where a special low-band probe is needed to measure ^{73}Ge NMR.[129] A major problem is also a baseline roll, due to acoustic ringing, which is especially problematic for broad lines. Thus, special pulse techniques like RIDE, PHASE or EXSPEC were applied for ^{73}Ge NMR analysis as well as proton polarization transfer sequences like INEPT.[130, 131]

Table 2.3.: NMR data for Group 14 elements.

Nucleus	**Nucleus spin**	**Gyromagnetic ratio** $[\cdot 10^7, rad \cdot s^{-1} \cdot T^{-1}]$	**Natural abundance** [%]	**Resonance frequency** [MHz][a]	**Relative sensitivity**[b]
^{13}C	1/2	6.725	1.11	125.7	1.00
^{29}Si	1/2	-5.314	4.67	99.3	2.10
^{73}Ge	9/2	-0.9332	7.76	17.4	0.62
^{119}Sn	1/2	-9.971	8.60	186.4	25.6
^{207}Pb	1/2	5.597	22.60	104.6	11.4

[a]Magnetic field of 11.74 T (^{1}H = 500 MHz)

[b]Sensitivity at natural abundance in a constant field (in reference to ^{13}C = 1.00).

The first developments in this field of research were made in the 1970s by the groups of Spinney and Schwenk and further progresses were made in the 1980s.[132, 133] Since the end of the 1990s, most advances were made in the field of solid state germanium NMR.[134–136] Over the years, due to the vast limitations, only a few hundred compounds analyzed using germanium NMR were published. Due to the limited size of the field, various comprehensive reviews have been published in the 1980s and recently by Takeuchi and Weinert in 2005 and 2012.[128, 129, 137, 138]

^{73}Ge NMR spectroscopy of arylgermanium hydrides

In literature, only a very limited number of arylgermanium compounds are characterized using ^{73}Ge NMR spectroscopy. This is owed to the sophisticated synthesis of such compounds and low molecular symmetry, which was thought to lead to broad resonances because of the 9/2 spin.[139] Nonetheless, surprisingly sharp signals were reported for various arylgermanes with aryl groups that cannot induce hypervalency.[39, 134] This is also true for the compounds measured within this thesis. As example the ^{73}Ge-NMR spectrum of 3,5 −xylylGeH$_3$ (**16**) is shown in Figure 2.16.

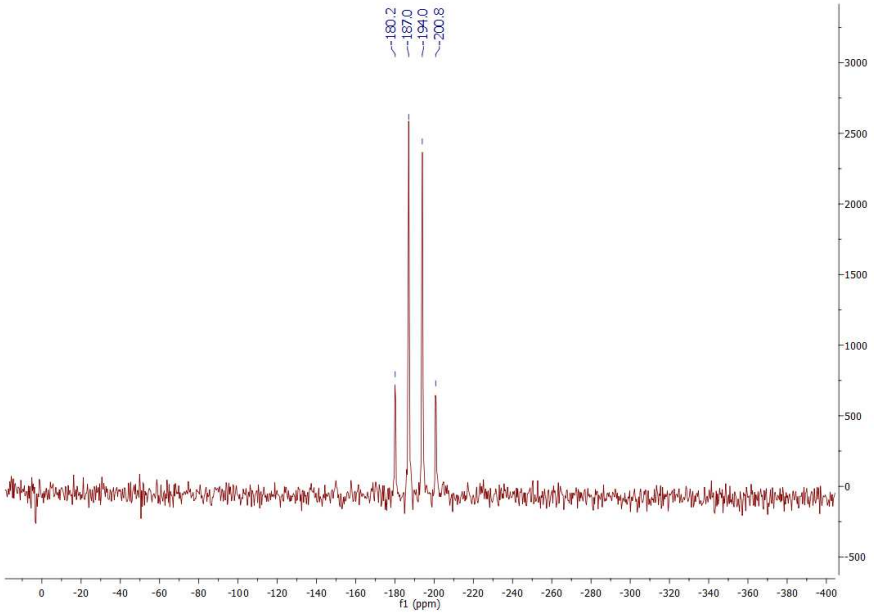

Figure 2.16.: Example ^{73}Ge NMR spectrum: 3,5 −xylylGeH$_3$ (**16**).

For most of the compounds the full width at half maximum is significantly lower than 100 Hz, allowing the determination of the *J*-coupling with the hydride protons (Table 2.4). For compounds bearing the L^{CN} residue, which allows for hypervalency, a significantly broader signal is detected. This results are in agreement with previously reported results, that hypervalency results in a large line broadening of signals in ^{73}Ge NMR spectroscopy in contrast to the upfield shift found for other group 14 organometallic compounds.[122, 134] When comparing the different xylyl compounds, it can be seen that also the residue symmetry has an effect on the signal width, since compounds with the unsymmetrically substituted xylyl residue (2,5 −xylyl) show broader signals than with symmetrically substituted xylyl residues (2,6 −xylyl, 3,5 −xylyl). Furthermore, also distinctively broader signals are detected with the 1 −naphthyl residue. In comparison to the peak widths, the magnitude of the dipolar coupling to the hydride protons shows neither dependence on the residue, nor on the number of hydride functionalities. Values are in the same magnitude as reported for literature known compounds. The coupling pattern shows a doublet for R$_3$GeH, a triplet for R$_2$GeH$_2$ and a quadruplet for RGeH$_3$ compounds.

A comprehensive list of δ^{73}Ge solution NMR shifts of arylhydrides is presented in Table 2.4 comparing the δ^{73}Ge chemical shifts of various literature known R_3GeH, R_2GeH_2 and $RGeH_3$ and the ^{73}Ge shifts of the products synthesized in our working group and measured in cooperation with Prof. Gudat at the University of Stuttgart. Spectral parameters are dependent on solvents. Thereof, all spectra prepared within this work were measured in toluene$-d_8$. Literature values have been recorded in different solvents, thus only approximate comparison is possible, even though it was reported previously, that shift ranges with solvent and concentration influences are within 5 ppm for δ^{73}Ge shifts.[137]

Table 2.4.: ^{73}Ge NMR shifts of arylgermanium hydrides prepared within this thesis and similar compounds in literature.

Compound	δ^{73}**Ge** [ppm]	^{1}**J(**^{73}**Ge**$-^{1}$**H)** [Hz]	$\nu_{1/2}$ [Hz]	**Solvent**
GeH_4[137]	-299	97.6	1.1	Bu_2O
		R_3GeH		
phenyl$_3$GeH[134]	-56.0	98.6	87	$CDCl_3$
o$-$tolyl$_3$GeH[122]	-84	n/a	70	$CDCl_3$
o$-$(MeOCH$_2$)phenyl$_3$GeH[122]	-85	n/a	350	$CDCl_3$
o$-$(EtOCH$_2$)phenyl$_3$GeH[122]	-85	n/a	350	$CDCl_3$
o$-$(^{t}butylOCH$_2$)phenyl$_3$GeH[122]	-84	n/a	350	$CDCl_3$
o$-$(MeSCH$_2$)phenyl$_3$GeH[122]	-93	n/a	270	$CDCl_3$
L$^{CN}{}_3$GeH^a [122]	-89	n/a	900	$CDCl_3$
o$-$(MeOCH$_2$)phenyl$_2-$ *o*$-$(HOCH$_2$)phenylGeH[122]	-85	n/a	250	$CDCl_3$
3,5 $-$xylyl$_3$GeH (synthesis: [38])	-52.6	n/a	39	toluene$-d_8$
2,5 $-$xylyl$_3$GeH (synthesis: [38])	-80.2	n/a	52	toluene$-d_8$
2,6 $-$xylyl$_3$GeH (synthesis: [38])	-129.5	94	10	toluene$-d_8$

R_2GeH_2				
phenyl$_2$GeH$_2$[134]	-108.5	96.6	28	$CDCl_3$
$p-$(MeO)phenyl$_2$GeH$_2$[39]	-112.0	n/a	n/a	C_6D_6
$p-^n$butylphenyl$_2$GeH$_2$ (**22**)	-109.3	97	26	toluene$-d_8$
3,5 $-$xylyl$_2$GeH$_2$ (**23**)	-107.5	98	35	toluene$-d_8$
2,5 $-$xylyl$_2$GeH$_2$ (**26**)	-125.6	107(5)	41	toluene$-d_8$
2,6 $-$xylyl$_2$GeH$_2$ (**24**)	-185.4	95	14	toluene$-d_8$
1 $-$naphthyl$_2$GeH$_2$ (**25**)	-127.0	n/a	110	toluene$-d_8$
$L^{CN}{}_2GeH_2{}^a$ (**27**)	-118.9	n/a	320	toluene$-d_8$
$RGeH_3$				
phenylGeH$_3$[134]	-187.5	96.6	25	$CDCl_3$
$p-$(MeO)phenylGeH$_3$[39]	-189.9	97	n/a	C_6D_6
$p-$tolylGeH$_3$[39]	-190.6	96	n/a	C_6D_6
2,4,6 $-$mesitylGeH$_3$[39]	-234.3	95	n/a	C_6D_6
$p-^n$butylphenylGeH$_3$ (**15**)	-190.8	97	8	toluene$-d_8$
3,5 $-$xylylGeH$_3$ (**16**)	-195.3	96	7	toluene$-d_8$
2,5 $-$xylylGeH$_3$ (**17**)	-200.6	96	20	toluene$-d_8$
2,6 $-$xylylGeH$_3$ (**18**)	-237.5	97	3	toluene$-d_8$
1 $-$naphthylGeH$_3$ (**19**)	-197.9	98	40	toluene$-d_8$
$L^{CN}GeH_3{}^a$ (**21**)	-189.0	99	92	toluene$-d_8$
other compounds within this thesis				
benzylGeH$_3$ (**20**)	-180	95	12	toluene$-d_8$

^{a} 2 $-$((dimethylamino)methyl)phenyl = L^{CN}

When comparing the chemical shifts of Table 2.4 it can be observed that the substitution of an aryl group with a hydride moiety results in an upfield shift of the signal. This behavior can be found for literature known compounds, as well as for newly synthesized compounds.[134] Furthermore, the same upfieild shift dependent on the number oh hydride functionality was found for alkylgermanium hydrides.[137] Figure 2.17 shows the ^{73}Ge chemical shifts for selected arylgermanium compounds, categorized by the number of hydrides.

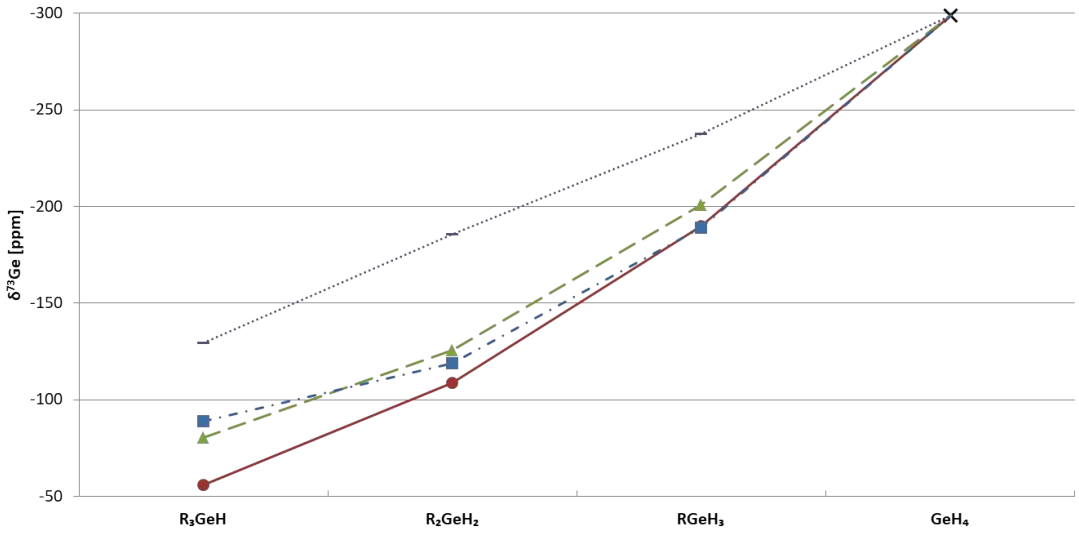

Figure 2.17.: ^{73}Ge shifts of selected arylgermanium hydrides (red circles = phenyl; blue squares = L^{CN}; green triangles = 2,5 −xylyl; purple dashes = 2,5 −xylyl).

It can be seen that within the categories, the chemical shifts range over nearly 80 ppm for arylgermanium mono- and dihydrides, and 40 ppm for trihydrides. Interestingly, this seems to be caused by the substitution pattern of the residue moiety in *ortho*-position. It can be seen that the introduction of one methyl group in *ortho*-position results in an upfield shift, which gets more pronounced when having methyl groups in both *ortho*-positions. Figure 2.18 shows this influence for various arylgermanium trihydrides. As shown, *para*-substituted residues (downfield category; red) show nearly the same chemical shift as phenylgermane. 3,5 −xylylGeH$_3$ (**16**) with its two methyl groups in *meta*-position shows only a slight deviation compared to the chemical shift of the phenyl derivative. The introduction of an increased aryl system in 1 −naphthylGeH$_3$ (**19**) or of a methyl group for 2,5 −xylylGeH$_3$ (**17**) in *ortho*-position shows in both cases a distinctive upfield shift (middle category; green). This shift is further pronounced when another methyl group occupies the second *ortho*-position as in a 2,6-substitution pattern found in compounds like 2,6 −xylylGeH$_3$ (**18**) or 2,4,6 −mesitylGeH$_3$ (upfield category; blue). The same behavior is also found for mono- and dihydride compounds.

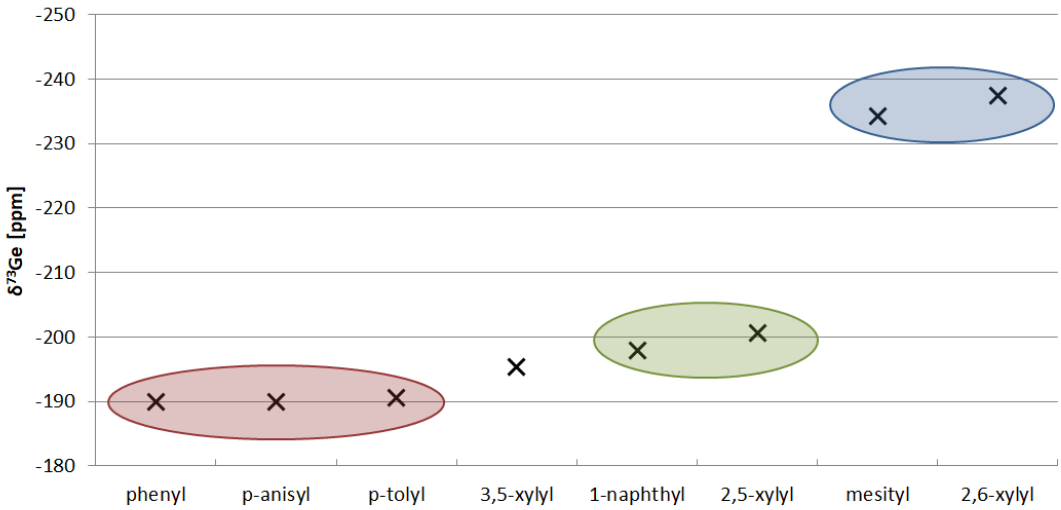

Figure 2.18.: Influence of substitution pattern of aryl residues in *ortho*-position on the ^{73}Ge shifts of arylgermanium trihydrides.

The only exception show compounds bearing the L^{CN} residue. Here the chemical shift is not changed by the $-CH_2N(CH_3)_2$ substituent. This off behavior may be caused by the hypervalency in the molecule, which could compensate the steric effect on the chemical shift. Nevertheless, it can be concluded, that the ^{73}Ge NMR shift is not only affected by the number of hydride residues, but also by the substitution pattern of the aryl residue itself. Despite all difficulties mentioned above, δ^{73}Ge NMR spectroscopy is a valuable tool for the determination of organogermanium hydride compounds.

2.3. X-ray crystallography

The elucidation of the crystal structure of novel compounds using single crystal X-ray crystallography is one of the most conclusive proof of the compounds prepared. Wolf presented various solid state structures of organogermanium compounds, including organogermanium dihydrides,[38] which were also prepared within this work *via* a different reaction route. Generally, arylgermanium hydride and halide compounds show presence of various non-covalent interactions in the solid state, like π-stacking of aromatic residues or Van der Waals interactions between halogenide moieties and adjacent hydrogen atoms, which result in a stabilization of the solid state structure and thus facilitate their crystallization. All organogermanium trihydrides prepared are liquids at room temperatures, and attempts to crystallize them at the diffractometer were unfortunately unsuccessful. Thus, organogermanium dichlorides and trichlorides are presented here, for 2,5 −xylyl, 2,6 −xylyl and 1 −naphthyl residues. Structural parameters are compared to literature known compounds and in addition, intermolecular interactions are determined and discussed with regard to the influence of the different residues on the solid state structure.

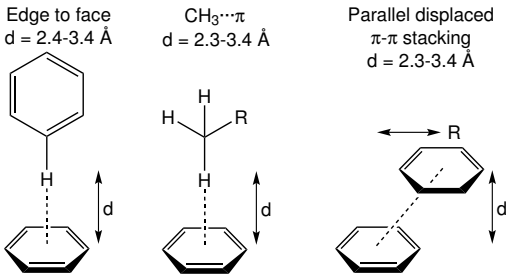

Figure 2.19.: Secondary electrostatic interactions possible with aromatic systems.

All compounds showing both Van der Waals interactions between the chloride substituent and adjacent hydrogen atoms (C−H· · ·Cl) and electrostatic interactions through their aromatic systems in the residues. Values for the distances of these interactions are presented and compared to literature values. Figure 2.19 shows types

of non-covalent secondary interactions with expected ranges.[140–144] Table A.4 in the appendix contains crystallographic data and details of measurements and refinement for compounds **8**, **9**, **10**, **12**, **13** and **14**.

2.3.1. Organogermanium trichlorides - $RGeCl_3$

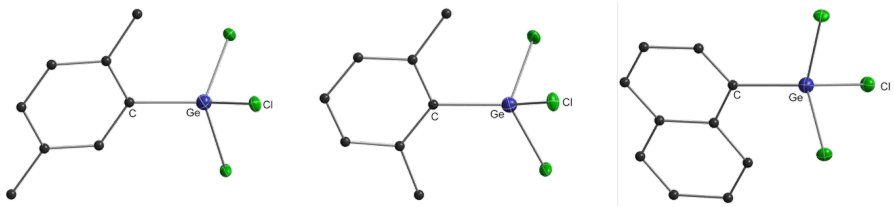

Figure 2.20.: Crystal structure of 2,5 −xylylGeCl$_3$ (**8**, left), 2,6 −xylylGeCl$_3$ (**9**, middle) and 1 −naphthylGeCl$_3$ (**10**, right). All non-carbon atoms shown as 30% shaded ellipsoids. Hydrogen atoms removed for clarity.

When comparing the Ge−C bond lengths of the organogermanium trichloride compounds, it becomes apparent that steric demand in *ortho*-position of the aromatic substituent results in an increased bond length with higher bulkiness. Both compounds which have one demanding group in *ortho*-position, 2,5 −xylylGeCl$_3$ (**8**) and 1 −naphthylGeCl$_3$ (**10**), show a bond length of 1.918(2) Å. This increases when introducing a second *ortho*-methyl group in 2,6 −xylylGeCl$_3$ (**9**). Furthermore, when introducing even bulkier groups in 2 and 6 positions like in the compounds prepared by Unno *et al.* or Johnson *et al.*, this effect becomes more pronounced with 1.970(2) Å for the 2,6 −(2,4,6 −^{i}propylphenyl)phenylGeCl$_3$.[145] In contrast to this, the Ge−Cl bond length is nearly similar for all compounds except the 2,6 −(2,4,6 −^{i}propylphenyl)−phenylGeCl$_3$. This could be a result of intramolecular interactions of the propyl groups of the residue and the chloride functionality. All compounds show a distorted tetrahedral arrangement around the germanium central atom with widened C−Ge−Cl angles of averaged 113.25(7)-115.51(8)° and and narrowed Cl−Ge−Cl angles of averaged 102.35(2)-105.47(2)°. Interestingly the largest distortion from tetrahedral sym-

metry shows not the sterically most demanding residue 2,6 −(2,4,6 −^{i}propylphenyl)−phenylGeCl$_3$, but 2,4,6 −^{t}butylphenylGeCl$_3$. It seems that especially the larger Ge−Cl bond distances in the bulkiest compound seem to facilitate less distortion of the bond angles.

Table 2.5.: List of selected bond lengths and angles for selected organogermnaium trichlorides.

	Space Group	**Ge−C (Å) (avg.)**	**Ge−Cl (Å) (avg.)**	**C−Ge−Cl (°) (avg.)**	**Cl−Ge−Cl (°) (avg.)**
2,5 −xylylGeCl$_3$ (**8**)	P2$_1$/m	1.918(2)	2.139(4)	113.37(3)	105.29(3)
2,6 −xylylGeCl$_3$ (**8**)	Pnma	1.935(3)	2.136(6)	114.49(4)	104.06(4)
1 −naphthylGeCl$_3$ (**10**)	Pbca	1.918(2)	2.138(3)	113.25(7)	105.47(2)
2,4,6 −^{t}butylphenylGeCl$_3$[126]	P2$_1$/n	1.944(4)	2.140(2)	115.51(8)	102.35(2)
2,6 −(2,4,6 −^{i}propylphenyl)phenylGeCl$_3$[145]	C222$_1$	1.970(2)	2.199(3)	114.43(7)	103.62(3)

Table 2.6.: List of non-covalent interactions for selected organogermanium trichlorides.

	$\pi-\pi$ **Stacking**		**Edge to face**	**CH$_3\cdots\pi$**	**C−H$\cdots$Cl**
	d	**R**			
2,5 −xylylGeCl$_3$ (**8**)	-	-	-	2.89	3.02-3.14
2,6 −xylylGeCl$_3$ (**9**)	-	-	-	3.23	3.03-3.25
1 −naphthylGeCl$_3$ (**10**)	3.76	0.77	2.816	-	2.81-3.14
2,4,6 −^{t}butylphenylGeCl$_3$[126]	-	-	-	-	-
2,6 −(2,4,6 −^{i}propylphenyl)phenylGeCl$_3$[145]	-	-	-	-	2.45-3.29

For all trichloride compounds synthesized within this work, non-covalent electrostatic interactions are found (Table 2.6), which results in the formation of ordered connectivity within the solid state structure of the molecules. All C−H$\cdots$Cl contacts of these compounds are between 2.81 and 3.25 Å, which are in the range of those interactions reported for 2,6 −(2,4,6 −^{i}propylphenyl)phenylGeCl$_3$ (2.45-3.29 Å). Notably, no secondary interactions were reported for the 2,4,6 −^{t}butylphenylGeCl$_3$ compound. 2,5 −xylylGeCl$_3$ (**8**) shows two CH$_3\cdots\pi$ interactions with an average distance of 2.89 Å, which results in the formation of a dimeric structure (Figure 2.21).

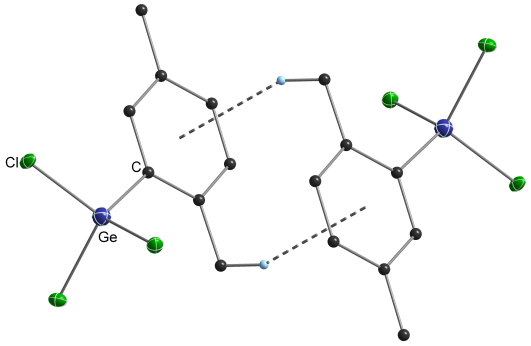

Figure 2.21.: Crystal packing diagram for 2,5 −xylylGeCl$_3$ (**8**). CH$_3$· · ·π interactions highlighted by dashed bonds. All non-carbon atoms shown as 30% shaded ellipsoids. C−H· · ·Cl contacts and hydrogen atoms not involved in intermolecular interactions removed for clarity.

In the solid state structure of 2,6 −xylylGeCl$_3$ (**9**) also CH$_3$· · ·π interactions are formed, but not pairwise interactions are gained. Each molecule forms interactions to four adjacent molecules, which results in the formation of a two dimensional sheet-like structure, where the organic residues are placed on the inside and the chloride on the outside, which themselves form C−H· · ·Cl contacts (Figure 2.22). Compared to the 2,5 −xylyl compound the CH$_3$· · ·π distances are increased to 3.23 Å, due to the interactions to various molecules.

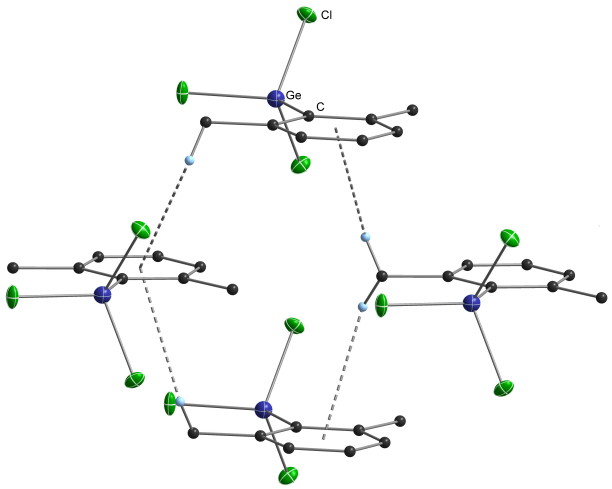

Figure 2.22.: Crystal packing diagram for 2,6 −xylylGeCl$_3$ (**9**). CH$_3$· · ·π interactions highlighted by dashed bonds. All non-carbon atoms shown as 30% shaded ellipsoids. C−H· · ·Cl contacts and hydrogen atoms not involved in intermolecular interactions removed for clarity.

As commonly observed for other 1 −naphthyl germanium compounds,1 −naphthylGeCl$_3$ (**10**) also displays close $\pi-\pi$-stacking between the naphthyl residues of adjacent molecules, which can be seen in Figure 2.23.[38] The distance between the π-systems is 3.76 Å with a small displacement of 0.77 Å. Furthermore, each molecule interacts *via* edge to face and C−H· · ·Cl contacts with other neighboring molecules, which results in a closely packed three dimensional network.

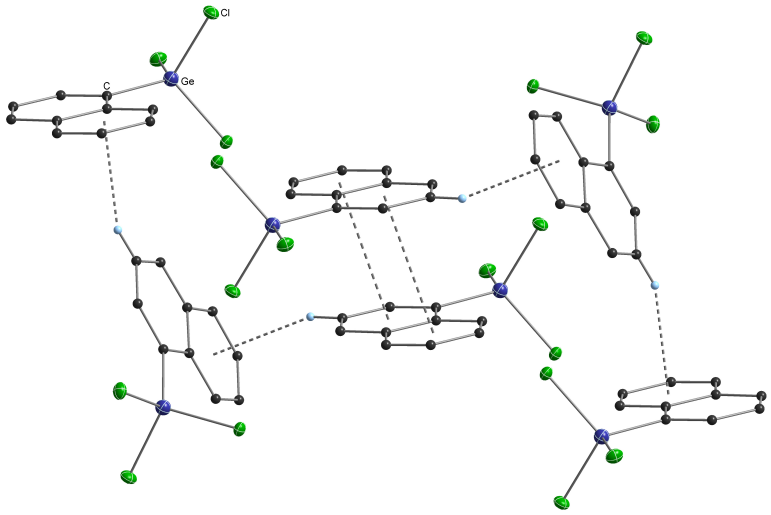

Figure 2.23.: Crystal packing diagram for 1 −naphthylGeCl$_3$ (**10**). π–π stacking and edge to face interactions highlighted by dashed bonds. All non-carbon atoms shown as 30% shaded ellipsoids. C−H· · ·Cl contacts and hydrogen atoms not involved in intermolecular interactions removed for clarity.

2.3.2. Organogermanium dichlorides - R_2GeCl_2

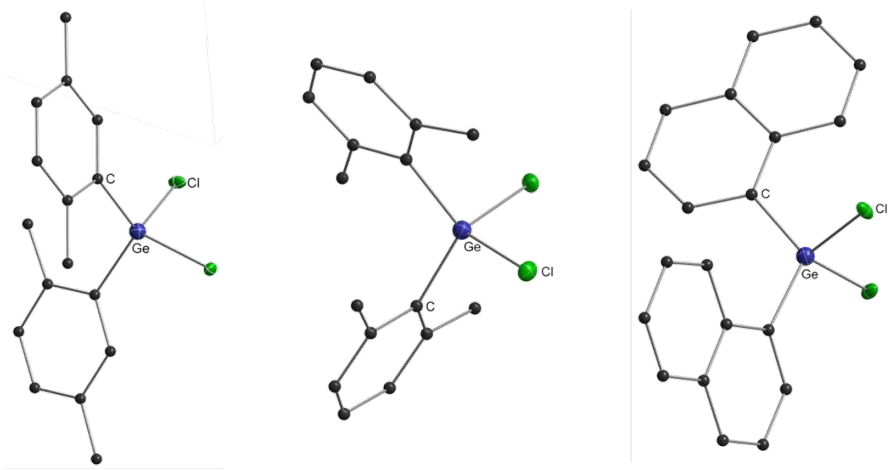

Figure 2.24.: Crystal structure of 2,5 −xylyl$_2$GeCl$_2$ (**12**, left), 2,6 −xylyl$_2$GeCl$_2$ (**13**, middle) and 1 −naphthyl$_2$GeCl$_2$ (**14**, right). All non-carbon atoms shown as 30% shaded ellipsoids. Hydrogen atoms removed for clarity.

The introduction of a second aryl residue results in an increase of the bond lengths of both Ge−C and Ge−Cl bonds in the solid state structures, compared to respective monoaryl compounds. The trend in Ge−C bond lengths with respect to steric demand in *ortho*-position can also be confirmed for organogermanium dichlorides, with an increased bond length of e.g. 1.948(2) Å in 2,6 −xylyl$_2$GeCl$_2$ (**13**). The tetrahedral arrangement in the molecules is further distorted by the second residue. C−Ge−C angles show a widening of average 115.41(8)-119.59(5)° and narrowed Cl−Ge−Cl angles of average 100.62(3)-105.12(15)°, whereas the C−Ge−Cl angles are only slightly distorted from the tetrahedron angle.

Table 2.7.: List of selected bond lengths and angles for selected organogermnaium dichlorides.

	Space Group	**Ge−C (Å) (avg.)**	**Ge−Cl (Å) (avg.)**	**C−Ge−C (°) (avg.)**	**Cl−Ge−Cl (°) (avg.)**	**C−Ge−Cl (°) (avg.)**
2,5 −xylyl$_2$GeCl$_2$ (**12**)	P2$_1$/c	1.934(3)	2.165(2)	118.63(4)	103.13(11)	108.49(3)
2,6 −xylyl$_2$GeCl$_2$ (**13**)	P-1	1.948(2)	2.169(7)	115.41(8)	100.62(3)	110.08(6)
1 −naphthyl$_2$GeCl$_2$ (**14**)	P2$_1$/n	1.928(2)	2.164(3)	119.59(5)	105.12(15)	107.79(3)

Table 2.8.: List of non-covalent interactions for selected organogermanium dichlorides.

	$\pi-\pi$ Stacking		Edge to face	$CH_3 \cdots \pi$	C−H···Cl
	d	R			
2,5 −xylyl$_2$GeCl$_2$ (**12**)	-	-	2.67	3.15-3.39	3.02-3.28
2,6 −xylyl$_2$GeCl$_2$ (**13**)	3.44	1.51	-	3.26-3.33	2.96-3.04
1 −naphthyl$_2$GeCl$_2$ (**14**)	3.52	1.68	2.98-3.29	-	3.03-3.25

The second residue moiety in the molecule promotes for all compounds further possibilities for interactions compared to the monoaryl trichlorides. In the extended solid state structure, 2,5 −xylyl$_2$GeCl$_2$ (**12**) crystallizes in a dense structure, propagated by edge to face interactions (2.67 Å) and $CH_3 \cdots \pi$ interactions (3.15-3.39 Å) in which all chloride molecules are turning away from the hydrocarbon residues (Figure 2.25). The chloride molecules itself engage C−H···Cl contacts of 3.02-3.28 Å.

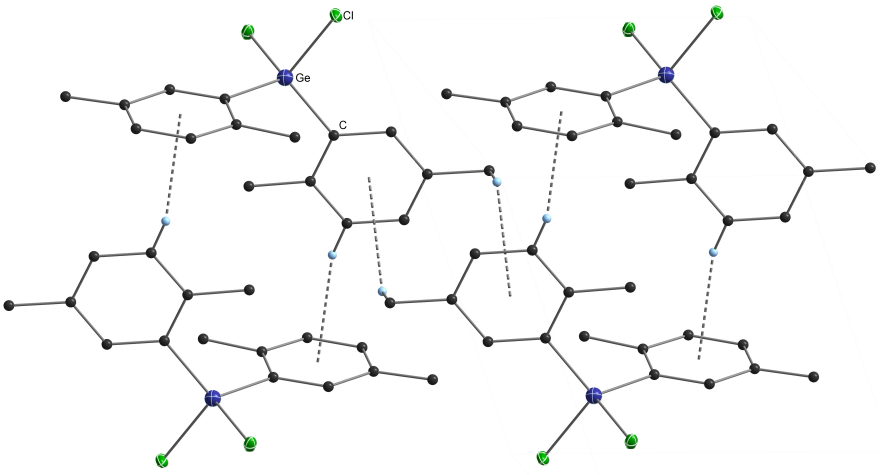

Figure 2.25.: Crystal packing diagram for 2,5 −xylyl$_2$GeCl$_2$ (**12**). $CH_3 \cdots \pi$ interactions highlighted by dashed bonds. All non-carbon atoms shown as 30% shaded ellipsoids. C−H···Cl contacts and hydrogen atoms not involved in intermolecular interactions removed for clarity.

2,6 −xylyl$_2$GeCl$_2$ (**13**) crystallizes in an infinite one dimensional chain structure of molecules, which is propagated by $\pi-\pi$-stacking (d = 3.44 Å; R = 1.51 Å) and $CH_3 \cdots \pi$ interactions (3.15-3.39 Å) between adjacent molecules (Figure 2.26). Moreover, chloride molecules are organized in this structure in a zigzag motif, where they

are alternating pointing in and out of the plane entering C−H· · ·Cl interactions with neighboring chains.

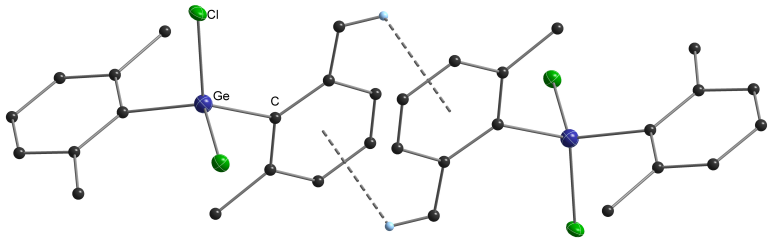

Figure 2.26.: Crystal packing diagram for 2,6 −xylyl$_2$GeCl$_2$ (**13**). CH$_3$· · ·π interactions highlighted by dashed bonds. All non-carbon atoms shown as 30% shaded ellipsoids. C−H· · ·Cl contacts and hydrogen atoms not involved in intermolecular interactions removed for clarity.

Similarly, the structure of 1 −naphthyl$_2$GeCl$_2$ (**14**) is also orientated in a linear extended solid state structure, where the naphthyl residues interact with neighboring molecules, by edge to face interactions (2.89-3.29 Å) and also $\pi-\pi$-stacking (d = 3.52 Å; R = 1.68 Å) (Figure 2.27). Compared to the respective trichloride, the stacking of the aromatic systems is closer, but with an increased dislocation. As found for the structure of 2,6 −xylyl$_2$GeCl$_2$ the chloride molecules are also arranged in the zigzag arrangement in and out of the plane.

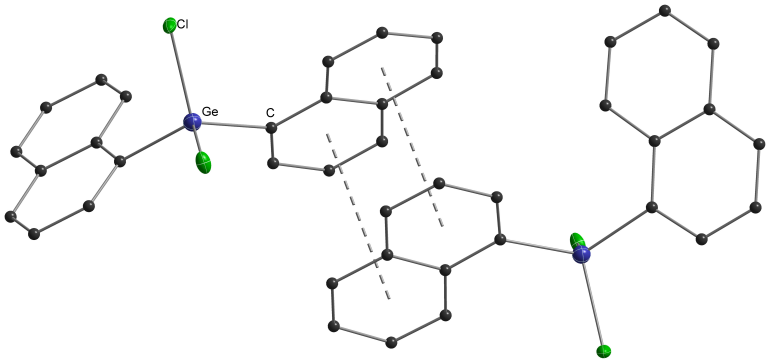

Figure 2.27.: Crystal packing diagram for 1 −naphthyl$_2$GeCl$_2$ (**14**). $\pi-\pi$ stacking interactions highlighted by dashed bonds. All non-carbon atoms shown as 30% shaded ellipsoids. C−H· · ·Cl contacts and hydrogen atoms not involved in intermolecular interactions removed for clarity.

2.3.3. ATR-IR spectroscopy

Infrared spectroscopy shows little to no use in the characterization of the organogermanium chlorides prepared within this work. Nevertheless, due to the characteristic Ge−H vibration, which can be observed using infrared spectroscopy, IR shifts were very important for the characterization of germanium hydrides. All shifts for the synthesized compounds show a Ge−H vibration in the very narrow range of 2067-2059 cm^{-1} for trihydrides and 2062-2044 cm^{-1} for dihydrides, which are in the expected ranges.[146] As an example, the spectrum of 2,5 −xylylGeH$_3$ is shown in Figure 2.28. Since the steric effect gets far less important in less crowded di- and trihydrides, shift ranges get narrower in comparison to monohydrides, making interpretation nearly impossible. Moreover, due to that, no trend seems to become apparent.

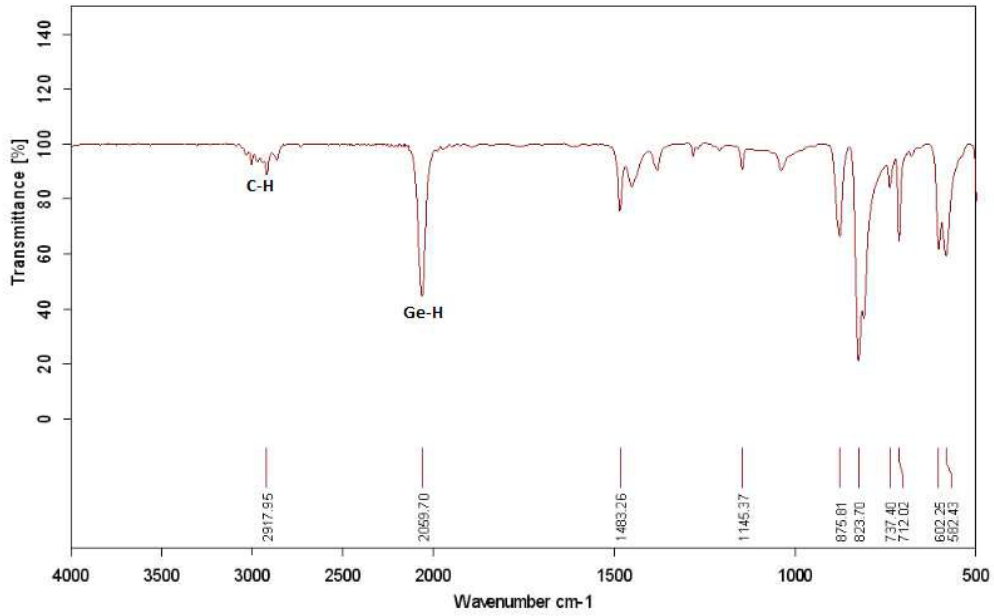

Figure 2.28.: Example ATR-IR spectrum: 2,5 −xylylGeH$_3$ (**17**).

Besides the distinct ν(Ge−H) vibration in the spectra of all compounds, signals with weak or medium intensity are found at 3100-2700 cm^{-1}, which can be attributed to aliphatic and/or aromatic C−H vibrations of the residue's protons (Figure 2.28).

2.3.4. Mass spectrometry

2.3.4.1. GCMS measurements

Since other analysis techniques like NMR are improper for reaction control for the synthesis of germanium organometallics, because they give too less information on mixtures, mass spectrometry has proven the most valuable characterization technique for reaction control in the synthesis of of organogermanium compounds. Coupled with gas chromatography, electron impact mass spectrometry (EI-MS) it shows not only product formation, but also product mixtures and is, in contrast to NMR spectroscopy, able to detect germanium routinely. Detailed information on the system used can be found in Section 4.1.2.

For the chromatography of the organogermanium compounds, it can be stated that retention time is decreased from diaryl- to monoarylgermanium compounds. Furthermore, halogenated species have a larger retention time than hydrides. For the halide mixtures which occur in the preparation of $RGeX_3$ and R_2GeX_2, the elution sequence is: $RGeCl_3$, $RGeCl_2Br$, $RGeClBr_2$, $RGeBr_3$, R_2GeCl_2, $R_2GeClBr$, R_2GeBr_2, R_3GeCl and R_3GeBr. This shows that the change from chloride to bromide does not affect the retention time as much as the substitution by an aryl residue. In the mass spectra, all compounds show a broad peak fingerprint of the molecular peaks, due to the different germanium isotopes. The highest peak was assigned as the peak for the most abundant molecular ion. Table 2.9 shows the different isotopes for the elements occurring in the molecules prepared with corresponding natural isotope abundance. The isotope pattern is nearly not influenced by the isotopes of hydrogen. Peak fingerprints are mainly dominated by the germanium pattern. This pattern is overlapped, when halides are present, which is easy to detect because of the special peak pattern which reflects their natural abundance. The presence of a nitrogen atom in the $L^{CN}GeH_3$ is proven by an odd molecular ion.

Table 2.9.: Isotopes and their abundance of Ge, C, H, Cl, Br and N.[2]

Element	Isotope mass	Abundance	Element	Isotope mass	Abundance
Ge	70	20.5%	C	12	98.9%
	72	27.4%		13	1.10%
	73	7.8%	H	1	99.9855%
	74	36.5%		2	0.0155%
Cl	35	75.77%	Br	79	50.69%
	37	24.23%		81	49.31%
N	14	99.634%			
	15	0.366%			

The fragmentation pattern within the electron impact (EI) ionization shows two main different fragmentation pathways for halide compounds, which occur by loss of aryl or halide in the primary step, which is in accordance with literature.[147] In hydride species, only the latter or decomposition of the aryl residue and the germanium functionality is possible. Furthermore, cleavage of protons within ionization is commonly observed.

For organogermanium trichlorides, the molecular ion peak corresponds to a m/z of 283.9 for xylyl substituted compounds (**7**, **8** and **9**), to m/z of 311.9 for $p-^n$butylphenylGeCl$_3$ (**6**) and to m/z of 305.9 for 1 $-$naphthylGeCl$_3$(**10**). Arylgermanium dichlorides show their $M^{+\bullet}$ at 354.0 for 2,5 $-$xylyl$_2$GeCl$_2$ (**12**) and 2,6 $-$xylyl$_2$GeCl$_2$ (**13**), as well as 398.0 for 1 $-$naphthyl$_2$GeCl$_2$ (**14**). The $M^{+\bullet}$ signal for organogermanium trihydrides show their highest abundance at 180.0 for xylyl compounds (**7**, **8** and **9**), 165.0 for $p-^n$butylphenylGeH$_3$ (**15**), 201.0 for 1 $-$naphthylGeH$_3$ (**41**), 166.0 for the benzylGeH$_3$ (**20**) and with the only odd m/z value 211,0 the L^{CN}GeH$_3$ (**21**). Contrary for L$^{CN}{}_2$GeH$_2$ (**27**), an even m/z with 342.1 is observed, with already two hydrogens cleaved off. The m/z for $p-^n$butylphenyl$_2$GeH$_2$ (**22**) is 341.2 with one proton cleaved off. All xylyl$_2$GeH$_2$ **23**, **24** and **26**) show a m/z of 268.1, 1 $-$naphthyl$_2$GeH$_2$ (**42**) at 330.1.

2.3.4.2. HRMS measurements

Selected compounds were further characterized using high resolution mass spectrometry (**8**, **9**, **10**, **12**, **13**, **14**, **17**, **18** and **19**). Generally, spectra with the expected high mass accuracy are obtained for organogermanium di- and trichlorides (**8**, **9**, **10**, **12**, **13** and **14**) with a mass accuracy of lower than 5 ppm and the measured peak pattern matches the calculated isotope pattern. As an example, the calculated and measured spectra are shown for 1 −naphthylGeCl$_3$ (**10**) in Figure 2.29.

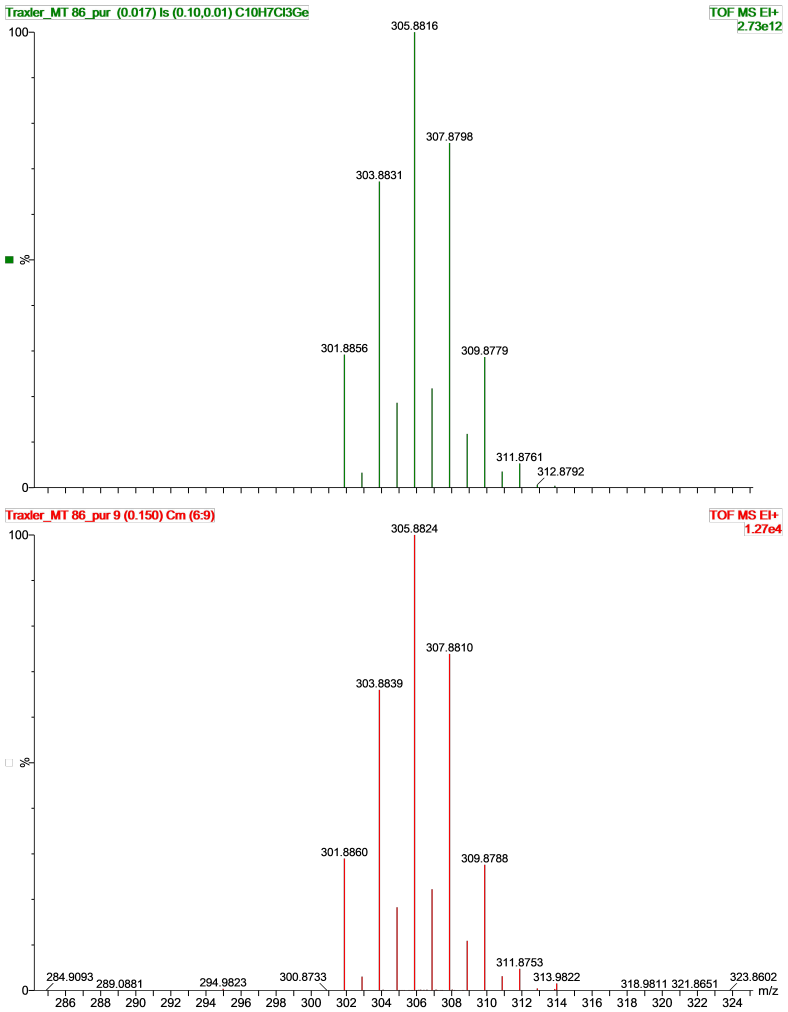

Figure 2.29.: Calculated (green; top) and measured (red; bottom) mass spectrum for the molecular ion of 1 −naphthylGeCl$_3$ (**10**).

In contrast to that, the measured trihydride compounds (**17**, **18** and **19**) defer from the calculated isotope pattern. This can be reasoned by the loss of hydrogen due to the harsh temperatures of the measurement conditions. Thus, the spectra is shifted to lower masses as demonstrated for the spectrum of 1 −naphthylGeH$_3$ (**19**; Figure 2.30) In addition, the mass determination is also less accurate.

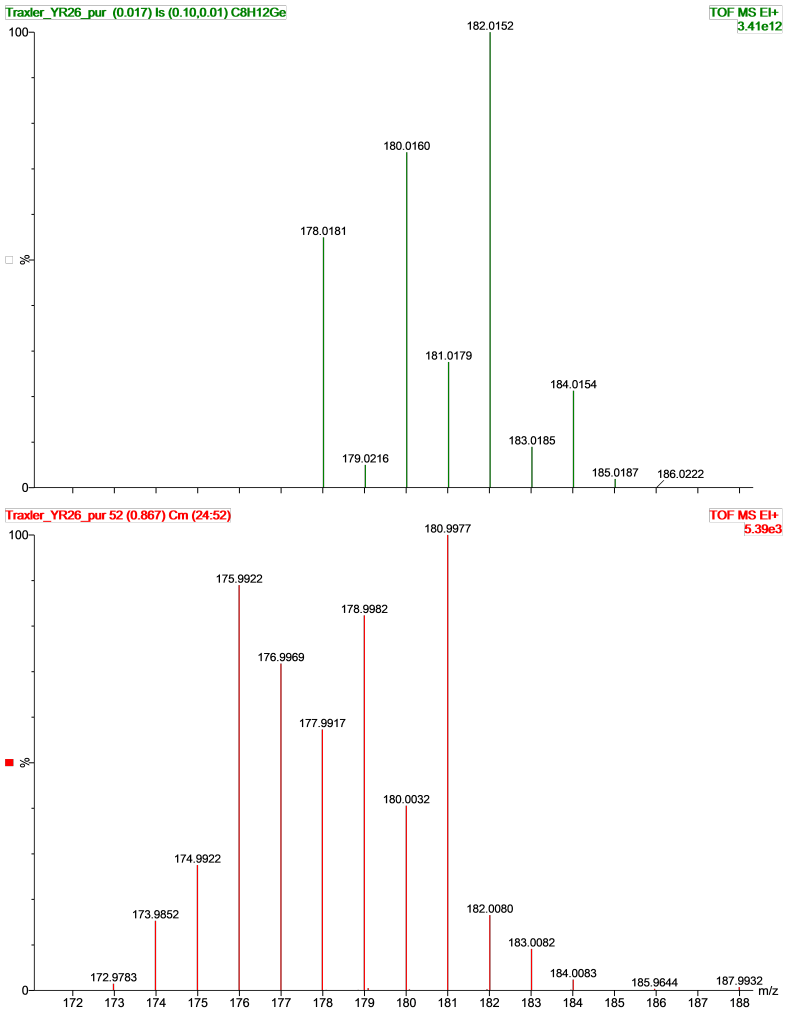

Figure 2.30.: Calculated (green; top) and measured (red; bottom) mass spectrum for the molecular ion of 1 −naphthylGeH$_3$ (**19**).

Detailed data on the most abundant molecular ion peak of the HRMS spectra for all measured compounds can be found in the experimental section.

2.4. Initial investigations on the polymerization of organogermanium trihydrides

2.4.1. Preparation of Ge@R nanoparticles

It was previously shown for higher Group 14 homologue tin that organotin trihydrides can undergo amine base catalyzed dehydrogenative coupling reactions upon the formation of aryl decorated nanoparticles, whereas *N,N,N',N'*−tetramethylethylenediamine (TMEDA) excelled as the most suitable catalyst.[58, 103, 104] Initial investigations were already performed by Wolf, showing formation of solids and loss of carbon and hydrogen content detected using elemental analysis.[38] Due to these initial results, the dehydrogenative coupling reaction of oranogermanium trihydrides is further investigated within this thesis.

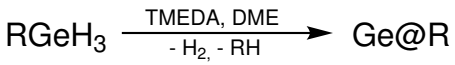

Figure 2.31.: Dehydrogenative coupling reaction of organogermanium trihydrides towards organometallic nanoparticles.

Initial experiments were tried using the reaction protocol used for tin derivatives, where the trihydrides are mixed with TMEDA and a solvent and the reaction proceeds within 20 minutes stirring at room temperature to give black a polymeric precipitate.[104] In contrast, when using organogermanium trihydrides, no precipitate was formed after 24h. At which point, the reaction was refluxed in toluene for 80h, which afforded a blurring of the reaction mixture and precipitate (Ge@2,5 −xylyl^{reflux,base}; **28**) was collected with very low yield. EDX-analysis confirmed presence of Ge and C in the material. Unfortunately, due to the low yield, no further analysis could be performed.

Thermal decomposition reactions were performed for 1 −naphthylGeH$_3$ (**19**) at around 220°C, which afforded formation of orange-brown solids in good yield. GCMS of the

pentane, with which the product was washed, showed cleaved naphthalene and traces of starting material. Elemental analysis showed a decrease in carbon content of 33% and of hydrogen content of 50%. These results show, that harsh reaction conditions are needed to perform the reaction in good yields.

Since base catalyzed reactions can not be performed at those high temperatures at ambient pressure, due to the boiling point of the TMEDA base being lower than the conversion temperature, reactions were performed as microwave assisted reactions. For those experiments, a 10 ml microwave vial was charged under inert conditions with the organogermanium trihydride and DME as solvent. To investigate the influence of the base, experiments were performed with and without TMEDA base. The reaction mixture was then heated in the synthesis microwave oven. Since no microwave oven with camera was available, systematic and controlled reactions conditions could not be developed. Nonetheless, certain trends can be proposed. Empirically, reactions starts at lower temperatures when TMEDA base is present in the reaction mixture, indicating that the reaction is indeed catalyzed. Furthermore, $1-$naphthylGeH$_3$ polymerizes already at lower temperatures than the $2,5-$xylylGeH$_3$ or benzylGeH$_3$. This can be reasoned due to naphthalene being the better leaving group. In all experiments, the pressure in the reaction vial increased within the progress of the experiment which was still present, when the reaction was cooled, which is due to the formation of gaseous elemental hydrogen.

GCMS of the liquid phase showed unreacted starting materials and aryl$-$H molecules. The presence of starting material after the reaction shows that the reaction, even at those harsh reaction conditions, is slow and once again confirms the higher stability of the germanium trihydrides, as compared to their tin homologues. On the other hand, reaction progress could be hindered, due to already high pressure inside the reaction vial because of the solvent. Elemental analysis of isolated precipitates also show loss of carbon and hydrogen in all experiments, compared to the starting trihydrides, confirming the loss of hydrogen and residue.

2.4.2. Characterization of Ge@R nanoparticles

Selected solid precipitates were further investigated with SEM, EDX, SAXS, GPC and MALDI-TOF mass spectrometry to get deeper insights on the size and morphology of the formed nanoparticles.

2.4.2.1. Secondary electron microscopy (SEM)

For the temperature induced amine catalyzed dehydrogenative coupling using reflux conditions (Ge@2,5 −xylyl$^{\text{reflux,base}}$, **28**), very distorted material was gained, consisting of irregular agglomerates (Figure 2.32 left). On the other hand, the material which was collected from the thermal decomposition reaction shows formation of a stacked plate like morphology (Figure 2.32 middle, right). This difference can be reasoned due to continuous distortion of the reaction mixture due to boiling and stirring, during the reflux reaction. The plate-like material formation shows similar morphology as organotin particles found by Reischauer for slow particle formation reactions.[104]

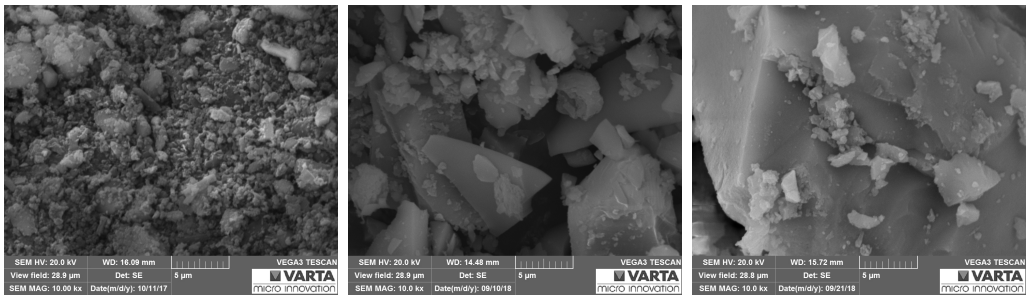

Figure 2.32.: SEM images of reflux and thermally induced dehydrogenative polymerized materials (left: Ge@2,5 −xylyl$^{\text{reflux,base}}$ (**28**); middle: Ge@1 −naphthyl$^{\text{T,base}}$ (**29**); right: Ge@1 −naphthyl$^{\text{T}}$ (**30**))

Compared to the reflux and thermal decomposition induced conversion, the material prepared *via* microwave induced reactions shows spherical morphology in μm range for the 2,5 −xylyl (Figure 2.33 left) and 1 −naphthyl (Figure 2.33 middle) residues.

In comparison to that, the conversion of $p-^{n}$butylphenylGeH$_3$ (Figure 2.33 right) led to a stacked plate-like material. The reason for this difference is the latter is soluble in the solvent used for the reaction and was isolated by evaporation of the solvent and could thus organize to its plate-like structure. For the other residues, the material precipitated during the reaction and was isolated by centrifugation. The sphere-like morphology is furthermore in agreement for the morphology found for fast reactions for the conversion of organotin trihydrides.[104]

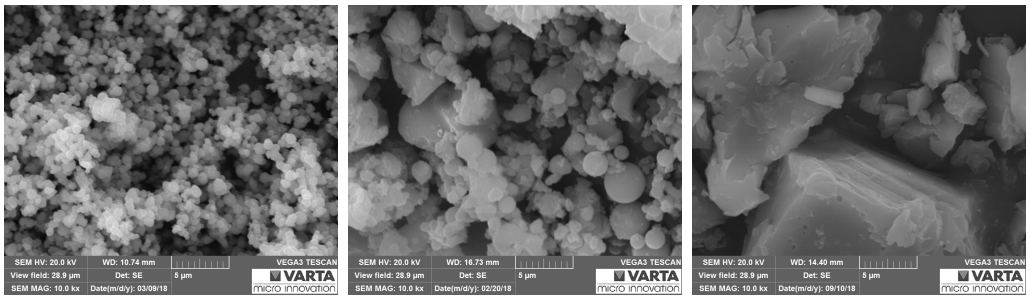

Figure 2.33.: SEM images of TMEDA catalyzed, microwave induced dehydrogenative polymerized materials (left: Ge@2,5 $-$xylyl$^{\text{micro,base,250°,10min}}$ (**32**); middle: Ge@1 $-$naphthyl$^{\text{micro,base,250°}}$ (**31**); right: Ge@benzyl$^{\text{micro,base,250°,3x5min}}$ (**36**))

First indications show that an increase of the reaction time changes the morphology towards more agglomerated particles, which could be reasoned due to a rearrangement of particles with increased reaction time.

2.4.2.2. Energy dispersive X-ray (EDX) analysis

EDX analysis was used to determine, the elemental composition of the prepared materials in a qualitative/semi-quantitative way. All samples consisted of germanium and carbon, with a reduced amount of carbon compared to the starting material, which again proves the cleavage of the organic groups within the conversion.

2.4.2.3. Small and wide angle X-ray scattering (S(W)AXS)

The gained solid polymeric material was further investigated using small and wide angle X-ray scattering (S(W)AXS). For this measurement the polymeric material was placed under inert gas conditions using a glove box into a sealable sample holder where the material is sandwiched between two polycarbonate foils. The gained correlation length q of the various prepared materials are in a very narrow range between 3.8 and 2.5 $1/\text{nm}$. Converting this values into real space, using the conversion $d = 2\pi \ / \ q$, gives reoccurring distances in the material, which reflect particle diameters d, of 1.7 - 2.5 nm. Although this range is very small it becomes apparent that the particles prepared with the benzyl residues d(Ge@benzyl$^{\text{micro,base,250°,3x5min}}$; **36**) = 1.7 nm are smaller than the one with the bigger naphthyl residue d = 2.0 - 2.5 nm. Figure 2.34 shows an example spectrum collected for Ge@1 $-$naphthyl$^{\text{micro,base,250°}}$ (**31**) with a correlation peak at 2.5 $1/\text{nm}$.

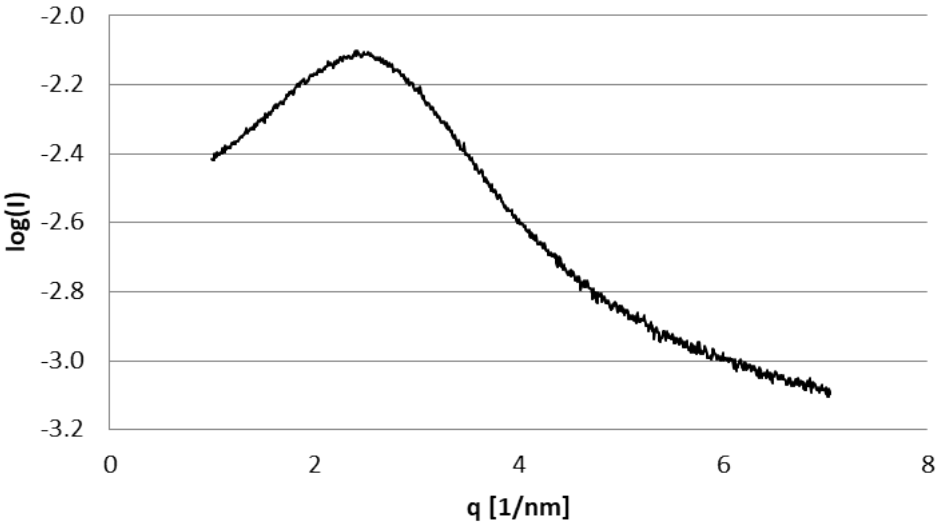

Figure 2.34.: Example SAXS spectrum: Ge@1 $-$naphthyl$^{\text{micro,base,250°}}$ (**31**).

Moreover, all prepared polymers did not generate any reflections in the WAXS area, which could be assigned to planes in a germanium(0) crystal structure.

2.4.2.4. Gel permeation chromatography (GPC)

The GPC analysis was performed for the partly dispersible particles. The hydrodynamic radius (R_h) of the particles was determined by the relation between the elution volume and the radius of the polystyrene samples used for calibration. For all samples, the hydrodynamic radius found was between 0.7 and 1.6 nm, which once again proves the formation of nanoparticles. The slightly bigger size compared to the SAXS analysis can be reasoned due to solvent molecules that can be incorporated into the organic shell of the particles. Base catalyzed microwave induced 1 −naphthyl decorated particles are with a radius of 1.6 nm bigger than respective benzyl particles (R_h = 1.2 nm). Although differences are only minor, it is apparent that particles prepared without the use of an amine base (TMEDA) are significantly smaller than the amine catalyzed one.

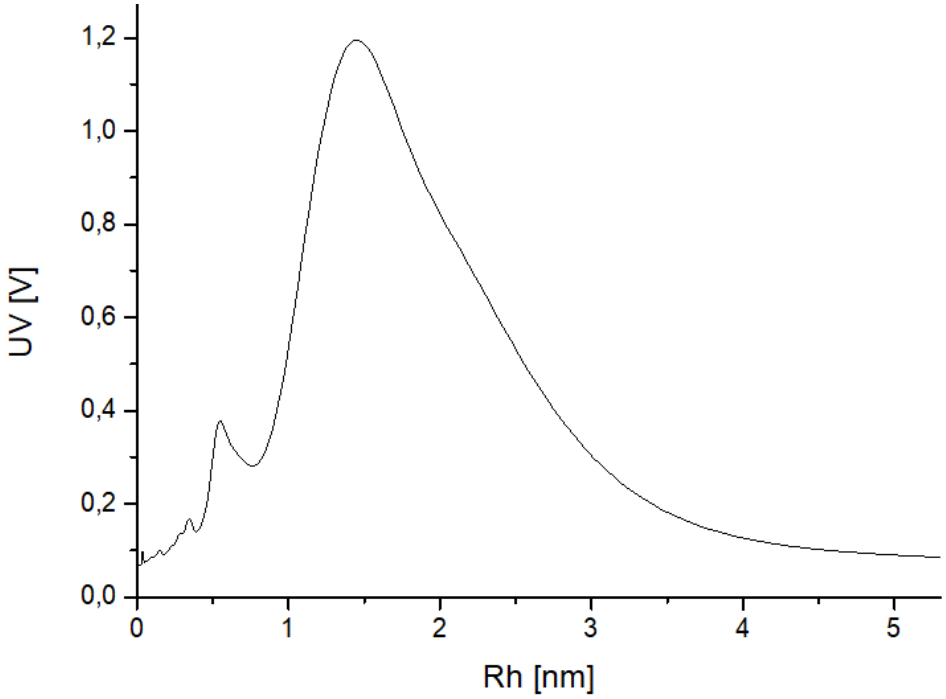

Figure 2.35.: Example GPC spectrum: Ge@1 −naphthyl$^{micro,base,250°}$ (**31**).

2.4.2.5. MALDI-TOF mass spectrometry

The particles prepared in the experiment with Ge@1 −naphthyl$^{micro,base,250°}$ (**31**) and Ge@benzyl$^{micro,base,250°,3x5min}$ (**36**) were further investigated using (MA)LDI-TOF mass spectrometry. The samples were investigated with DCTB as matrix and without matrix and showed for both the same results. Thus, it can be concluded that the samples are photoionizing. Both samples show in reflectron mode Ge clusters that are partly decorated with organic residues, which are ejected from the particles upon ionization using the laser energy. Figure 2.37 shows the measured spectrum versus calculated clusters of the 1 −naphthyl decorated particles, which are perfectly matching.

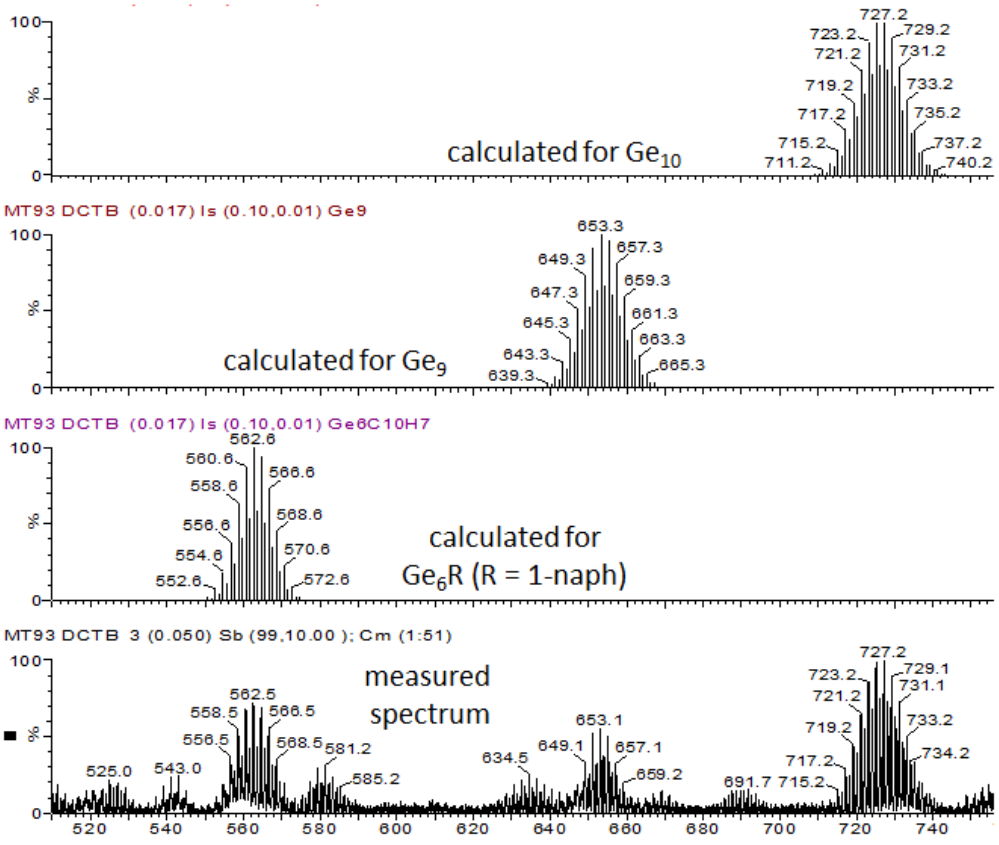

Figure 2.36.: MALDI-TOF spectrum in reflectron mode of Ge@1 −naphthyl$^{micro,base,250°}$ (**31**). Comparison of measured and calculated clusters.

In linear mode, respectively, the mass of the nanoparticles can be detected. For Ge@1 $-$naphthyl$^{micro,base,250^{\circ}}$ (**31**) particles, a peak in the mass range of 40-60 kDa is found, whereas the Ge@benzyl$^{micro,base,250^{\circ},3x5min}$ (**36**) particles show a peak at lower masses in the range of about 4-8 kDa. These results are also in agreement, with GPC and SAXS analysis, where the benzyl particles are as well smaller than respective naphthyl particles. Furthermore, what at first glance looks like noise in the peak maximum of the spectrum of the benzyl decorated particles in linear mode, shows actually peaks of particles with a mass difference of 72 Da, which reflects the addition of the mass of a germanium molecule.

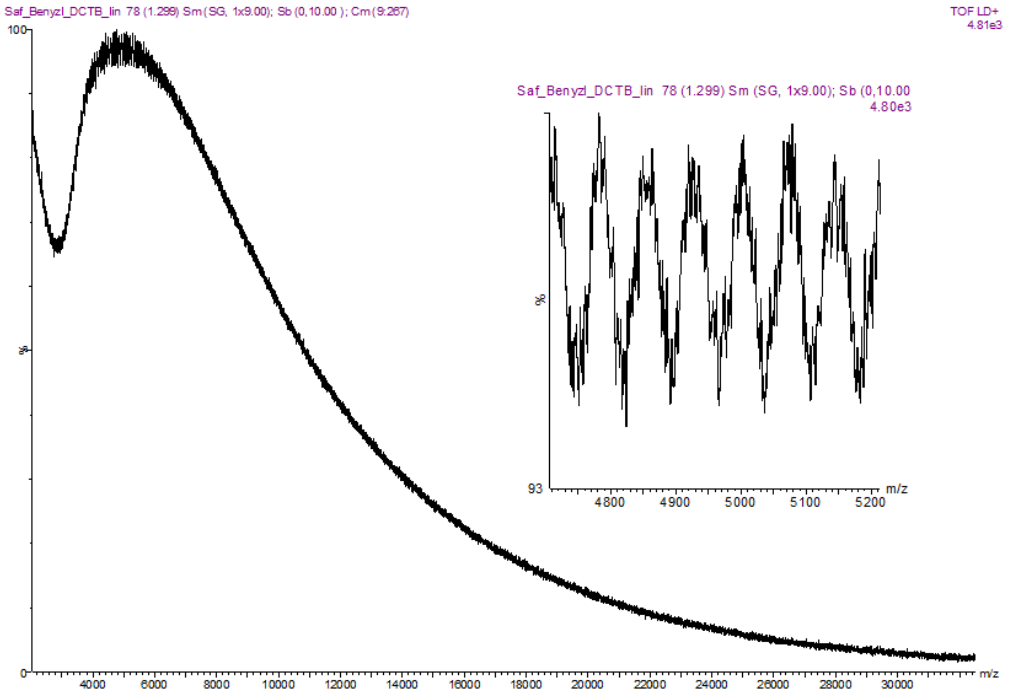

Figure 2.37.: MALDI-TOF spectrum in linear mode of Ge@benzyl$^{micro,base,250^{\circ},3x5min}$ (**36**).

3. Summary & outlook

Within the course of this master thesis various novel organogermanium hydrides and halides bearing aromatic residues have been synthesized using a high-yielding reaction route. The reaction procedure *via* the Grignard route, which shows inevitable formation of product mixtures, has been optimized towards organogermanium di- or trihalides, as desired. After hydrogenation using lithium aluminum hydride, sophisticated separation of the formed mixture of the different hydrides was needed, using their thermal behavior and their solubility in pentane. Using this optimized route, isolated yields of more than 70% were reached in the synthesis of organogermanium trihydrides. Additionally, this reaction, in contrast to other literature known routes towards such organogermanium compounds, can be scaled up to more than 10 g of product per experiment. All prepared compounds were fully characterized using various analysis techniques including ^{73}Ge NMR spectroscopy for organogermanium hydrides. Spectra showed peaks in the expected chemical shift range and showed surprisingly good resolution, even though the nucleus investigated shows unfavorable characteristics such as high nuclear spin or large quadrupolar momentum.

Subsequently, the behavior of the synthesized organogermanium trihydrides in a dehydrogenative coupling reaction towards a nanoparticular material was investigated. Performing the reaction at reflux conditions yielded in low product formation. However, when applying harsher reaction conditions, such as using microwave assisted synthesis, particular material is formed in higher yields. The collected solid material

was investigated using various techniques, which conclusively suggest particles in the range of 1-5 nm.

In future, efforts should be directed towards the synthesis of the nanoparticular materials using a reaction system with increased reaction control. For example, a microwave oven with a camera would be highly crucial to deeper investigate the particle formation or develop a reaction procedure. Furthermore, differences in residues could be investigated and compared to calculated bond stability values. In addition, thermal decomposition in an oven could also be a worthwhile alternative to the microwave synthesis.

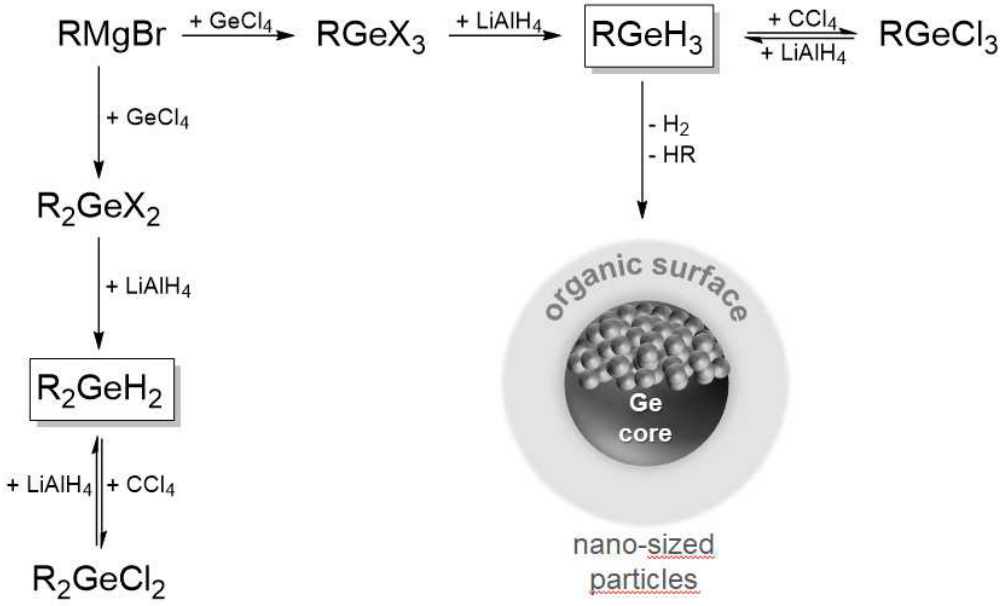

Figure 3.1.: Summary of the synthesis of organogermanium compounds and nanoparticles within this thesis.

Additionally, the results of the aminophenol based processing of germanium shows in Grignard conversion reactions selectivity towards organogermanium monochlorides, for residues bearing no substituent in *ortho*-position. Within this field of research, the focus should be directed towards the synthesis of $Ge(ap)_2$ from GeO_2 and the adaption of reaction conditions in the conversion to yield difunctional germanes.

4. Experimental

4.1. Materials, methods and analysis techniques

All reactions were performed using standard Schlenk line techniques or glove-box operated both under N_2 atmosphere. All solvents were dried and deoxygenated prior to usage. Toluene, pentane, diethyl ether, DME and THF were obtained from a solvent drying system (Innovative Technology Inc.). THF was further distilled over $LiAlH_4$. CCl_4 was dried over P_2O_5 and distilled prior usage. TMEDA (*N,N,N',N'*-tetramethylethylenediamine) was distilled over Na. $GeCl_4$ was purchased from abcr; $LiAlH_4$ was freshly grounded before addition. Benzylgermanium trichloride was purchased from abcr; $L^{CN}{}_2GeCl_2$ and $L^{CN}GeCl_3$ were prepared in the working group of Prof. Ruzicka at the University of Pardubice (Czech Republic) *via* lithiation route. All other chemicals were purchased from commercial sources and utilized without a further purification step. H_2SO_4 (95%) and HCl (32%) were diluted with deionized and degassed water. As filtration support was Celite® 512 used (average particle size 16.4 μm).

4.1.1. NMR spectroscopy

^1H (300.22 MHz) and ^{13}C (75.5 MHz) NMR spectra were recorded on a Mercury 300 MHz spectrometer from Varian at 25°C. ^{73}Ge (13.96 MHz) were measured on a Bruker

Avance 400 spectrometer at 30°C or, if no signal was detected at lower temperatures, at 70°C with the antiring pulse sequence "ARING". Chemical shifts are given in part per million (ppm) relative to TMS ($\delta = 0.00$ ppm) for ^{1}H and ^{13}C spectra and relative to trimethylgermane for ^{73}Ge. Coupling constants (J) and peak width ($\nu_{1/2}$) are reported in Hertz (Hz). ^{1}H and ^{13}C NMR spectra were recorded in $CDCl_3$ or C_6D_6; ^{73}Ge NMR spectra in toluene-d_8. The letters s, d, t, q, h and m are used for indication of singlet, doublet, triplet, quadruplet, quintet, sextet and multiplet.

4.1.2. GCMS measurements

GCMS measurements were performed on an Agilent Technologies 7890A GC system coupled to an Agilent Technologies 5975C VLMSD mass spectrometer using a HP5 column (30 m x 0.250 mm x 0.025 μm) and helium as a carrier gas with a flow of 0.92726 ml/min. A hot-needle manual injection method at an injector temperature of 280°C was used. The MS conditions used are positive EI ionization with an ionization energy of 70 eV and a full scan mode (50–500 m/z). The methods used within this Thesis are presented in the Appendix (Table A.2 and Table A.3).

4.1.3. HRMS measurements

High resolution mass spectroscopy was performed for selected samples on a Waters GCT Premier with direct insertion EI ionization at an energy of 70 eV and an ion source temperature of 200°C. Samples were prepared in THF with a concentration of 1 mg/ml. The data was interpreted using Masslynx software.

4.1.4. Crystal structure determination

All crystals suitable for single crystal X-ray diffractometry were removed from a vial or a Schlenk and immediately covered with a layer of silicone oil. A single crystal was selected, mounted on a glass rod on a copper pin, and placed in the cold N_2 stream provided by an Oxford Cryosystems cryostream. Single crystal X-ray diffraction data collection was performed for compounds **8**, **9**, **10**, **12**, **13** and **14**, on a Bruker APEX II diffractometer with use of an Incoatec microfocus sealed tube of Mo Kα radiation (λ= 0.71073 Å) and a CCD area detector. Empirical absorption corrections were applied using SADABS or TWINABS.[148, 149] The structures were solved with use of the intrinsic phasing option in SHELXT and refined by the full-matrix least-squares procedures in SHELXL.[150–152] The space group assignments and structural solutions were evaluated using PLATON.[153, 154] Non-hydrogen atoms were refined anisotropically. Hydrogen atoms were located in calculated positions corresponding to standard bond lengths and angles. In the case of **10**, anisotropic U^{ij}-values a naphthyl carbon atom were restrained (ISOR) to behave more isotropically. Electrostatic non-covalent intermolecular interactions[140–143] and van der Waals contacts (C-H$\cdot\cdot\cdot$Cl)[144, 155, 156] for presented and published compounds were based on a Cambridge Structural Database[157] search and fall within expected ranges. Centroids and planes were determined by features of the programs Mercury[158] and Diamond.[159] All crystal structures representations were made with the program Diamond. Table A.4 contains crystallographic data and details of measurements and refinement for compounds **8**, **9**, **10**, **12**, **13** and **14**.

4.1.5. S(W)AXS and measurements

Solid powder samples are transferred in the dry box into a sealable (by screw caps) sample holder (Anton Paar, Graz, Austria) where the sample is sandwiched (less than 1 mm) between two vacuum-tight sealing polycarbonate foils (100 μm each). Small-angle

(and wide-angle) X-ray scattering (S(W)AXS) measurements are carried at a laboratory SAXS instrument (SAXSpoint 2.0, Anton Paar, Austria) using point-collimated Cu-Kα radiation with wavelength of 0.154 nm from a micro-source and a Dectris EIGER2 R 500K area detector. SAXS and WAXS patterns were recorded by choosing a variable sample-to-detector distance in the range from 70 to 540 mm. All recorded 2D-SAXS patterns were azimuthally integrated in order to obtain the 1D-SAXS curves with the scattered intensities as a function of the scattering angle. Instead of the scattering angle 2Θ we used the magnitude of the scattering vector q, by applying the conversion $q\ [\ nm^{-1}\ ] = 4\pi(sin\Theta)/\lambda$ with 2Θ being the scattering angle with respect to the incident beam and λ the wavelength of the X-rays.

4.1.6. SEM measurements

Scanning electron microscopy (SEM) analysis was performed on a Vega 3 SBU SEM using a tungsten hairpin cathode for electron generation. All samples were sputtered with gold because of non-conductive samples. Qualitative composition analysis was performed by energy dispersive X-ray microanalysis (EDX) (Oxford Instruments, model INCA X-act).

4.1.7. GPC

Gel permeation chromatography (GPC) was carried out on a system provided by WGE Dr. Bures operated with THF (separating columns from MZ-Gel SD plus, linear 5μ; UV and RI detector SEC 3010). Poly(styrene) standards purchased from Polymer Standard Service were used for calibration.

4.1.8. MALDI-TOF mass spectroscopy

Matrix assisted laser desorption/ionisation (MALDI) time of fight mass spectrometry was performed on a Waters Micro MX (nitrogen laser, 337 nm; operated at 5 Hz). Positive ion spectra were recorded in reflectron as well as in linear mode. Typically the spectra from 100-150 laser shots were averaged and externally calibrated with a suitable mixture of poly(ethyleneglycol)s (PEG). Samples were prepared by mixing solutions of DCTB (*trans*–2–[3–(4–*tert*–butylphenyl)–2–methyl–2–propenylidene]malononitrile; c = 10 mg/ml in THF) and the analyte (c = 1 mg/ml in THF) in a ratio of 10:1 (v/v). 0.5 μl of the resulting mixture were deposited on the sample plate (stainless steel) and allowed to dry under air.

4.1.9. Complementary techniques

Microwave assisted reactions were performed in a microwave synthesis reactor Monowave 300 from Anton Paar using 10 ml reaction vials. Elemental analysis was performed on an Elementar vario MICRO cube by double determination. IR spectra were performed on a Bruker ALPHA FT-IR spectrometer charged with a platinum ATR diamond top. Melting point measurements were performed on a Stuart Scientific SMP 10 in threefold determination.

General considerations for reactions performed at the University of Western Ontario (Canada)

All reactions were carried out using flame dried apparatus under an inert atmosphere of argon using general Schlenk techniques or in an MBraun glovebox under an atmosphere of nitrogen, unless otherwise stated. All anhydrous solvents were collected from an Innovative Technology solvent purification system and dried over 4 Å molecular sieves. $GeCl_4$ was distilled over CaH_2. *t*-buNH$_2$ and pyridine were distilled prior usage. All reagents were purchased from Millipore Sigma or Alfa Aesar.

NMR spectra were acquired using a Varian INOVA I600 FT-NMR spectrometer or a Bruker AvIII HD 400 spectrometer. Chemical shifts are given in part per million (ppm) relative to TMS ($\delta = 0.00$ ppm) for ^{1}H and ^{13}C spectra. Electrospray ionization time of flight mass spectrometry was performed using the Bruker microOTOF 11 instrument in positive ion mode. Reaction mixtures were purified outside of the glovebox using preparative thin-layer chromatography on 20 x 20 cm plastic TLC plates consisting of silica gel coated with a fluorescent indicator and purchased from Millipore Sigma. GC-MS were obtained on a GCMS-QP2010S instrument with a GC-2010 gas chromatograph at an ionizing voltage of 70 eV and a DB-5MS 30 m x 0.25 μm column from J & W Scientific utilizing the following temperature program: 3 min at 65°C; 17 min constant heating rate of 15 °C / min; 5 min at 320 °C.

4.2. Synthesis

4.2.1. Germanium halides

4.2.1.1. Preparation of $RGeX_3$ (X = Cl, Br)

Organogermanium trihalide compounds ($RGeX_3$ (X = Cl, Br)) were prepared using the direct synthesis using the Grignard route with corresponding side products of R_2GeX_2 and R_3GeX. No pure halides were gained due to halogen-halogen exchange. Because of the presence of these mixtures, only semi-quantitative GCMS analysis was performed to determine the product distribution. The distribution is dependent on the solubility of respective compounds, solvent, concentration and GC-method, presenting distribution trends, but no exact values.

A flask equipped with a dropping funnel and a reflux condenser was charged with Mg and THF. The dropping funnel was charged with arylbromide in THF; about 10% of the solution was added to the reaction vessel and, in order to start the reaction, it

was carefully heated or dibromoethane was added. The arylbromide was subsequently added dropwise at reflux. After complete addition, the reaction was refluxed for about 3 hours. Residual Mg was filtered off using a filter cannula or a Schlenk-frit charged with Celite®. A flask was charged with germanium tetrachloride ($GeCl_4$) and THF. The Grignard solution was added dropwise at 0°C while stirring the solution. The reaction was allowed to warm up to room temperature and stirred for about 12 hours. After quenching with 10% degassed HCl at 0°C, the phases were separated and the organic layer was filtered of *via* a cannula; the watery layer was washed twice with THF. The organic layers were dried over Na_2SO_4. After removal of solvent under reduced pressure, the product was heated carefully with a heat gun under reduced pressure in order remove unreacted arylbromide and arylhydride formed by quenching the reaction. As product, an oily off white mixture of $RGeX_3$, R_2GeX_2 and R_3GeX compounds is gained.

p−^{n}butylphenylGeX$_3$ (1): 1.00 g (41.3 mmol, 1.22 eq.) Mg in 25 ml THF, 8.00 g (37.5 mmol, 1.11 eq.) 1-bromo−4-^{n}butylbenzene in 55 ml THF, 7.23 g (33.8 mmol, 1.00 eq.) $GeCl_4$ in 40 ml THF at 0°C; GCMS (Method 1): *p*−^{n}butylphenyl$GeCl_3$ (63%): t_R = 11.780 min, m/z: 311.9 ($M^{+\bullet}$), 268.9 ($M^{+\bullet}$ - C_3H_7), 125.0 ($M^{+\bullet}$ - $GeCl_2$, - C_3H_7), 91.0 ($M^{+\bullet}$ - $GeCl_3$, - C_3H_7); *p*−^{n}butylphenyl$GeCl_2Br$ (1%): t_R = 12.439 min, m/z: 355.9 ($M^{+\bullet}$), 312.8 ($M^{+\bullet}$ - C_3H_7), 277.0 ($M^{+\bullet}$ - Br), 125.0 ($M^{+\bullet}$ - GeClBr, - C_3H_7), 91.0 ($M^{+\bullet}$ - $GeCl_2Br$, - C_3H_7); *p*−^{n}butylphenyl$GeClBr_2$ (1%): t_R = 13.120 min, m/z: 401.9 ($M^{+\bullet}$), 358.8 ($M^{+\bullet}$ - C_3H_7), 320.9 ($M^{+\bullet}$ - Br), 125.0 ($M^{+\bullet}$ - GeBr2, - C_3H_7), 91.0 ($M^{+\bullet}$ - $GeClBr_2$, - C_3H_7); *p*−^{n}butylphenyl$GeBr_3$ (traces): t_R = 13.810 min, m/z: 445.9 ($M^{+\bullet}$), 402.7 ($M^{+\bullet}$ - C_3H_7), 336.9 ($M^{+\bullet}$ - Br, -C_2H_5), 91.0 ($M^{+\bullet}$ - $GeBr_3$, - C_3H_7); *p*−^{n}butylphenyl$_2GeCl_2$ (26%): t_R = 18.485 min, m/z: 410.1 ($M^{+\bullet}$), 367.1 ($M^{+\bullet}$ - C_3H_7), 277.1 ($M^{+\bullet}$ - *p*−^{n}butylphenyl, 125.0 ($M^{+\bullet}$ - GeCl, - *p*−^{n}butylphenyl, - C_3H_7), 91.0 ($M^{+\bullet}$ - $GeCl_2$, - *p*−^{n}butylphenyl, - C_3H_7); *p*−^{n}butylphenyl$_2$GeClBr (3%): t_R = 18.996 min, m/z: 454.0 ($M^{+\bullet}$), 375.1 ($M^{+\bullet}$ - C_3H_7), 180.0 ($M^{+\bullet}$ - *p*−^{n}butylphenyl, - Br, - Cl, -C_2H_5), 125.0 ($M^{+\bullet}$- GeBr, -

p−^{n}butylphenyl, - C_3H_7), 91.0 ($M^{+\bullet}$ - GeClBr, - *p*−^{n}butylphenyl, - C_3H_7); *p*−^{n}butylphenyl$_2$GeBr$_2$ (traces): t_R = 19.506 min, m/z: 500.0 ($M^{+\bullet}$), 180.0 ($M^{+\bullet}$ - *p*−^{n}butylphenyl, - Br_2, - C_2H_5), 91.0 ($M^{+\bullet}$ - $GeBr_2$, - *p*−^{n}butylphenyl, - C_3H_7); *p*−^{n}butylphenyl$_3$GeCl (6%): t_R = 23.195 min, m/z: 508.3 ($M^{+\bullet}$), 375.1 ($M^{+\bullet}$ - *p*−^{n}butylphenyl), 266.1 ($M^{+\bullet}$ - *p*−^{n}butylphenyl, - GeCl), 91.0 ($M^{+\bullet}$ - GeCl, - *p*−^{n}butylphenyl, -C_3H_7); *p*−^{n}butylphenyl$_3$GeBr (traces): t_R = 23.808 min, m/z: 552.2 ($M^{+\bullet}$), 473.3 ($M^{+\bullet}$ - Br), 419.1 ($M^{+\bullet}$ - *p*−^{n}butylphenyl), 207.0 ($M^{+\bullet}$ - Br, - *p*−^{n}butylphenyl$_2$), 91.0 ($M^{+\bullet}$ - GeBr, - *p*−^{n}butylphenyl$_2$, - C_3H_7);
Product distribution: *p*−^{n}butylphenylGeX$_3$:*p*−^{n}butylphenyl$_2$GeX$_2$:*p*−^{n}butylphenyl$_3$GeX = 62:26:6.

3,5 −xylylGeX$_3$ (**2**): 1.36 g (56.0 mmol, 1.23 eq.) Mg in 30 ml THF, 9.0 g (49 mmol, 1.11 eq.) 5 −bromo−*m*−xylene in 90 ml THF, 9.4 g (43.9 mmol, 1.00 eq.) $GeCl_4$ in 30 ml THF at 0°C; GCMS (Method 2): 3,5 −xylylGeCl$_3$ (60%): t_R = 10.202 min, m/z: 283.9 ($M^{+\bullet}$), 248.9 ($M^{+\bullet}$ - Cl), 105.1 ($M^{+\bullet}$ - GeCl$_3$); 3,5 −xylylGeCl$_2$Br (3%): t_R = 10.791 min, m/z: 327.9 ($M^{+\bullet}$), 248.9 ($M^{+\bullet}$ - Br), 105.0 ($M^{+\bullet}$ - GeCl$_2$Br); 3,5 −xylylGeClBr$_2$ (3%): t_R = 11.375 min, m/z: 373.8 ($M^{+\bullet}$), 292.9 ($M^{+\bullet}$ - Br), 105.0 ($M^{+\bullet}$ - GeClBr$_2$); 3,5 −xylylGeBr$_3$ (8%): t_R = 11.944 min, m/z: 417.8 ($M^{+\bullet}$), 336.9 ($M^{+\bullet}$ - Br), 105.0 ($M^{+\bullet}$ - GeBr$_3$); 3,5 −xylyl$_2$GeCl$_2$ (14%): t_R = 14.353 min, m/z: 354.1 ($M^{+\bullet}$), 319.1 ($M^{+\bullet}$ - Cl), 210.1 ($M^{+\bullet}$ - GeCl$_2$), 105.0 ($M^{+\bullet}$ - GeCl$_2$, - 3,5 −xylyl); 3,5 −xylyl$_2$GeClBr (8%): t_R = 14.721 min, m/z: 398.0 ($M^{+\bullet}$), 319.1 ($M^{+\bullet}$ - Br), 105.0 ($M^{+\bullet}$ - GeClBr, - 3,5 −xylyl); 3,5 −xylyl$_2$GeBr$_2$ (1%): t_R = 15.081 min, m/z: 442.0 ($M^{+\bullet}$), 363.0 ($M^{+\bullet}$ - Br), 105.0 ($M^{+\bullet}$ - GeBr$_2$, - 3,5 −xylyl); 3,5 −xylyl$_3$GeCl (2%): t_R = 16.723 min, m/z: 424.2 ($M^{+\bullet}$), 319.1 ($M^{+\bullet}$ - 3,5-xylyl), 210.1 ($M^{+\bullet}$ - 3,5 −xylyl, - GeCl), 105.0 ($M^{+\bullet}$ - GeCl, - 3,5 −xylyl$_2$); 3,5 −xylyl$_3$GeBr (1%): t_R = 17.117 min, m/z: 468.1 ($M^{+\bullet}$), 389.2 ($M^{+\bullet}$ - Br), 210.1 ($M^{+\bullet}$ - 3,5-xylyl, - GeBr), 105.0 ($M^{+\bullet}$ - GeBr, - 3,5 −xylyl$_2$);
Product distribution: 3,5 −xylylGeX$_3$:3,5 −xylyl$_2$GeX$_2$:3,5 −xylyl$_3$GeX = 74:23:3.

2,5 −xylylGeX$_3$ (**3**): 2.61 g (107 mmol, 1.22 eq.) Mg in 40 ml THF, 18.0 g (97.5

mmol, 1.11 eq.) 2 −bromo−*p*−xylene in 100 ml THF, 18.8 g (87.8 mmol, 1.00 eq.) $GeCl_4$ in 60 ml THF at 0°C; GCMS (Method 2): 2,5 −xylylGeCl_3 (65%): t_R = 9.891, 9.971, 10.027 min, m/z: 283.9 ($M^{+\bullet}$), 247.9 ($M^{+\bullet}$ - Cl), 104.1 ($M^{+\bullet}$ - GeCl_3); 2,5 −xylylGeCl_2Br (24%): t_R = 10.987 min, m/z: 327.9 ($M^{+\bullet}$), 291.9 ($M^{+\bullet}$ - Cl), 248.9 ($M^{+\bullet}$ - Br), 104.1 ($M^{+\bullet}$ - GeCl_2Br); 2,5 −xylylGeClBr$_2$ (3%): t_R = 10.987 min, m/z: 373.8 ($M^{+\bullet}$), 335.8 ($M^{+\bullet}$ - Cl), 292.9 ($M^{+\bullet}$ - Br), 105.0 ($M^{+\bullet}$ - GeClBr$_2$); 2,5 −xylylGeBr_3 (traces): t_R = 11.514 min, m/z: 417.7 ($M^{+\bullet}$), 336.8 ($M^{+\bullet}$ - Br), 105.0 ($M^{+\bullet}$ - GeBr_3); 2,5 −xylyl$_2$GeCl_2 (7%): t_R = 13.504 min, m/z: 354.1 ($M^{+\bullet}$), 318.0 ($M^{+\bullet}$ - Cl), 247.0 ($M^{+\bullet}$ - 2,5 −xylyl), 105.0 ($M^{+\bullet}$ - GeCl_2, - 2,5 −xylyl); 2,5 −xylyl$_2$GeClBr (1%): t_R = 13.860 min, m/z: 397.9 ($M^{+\bullet}$), 319.0 ($M^{+\bullet}$ - Br), 291.9 ($M^{+\bullet}$ - 2,5 −xylyl), 105.0 ($M^{+\bullet}$ - GeClBr, - 2,5 −xylyl);
Product distribution: 2,5 −xylylGeX_3:2,5 −xylyl$_2$GeX_2:2,5 −xylyl$_3$GeX = 92:8:traces.

2,6 −xylylGeX_3 (**4**): 2.62 g (108 mmol, 1.23 eq.) Mg in 30 ml THF, 18.0 g 97.5 mmol, 1.11 eq.) 2 −bromo−*m*−xylene in 100 ml THF, 18.8 g (87.8 mmol, 1.00 eq.) $GeCl_4$ in 40 ml THF at 0°C; GCMS (Method 1): 2,6 −xylylGeCl_3 (67%): t_R = 10.793, 10.912 min, m/z: 283.9 ($M^{+\bullet}$), 247.9 ($M^{+\bullet}$ - Cl), 104.1 ($M^{+\bullet}$ - GeCl_3); 2,6 −xylylGeCl_2Br (9%): t_R = 11.403, 11.594 min, m/z: 327.8 ($M^{+\bullet}$), 291.8 ($M^{+\bullet}$ - Cl), 104.0 ($M^{+\bullet}$ - GeCl_2Br); 2,6 −xylylGeClBr$_2$ (traces): t_R = 12.030, 12.296 min, m/z: 373.8 ($M^{+\bullet}$), 337.8 ($M^{+\bullet}$ - Cl), 292.9 ($M^{+\bullet}$ - Br), 104.0 ($M^{+\bullet}$ - GeClBr$_2$); 2,6 −xylyl$_2$GeCl_2 (19%): t_R = 15.881 min, m/z: 354.1 ($M^{+\bullet}$), 247.9 ($M^{+\bullet}$ - 2,6 −xylyl), 210.1 ($M^{+\bullet}$ - GeCl_2), 105.0 ($M^{+\bullet}$ - GeCl_2, - 2,6 −xylyl); 2,6 −xylyl$_2$GeClBr (4%): t_R = 14.721 min, m/z: 398.0 ($M^{+\bullet}$), 291.8 ($M^{+\bullet}$ - 2,6 −xylyl), 105.0 ($M^{+\bullet}$ - GeClBr, - 2,6 −xylyl);
Product distribution: 2,6 −xylylGeX_3:2,6 −xylyl$_2$GeX_2:2,6 −xylyl$_3$GeX = 76:23:traces.

1 −naphthylGeX_3 (**5**): 2.00 g (82.3 mmol, 1.22 eq.) Mg in 50 ml THF, 15.5 g (74.8 mmol, 1.11 eq.) 1 −bromo−naphthalene in 250 ml THF, 14.4 g (67.3 mmol, 1.00 eq.) $GeCl_4$ in 80 ml THF at 0°C; GCMS (Method 2): 1 −naphthylGeCl_3 (63%): t_R = 11.845, 11.915 min, m/z: 305.9 ($M^{+\bullet}$), 270.9 ($M^{+\bullet}$ - Cl), 127.1 ($M^{+\bullet}$ - GeCl_3); 1 −naphthylGeCl_2Br (26%): t_R = 12.362 min, m/z: 349.9 ($M^{+\bullet}$), 270.9 ($M^{+\bullet}$ - Br),

127.1 ($M^{+\bullet}$ - $GeCl_2Br$); 1 −naphthylGeClBr$_2$ (4%): t_R = 12.865 min, m/z: 395.8 ($M^{+\bullet}$), 316.9 ($M^{+\bullet}$ - Br), 127.1 ($M^{+\bullet}$ - $GeClBr_2$); 1 −naphthyl$_2$GeCl$_2$ (7%): t_R = 17.020 min, m/z: 398.0 ($M^{+\bullet}$), 362.0 ($M^{+\bullet}$ - Cl), 127.1 ($M^{+\bullet}$ - $GeCl_2$, - 1 −naphthyl); 1 −naphthyl$_2$GeClBr (traces): t_R = 17.593 min, m/z: 442.0 ($M^{+\bullet}$), 363.0 ($M^{+\bullet}$ - Br), 127.1 ($M^{+\bullet}$ - GeClBr, - 1 −naphthyl);
Product distribution: 1 −naphthylGeX$_3$:1 −naphthyl$_2$GeX$_2$:1 −naphthyl$_3$GeX = 93:7:traces.

4.2.1.2. Preparation of $RGeCl_3$

Chlorination of organogermanium trihydride compounds using CCl_4 and a palladium catalyst, gives pure compounds, which can be fully characterized.

A Schlenk was charged with $RGeH_3$ and freshly distilled CCl_4. After addition of catalytic amounts of a powder of elemental Pd on carbon, the reaction was refluxed. After filtration *via* cannula, the solvent was removed under *vacuo*.

p−^{n}butylphenylGeCl$_3$ (**6**): 0.58 g (2.8 mmol, 1.00 eq.) *p*−^{n}butylphenylGeH$_3$ (**15**) in 15 ml freshly distilled CCl_4, catalytic amounts of Pd, refluxed for 18 hours. A colorless oily liquid was gained. Yield: 84%. M.p.: $< 0^\circ$C. Elemental analysis (%) for $C_{10}H_{13}GeCl_3$: C, 38.47; H, 4.20. Found: C, 38.72; H, 4.03. ^{1}H NMR ($CDCl_3$, 300 MHz): δ 7.65 (d, 2H, 2,6 −H, ArH), 7.37 (d, 2H, 3,5 −H, ArH), 2.68 (t, 2H, C_αH), 1.62 (p, 2H, C_βH), 1.37 (h, 2H, C_γH), 0.94 (t, 3H, C_δH) ppm. ^{13}C NMR ($CDCl_3$, 75.5 MHz): δ 148.92, 132.13, 131.48, 129.68, 35.90, 33.41, 22.43, 14.03 ppm. GCMS (Method 1): t_R = 11.767 min, m/z: 311.9 ($M^{+\bullet}$), 268.9 ($M^{+\bullet}$ - C_3H_7), 125.0 ($M^{+\bullet}$ - $GeCl_2$, - C_3H_7), 91.0 ($M^{+\bullet}$ - $GeCl_3$, - C_3H_7).

3,5 −xylylGeCl$_3$ (**7**): 1.16 g (6.4 mmol, 1.00 eq.) 3,5 −xylylGeH$_3$ (**16**) in 15 ml freshly distilled CCl_4, catalytic amounts of Pd, refluxed for 20 hours. A colorless liquid was gained which solidified in the freezer. Yield: 86%. M.p.: $< 0^\circ$C. Elemental analysis (%) for $C_8H_9GeCl_3$: C, 33.82; H, 3.19. Found: C, 34.02; H, 3.13. ^{1}H NMR ($CDCl_3$,

300 MHz): δ 7.33 (s, 2H, 2,6 −H, ArH), 7.25 (s, 1H, 4-H, ArH), 2.40 (s, 6H, CH_3) ppm. ^{13}C NMR ($CDCl_3$, 75.5 MHz): δ 139.50, 134.96, 134.77, 128.88, 21.48 (CH_3) ppm. GCMS (Method 1): t_R = 10.211 min, m/z: 283.9 ($M^{+\bullet}$), 248.9 ($M^{+\bullet}$ - Cl), 105.1 ($M^{+\bullet}$ - $GeCl_3$), 77.1 ($M^{+\bullet}$ - $GeCl_3(CH_3)_2$).

2,5 −xylylGeCl$_3$ (**8**): 0.50 g (2.7 mmol, 1.00 eq.) 2,5 −xylylGeH$_3$ (**17**) in 20 ml freshly distilled CCl_4, catalytic amounts of Pd, refluxed for 16 hours. A colorless solid was gained which recrystallized when cooled down from melting point. Yield: 88%. M.p.: 61.9°C. Elemental analysis (%) for $C_8H_9GeCl_3$: C, 33.82; H, 3.19. Found: C, 33.90; H, 3.23. ^1H NMR (C_6D_6, 300 MHz): δ 7.45 (s, 1H, 6 −H, ArH), 6.77 (d, 1H, 3 −H, ArH), 6.68 (d, 1H, 4 −H, ArH), 2.34 (s, 3H, CH_3), 1.85 (s, 3H, CH_3) ppm; ($CDCl_3$, 300 MHz): δ 7.57 (s, 1H, 6 −H, ArH), 7.31 (d, 1H, 3 −H, ArH), 7.22 (d, 1H, 4 −H, ArH), 2.61 (s, 3H, CH_3), 2.38 (s, 3H, CH_3) ppm. ^{13}C NMR (C_6D_6, 75.5 MHz): δ 138.82, 136.22, 134.13, 133.53, 132.74, 131.62, 21.66 (CH_3), 21.03 (CH_3) ppm; ($CDCl_3$, 75.5 MHz): δ 138.92, 136.34, 134.12, 133.69, 132.88, 131.73, 21.50 (CH_3), 20.59 (CH_3) ppm. GCMS: (Method 2): t_R = 9.900 min, m/z: 283.9 ($M^{+\bullet}$), 247.9 ($M^{+\bullet}$ - Cl), 177.0 ($M^{+\bullet}$ - 2,5−xylyl), 104.1 ($M^{+\bullet}$ - $GeCl_3$), 77.1 ($M^{+\bullet}$ - $GeCl_3(CH_3)_2$). HRMS: Calcd. for $C_8H_9GeCl_3$: 283.8972, Found: 283.8977.

2,6 −xylylGeCl$_3$ (**9**): 0.44 g (2.4 mmol, 1.00 eq.) 2,6 −xylylGeH$_3$ (**18**) in 15 ml freshly distilled CCl_4, catalytic amounts of Pd, refluxed for 20 hours. A colorless solid was gained which recrystallized when cooled down from melting point. Yield: 90%. M.p.: 70.7°C. Elemental analysis (%) for $C_8H_9GeCl_3$: C, 33.82; H, 3.19. Found: C, 33.96; H, 3.11. ^1H NMR (C_6D_6, 300 MHz): δ 6.81 (t, 1H, 4 −H, ArH), 6.57 (d, 2H, 3,5 −H, ArH), 2.38 (s, 6H, CH_3) ppm; ($CDCl_3$, 300 MHz): δ 7.35 (t, 1H, 4 −H, ArH), 7.13 (d, 2H, 3,5 −H, ArH), 2.72 (s, 6H, CH_3) ppm. ^{13}C NMR ($CDCl_3$, 75.5 MHz): δ 142.78, 132.77, 130.00, 24.17 (CH_3) ppm. GCMS (Method 2): t_R = 10.245 min, m/z: 283.9 ($M^{+\bullet}$), 248.0 ($M^{+\bullet}$ - Cl), 176.9 ($M^{+\bullet}$ - 2,6 −xylyl), 104.1 ($M^{+\bullet}$ - $GeCl_3$), 77.1 ($M^{+\bullet}$ - $GeCl_3(CH_3)_2$). HRMS: Calcd. for $C_8H_9GeCl_3$: 283.8972, Found: 283.8976.

1 −naphthylGeCl$_3$ (10): 0.49 g (2.4 mmol, 1.00 eq.) 1 −naphthylGeH$_3$ (**19**) in 15 ml freshly distilled CCl_4, catalytic amounts of Pd, refluxed for 24 hours. The colorless solid was washed with pentane and could be recrystallized from toluene. Yield: 83%. M.p.: 70.9°C. Elemental analysis (%) for $C_{10}H_7GeCl_3$: C, 39.23; H, 2.30. Found: C, 41.54; H, 2.38. ^{1}H NMR ($CDCl_3$, 300 MHz): δ 8.27 (d, 1H, 8 −H, ArH), 8.10 (dd, 2H, 2,4 −H, ArH), 7.98 (d, 1H, 5 −H, ArH), 7.65 (m, 3H, ArH) ppm. ^{13}C NMR ($CDCl_3$, 75.5 MHz): δ 134.34, 134.21, 133.35, 132.91, 132.32, 129.46, 128.21, 127.24, 126.46, 125.08 ppm. GCMS (Method 2): t_R = 13.038 min, m/z: 305.9 ($M^{+\bullet}$), 270.9 ($M^{+\bullet}$ - Cl), 234.9 ($M^{+\bullet}$ - Cl_2), 199.0 ($M^{+\bullet}$ - Cl_3), 127.1 ($M^{+\bullet}$ - $GeCl_3$). HRMS: Calcd. for $C_{10}H_7GeCl_3$: 305.8816, Found: 305.8824.

4.2.1.3. Preparation of R_2GeX_2 (X = Cl, Br)

Organogermanium dihalide compounds ($RGeX_3$ (X = Cl, Br)) were prepared using the direct synthesis using the Grignard route with corresponding side products of $RGeX_3$ and R_3GeX. No pure halides were gained due to halogen-halogen exchange. Because of the presence of these mixtures, only semi-quantitative GCMS analysis was performed to determine the product distribution. The distribution is dependent on the solubility of respective compounds, solvent, concentration and GC-method, presenting distribution trends, but no exact values. Due to the fact that the desired products are mostly organogermanium trihydrides, the optimization towards R_2GeX_2 was only exemplary applied for the preparation of 2,5 −xylyl$_2$GeX$_2$.

A flask equipped with a dropping funnel and a reflux condenser was charged with Mg and Et_2O. The dropping funnel was charged with arylbromide in Et_2O; about 10% of the solution was added to the reaction vessel and, in order to start the reaction, it was carefully heated or dibromoethane was added. The arylbromide was subsequently added dropwise at reflux. After complete addition, the reaction was refluxed for about 3 hours. Residual Mg was filtered off using a filter cannula. A flask was charged with germanium

tetrachloride ($GeCl_4$) and Et_2O. The Grignard solution was added dropwise at 0°C while stirring the solution. The reaction was allowed to warm up to room temperature and stirred for about 12 hours. After quenching with 10% degassed HCl at 0°C, the phases were separated and the organic layer was filtered of *via* a cannula; the watery layer was washed twice with THF. The organic layers were dried over Na_2SO_4. After removal of solvent under reduced pressure, the product was heated carefully with a heat gun under reduced pressure in order to remove unreacted arylbromide and arylhydride formed by quenching. As product, an oily off white mixture of $RGeX_3$, R_2GeX_2 and R_3GeX compounds is gained.

2,5 −xylyl$_2$GeX$_2$ (11): 3.00 g (125 mmol, 2 eq) Mg in 40 ml Et_2O, 19.3 g (104 mmol, 1.67 eq.) 2-−bromo−*p*−xylene in 100 ml Et_2O, 13.4 g (62.5 mmol, 1 eq.) $GeCl_4$ in 60 ml Et_2O at 0°C; GCMS (Method 1): 2,5 −xylylGeCl$_3$ (1%): t_R = 10.510 min, m/z: 283.9 ($M^{+\bullet}$), 247.9 ($M^{+\bullet}$ - Cl), 104.1 ($M^{+\bullet}$ - $GeCl_3$); 2,5 −xylylGeCl$_2$Br (1%): t_R = 11.193 min, m/z: 327.9 ($M^{+\bullet}$), 291.9 ($M^{+\bullet}$ - Cl), 248.9 ($M^{+\bullet}$ - Br), 104.1 ($M^{+\bullet}$ - $GeCl_2Br$); 2,5 −xylylGeClBr$_2$ (1%): t_R = 11.871 min, m/z: 373.8 ($M^{+\bullet}$), 335.9 ($M^{+\bullet}$ - Cl), 292.9 ($M^{+\bullet}$ - Br), 105.1 ($M^{+\bullet}$ - $GeClBr_2$); 2,5 −xylylGeBr$_3$ (traces): t_R = 12.557 min, m/z: 417.8 ($M^{+\bullet}$), 336.8 ($M^{+\bullet}$ - Br), 105.1 ($M^{+\bullet}$ - $GeBr_3$); 2,5 −xylyl$_2$GeCl$_2$ (27%): t_R = 15.459 min, m/z: 354.0 ($M^{+\bullet}$), 318.1 ($M^{+\bullet}$ - Cl), 247.9 ($M^{+\bullet}$ - 2,5-xylyl), 210.1 ($M^{+\bullet}$ - $GeCl_2$), 104.1 ($M^{+\bullet}$ - $GeCl_2$, - 2,5 −xylyl); 2,5 −xylyl$_2$GeClBr (35%): t_R = 15.995 min, m/z: 398.0 ($M^{+\bullet}$), 362.0 ($M^{+\bullet}$ - Cl), 319.0 ($M^{+\bullet}$ - Br), 291.9 ($M^{+\bullet}$ - 2,5-xylyl), 104.1 ($M^{+\bullet}$ - GeClBr, - 2,5 −xylyl); 2,5 −xylyl$_2$GeBr$_2$ (23%): t_R = 16.533 min, m/z: 444.0 ($M^{+\bullet}$), 363.0 ($M^{+\bullet}$ - Br), 335.8 ($M^{+\bullet}$ - 2,5-xylyl), 104.1 ($M^{+\bullet}$ - $GeBr_2$, - 2,5 −xylyl); 2,5 −xylyl$_3$GeCl (6%): t_R = 18.417 min, m/z: 424.1 ($M^{+\bullet}$), 318.1 ($M^{+\bullet}$ - 2,5-xylyl), 209.1 (- 2,5 −xylyl, - GeCl), 105.1 ($M^{+\bullet}$ - GeCl, - 2,5 −xylyl$_2$); 2,5 −xylyl$_3$GeBr (5%): t_R = 18.917 min, m/z: 468.1 ($M^{+\bullet}$), 389.1 ($M^{+\bullet}$ - Br), 362.1 ($M^{+\bullet}$ - 2,5−xylyl), 105.1 ($M^{+\bullet}$ - GeBr, - 2,5 −xylyl$_2$); Product distribution: 2,5 −xylylGeX$_3$:2,5 −xylyl$_2$GeX$_2$:2,5 −xylyl$_3$GeX = 3:85:11.

4.2.1.4. Preparation of $RGeCl_3$

Chlorination of organogermanium dihydride compounds using CCl_4 and a palladium catalyst, gives pure compounds, which can be fully characterized.

A Schlenk was charged with R_2GeH_2 and freshly distilled CCl_4. After addition of catalytic amounts of a powder of elemental Pd on carbon, the reaction was refluxed. After filtration *via* cannula, the solvent was removed under *vacuo*.

2,5 −xylyl$_2$GeCl$_2$ (12): 0.64 g (2.3 mmol, 1.00 eq.) 2,5 −xylyl$_2$GeH$_2$ (**26**) in 15 ml freshly distilled CCl_4, catalytic amounts of Pd, refluxed for 22 hours. A colorless solid was gained which recrystallized when cooled down from melting point. Yield: 90%. M.p.: 127.6°C. Elemental analysis (%) for $C_{16}H_{18}GeCl_2$: C, 54.31; H, 5.13. Found: C, 54.23; H, 5.01. ^{1}H NMR (C_6D_6, 300 MHz): δ 7.92 (s, 2H, 6 −H, ArH), 6.89 (d, 2H, 3 −H, ArH), 6.79 (d, 2H, 4 −H, ArH), 2.26 (s, 6H, CH_3), 1.98 (s, 6H, CH_3) ppm; ($CDCl_3$, 300 MHz): δ 7.66 (s, 2H, 6 −H, ArH), 7.23 (d, 2H, 3 −H, ArH), 7.12 (d, 2H, 4 −H, ArH), 2.36 (s, 6H, CH_3), 2.31 (s, 6H, CH_3) ppm. ^{13}C NMR (C_6D_6, 75.5 MHz): δ 139.23, 136.29, 135.00, 133.98, 132.91, 131.14, 21.88 (CH_3), 20.80 (CH_3) ppm; ($CDCl_3$, 75.5 MHz): δ 139.04, 135.97, 134.44, 133.71, 132.78, 130.88, 21.95 (CH_3), 21.18 (CH_3) ppm. GCMS (Method 2): t_R = 13.503 min, m/z: 354.0 ($M^{+\bullet}$), 318.0 ($M^{+\bullet}$ - Cl), 281.1 ($M^{+\bullet}$ - Cl_2), 247.9 ($M^{+\bullet}$ - 2,5 −xylyl), 209.1 ($M^{+\bullet}$ - 2,5 −xylyl, - Cl) , 194.1 ($M^{+\bullet}$ - 2,5 −xylyl, - CH_3, - Cl) , 179.1 ($M^{+\bullet}$ - 2,5 −xylyl, -Cl_2), 104.1 ($M^{+\bullet}$ - 2,5 −xylyl, - $GeCl_2$), 77.1 ($M^{+\bullet}$ - 2,5 −xylyl, - $GeCl_2$, - $(CH_3)_2$). HRMS: Calcd. for $C_{16}H_{18}GeCl_2$: 353.9992, Found: 353.9996.

2,6 −xylyl$_2$GeCl$_2$ (13): 0.45 g (1.6 mmol, 1.00 eq.) 2,6 −xylyl$_2$GeH$_2$ (**26**) in 12 ml freshly distilled CCl_4, catalytic amounts of Pd, refluxed for 18 hours. A colorless solid was gained which could be recrystallized from toluene. Yield: 89%. M.p.: 98.6°C. Elemental analysis (%) for $C_{16}H_{18}GeCl_2$: C, 54.31; H, 5.13. Found: C, 55.10; H, 5.31. ^{1}H NMR (C_6D_6, 300 MHz): δ 6.93 (t, 2H, 4 −H, ArH), 6.71 (d, 4H, 3,5 −H, ArH), 2.45 (s, 12H, CH_3) ppm; (C_6D_6, 300 MHz): δ 7.25 (t, 2H, 4 −H, ArH), 7.04 (d, 4H,

3,5 −H, ArH), 2.53 (s, 12H, CH_3) ppm. ^{13}C NMR ($CDCl_3$, 75.5 MHz): δ 142.13, 138.12, 131.10, 129.56, 23.83 (CH_3) ppm. GCMS (Method 2): t_R = 13.809 min, m/z: 354.0 ($M^{+\bullet}$), 319.1 ($M^{+\bullet}$ - Cl), 247.9 ($M^{+\bullet}$ - 2,6 −xylyl, 210.2 ($M^{+\bullet}$ - 2,6 −xylyl, - Cl) , 195.1 ($M^{+\bullet}$ - 2,6 −xylyl, - CH_3, - Cl) , 179.1 ($M^{+\bullet}$ - 2,6 −xylyl, - Cl_2), 106.1 ($M^{+\bullet}$ - 2,6 −xylyl, - $GeCl_2$), 77.1 ($M^{+\bullet}$ - 2,6 −xylyl, - $GeCl_2$, - $(CH_3)_2$). HRMS: Calcd. for $C_{16}H_{18}GeCl_2$: 353.9992, Found: 354.0008.

1 −naphthyl$_2$GeCl$_2$ (**43**): 0.57 g (1.7 mmol, 1.00 eq.) 1 −naphthyl$_2$GeH$_2$ (**44**) in 12 ml freshly distilled CCl_4, catalytic amounts of Pd, refluxed for 16 hours. A colorless solid was gained which was washed with pentane and could then be recrystallized from toluene. Yield: 85%. M.p.: 165.9°C. Elemental analysis (%) for $C_{20}H_{14}GeCl_2$: C, 60.38; H, 3.55. Found: C, 61.69; H, 3.69. ^{1}H NMR ($CDCl_3$, 300 MHz): δ 8.10 (m, 6H, ArH), 7.93 (d, 2H, ArH), 7.52 (m, 6H, ArH) ppm. ^{13}C NMR ($CDCl_3$, 75.5 MHz): δ 134.74, 134.14, 133.80, 133.11, 132.93, 129.27, 127.42, 127.33, 126.70, 125.45 ppm. GCMS (Method 2): t_R = 13.503 min, m/z: 398.0 ($M^{+\bullet}$), 362.0 ($M^{+\bullet}$ - Cl), 253.1 ($M^{+\bullet}$ - $GeCl_2$), 127.1 ($M^{+\bullet}$ - $GeCl_2$, - 1 −naphthyl). HRMS: Calcd. for $C_{20}H_{14}GeCl_2$: 397.9680, Found: 397.9676.

4.2.2. Germanium hydrides

4.2.2.1. Preparation of RGeH$_3$

The trihydrides with R = 2,5 −xylyl and 2,6 −xylyl have previously been prepared by Wolf over another reaction route, but not fully characterized.[38] Organogermanium trihydrides prepared within this work were synthesized using two different reaction procedures, starting either from a mixture of halogenides (Route A; starting materials: **1**, **2**, **3**, **4** and **5**) or from pure the pure chloride derivative (Route B: starting materials benzylGeCl$_3$, L^{CN}GeCl$_3$). Due to the different reaction behavior of the L^{CN}-residue, a slightly different reaction procedure was applied compared to the benzyl residue (Route

B-1, Route B-2). All yields for Route A are given as overall yields including the Grignard conversion reaction and are calculated with respect to the germanium source $GeCl_4$.

Route A: To the mixture of $RGeX_3$ and R_2GeX_2 and R_3GeX (Compounds **1**, **2**, **3**, **4** and **5**) Et_2O was added and freshly grounded lithium aluminum hydride was slowly added as a powder at 0°C. The reaction was stirred 2 hours at 0°C and, after letting it warm up to room temperature, for another 30 minutes. The reaction was now quenched with 3% H_2SO_4 at 0°C, stirred for 10 minutes and then extracted with a saturated potassium tartrate solution. The phases were separated and the organic layer was filtered of *via* a cannula; the watery layer was washed twice with Et_2O. The combined organic layers were dried over Na_2SO_4. The solvent was removed under reduced pressure giving a mixture of $RGeH_3$, R_2GeH_2 and R_3GeH. The liquid $RGeH_3$ compound was then condensed into a Schlenk under reduced pressure giving a colorless liquid. For further purification the product could be subjected to a vacuum distillation.

p−^{n}butylphenylGeH$_3$ (**15**): 33.8 mmol (1.00 eq) *p*−^{n}butylphenyl$_{4-n}$GeX$_n$ (**1**) were suspended in 150 ml Et_2O and at 0°C 3.00 g (79.1 mmol, 2.3 eq.) lithium aluminum hydride added. Overall yield: 61%. Elemental analysis (%) for $C_{10}H_{16}Ge$: C, 57.51; H, 7.72. Found: C, 56.78; H, 7.23. ^{1}H NMR ($CDCl_3$, 300 MHz): δ 7.45 (d, 2H, ArH), 7.18 (d, 2H, ArH), 4.25 (s, 3H, Ge−H), 2.61 (t, 2H, C_αH), 1.60 (p, 2H, C_βH), 1.36 (h, 2H, C_γH), 0.93 (t, 3H, C_δH) ppm. ^{13}C NMR ($CDCl_3$, 75.5 MHz): δ 143.99, 135.52, 128.68, 127.84, 35.72, 33.73, 22.50, 14.10 ppm. ^{73}Ge NMR (toluene−d_8, 13.96 MHz): δ -190.8 ($^1J(^{73}Ge-^1H) = 97$ Hz; $\nu_{1/2} = 8$ Hz) ppm. ATR-IR: 2066.7 cm^{-1} (Ge−H). GCMS (Method 2): $t_R = 8.093$ min, m/z: 208.0 ($M^{+\bullet}$), 165.0 ($M^{+\bullet}$ - H_3, - C_3H_7), 150.9 ($M^{+\bullet}$ - H_3, - C_4H_9), 133.1 ($M^{+\bullet}$ - GeH_3), 105.1 ($M^{+\bullet}$ - GeH_3, - C_3H_5), 91.1 ($M^{+\bullet}$ - GeH_3, - C_3H_7).

3,5 −xylylGeH$_3$ (**16**): 43.9 mmol (1.00 eq.) 3,5 −xylyl$_{4-n}$GeX$_n$ (**2**) were suspended in 150 ml Et_2O and at 0°C 3.48 g (101 mmol, 2.3 eq.) lithium aluminum hydride added. Overall yield: 72%. Elemental analysis (%) for $C_8H_{12}Ge$: C, 53.14; H, 6.69. Found: C,

52.47; H, 6.25. ^{1}H NMR ($CDCl_3$, 300 MHz): δ 7.17 (s, 1H, 4 −H, ArH), 7.02 (s, 2H, 2,6 −H, ArH), 4.24 (s, 3H, Ge−H), 2.33 (s, 6H, CH_3) ppm. ^{13}C NMR ($CDCl_3$, 75.5 MHz): δ 137.87, 133.22, 130.94, 130.77, 21.37 (CH_3) ppm. ^{73}Ge NMR (toluene−d_8, 13.96 MHz): δ -195.3 ($^{1}J(^{73}Ge-^{1}H) = 96$ Hz; $\nu_{1/2} = 7$ Hz) ppm. ATR-IR: 2064.3 cm^{-1} (Ge−H). GCMS (Method 2): $t_R = 6.506$ min, m/z: 180.0 ($M^{+\bullet}$), 165.0 ($M^{+\bullet}$ - CH_3), 150.9 ($M^{+\bullet}$ - $(CH_3)_2$), 107.1 ($M^{+\bullet}$ - GeH_3), 91.1 ($M^{+\bullet}$ - GeH_3, - CH_3), 77.1 ($M^{+\bullet}$ - GeH_3, - $(CH_3)_2$).

2,5 −xylylGeH$_3$ (**17**): 87.8 mmol (1.00 eq.) 2,5 −xylyl$_{4-n}$GeX$_n$ (**3**) were suspended in 150 ml Et_2O and at 0°C 5.00 g (132 mmol, 1.5 eq.) lithium aluminum hydride added. Overall yield: 72%. B.p.: 45°C at 5 mbar. Elemental analysis (%) for $C_8H_{12}Ge$: C, 53.14; H, 6.69. Found: C, 52.47; H, 6.25. ^{1}H NMR (C_6D_6, 300 MHz): δ 7.25 (s, 1H, 6 −H, ArH), 6.94 (d, 2H, 3,4 −H, ArH), 4.26 (s, 3H, Ge−H), 2.19 (s, 3H, CH_3), 2.08 (s, 3H, CH_3) ppm; ($CDCl_3$, 300 MHz): δ 7.23 (s, 1H, 6 −H, ArH), 7.00 (d, 2H, 3,4 −H, ArH), 4.14 (s, 3H, Ge−H), 2.27 (s, 3H, CH_3), 2.21 (s, 3H, CH_3) ppm. ^{13}C NMR (C_6D_6, 75.5 MHz): δ 140.00, 137.15, 134.55, 130.96, 130.30, 129.14, 22.31 (CH_3), 20.41 (CH_3) ppm; ($CDCl_3$, 75.5 MHz): δ 140.45, 137.37, 134.98, 131.59, 130.53, 129.40, 22.85 (CH_3), 21.02 (CH_3) ppm. ^{73}Ge NMR (toluene−d_8, 13.96 MHz): δ -200.6 ($^{1}J(^{73}Ge-^{1}H) = 96$ Hz; $\nu_{1/2} = 20$ Hz) ppm. ATR-IR: 2059.7 cm^{-1} (Ge−H). GCMS (Method 2): $t_R = 6.815$ min, m/z: 180.0 ($M^{+\bullet}$), 165.0 ($M^{+\bullet}$ - CH_3), 151.0 ($M^{+\bullet}$ - $(CH_3)_2$), 105.1 ($M^{+\bullet}$ - GeH_3), 91.1 ($M^{+\bullet}$ - GeH_3, - CH_3), 77.1 ($M^{+\bullet}$ - GeH_3, - $(CH_3)_2$). HRMS: Calcd. for $C_8H_{12}Ge$: 182.0152, Found: 180.0085 ($M^{+\bullet}$ - 2 H).

2,6 −xylylGeH$_3$ (**18**): 87.8 mmol (1.00 eq.) 2,6 −xylyl$_{4-n}$GeX$_n$ (**4**) were suspended in 250 ml Et_2O and at 0°C 5.00 g (132 mmol, 1.5 eq.) lithium aluminum hydride added. Overall yield: 71%. B.p.: 39°C at 4 mbar. Elemental analysis (%) for $C_8H_{12}Ge$: C, 53.14; H, 6.69. Found: C, 52.47; H, 6.25. ^{1}H NMR (C_6D_6, 300 MHz): δ 6.98 (t, 1H, 4 −H, ArH), 6.86 (d, 2H, 3,5 −H, ArH), 4.06 (s, 3H, Ge−H), 2.23 (s, 6H, CH_3) ppm; ($CDCl_3$, 300 MHz): δ 7.10 (t, 1H, 4 −H, ArH), 6.96 (d, 2H, 3,5 −H, ArH), 4.12 (s, 3H, Ge−H), 2.36 (s, 6H, CH_3) ppm. ^{13}C NMR ($CDCl_3$, 75.5 MHz): δ 143.96,

131.37, 129.12, 24.34 (CH_3) ppm. ^{73}Ge NMR (toluene−d_8, 13.96 MHz): δ -237.5 ($^1J(^{73}Ge-^1H)$ = 97 Hz; $\nu_{1/2}$ = 3 Hz) ppm. ATR-IR: 2060.1 cm^{-1} (Ge−H). GCMS (Method 2): t_R = 7.149 min, m/z: 180.0 ($M^{+\bullet}$), 165.0 ($M^{+\bullet}$ - CH_3), 151.0 ($M^{+\bullet}$ - $(CH_3)_2$), 107.1 ($M^{+\bullet}$ - GeH_3), 91.1 ($M^{+\bullet}$ - GeH_3, - CH_3), 77.1 ($M^{+\bullet}$ - GeH_3, - $(CH_3)_2$). HRMS: Calcd. for $C_8H_{12}Ge$: 182.0152, Found: 180.9977 ($M^{+\bullet}$ - H).

1−naphthylGeH$_3$ (**19**): 67.3 mmol (1.00 eq.) 1−naphthyl$_{4-n}$GeX$_n$ (**5**) were suspended in 200 ml Et_2O and at 0°C 4.00 g (105 mmol, 1.6 eq.) lithium aluminium hydride added. Overall yield: 88%. B.p.: 102-104°C at 7 mbar. Elemental analysis (%) for $C_{10}H_{10}Ge$: C, 59.22; H, 4.97. Found: C, 60.73; H, 4.93. ^{1}H NMR ($CDCl_3$, 300 MHz): δ 7.90 (m, 3H, ArH), 7.77 (d, 1H, ArH), 7.51 (m, 3H, ArH), 4.54 (s, 3H, Ge−H) ppm. ^{13}C NMR ($CDCl_3$, 75.5 MHz): δ 137.27, 135.77, 133.44, 131.02, 130.07, 128.91, 128.43, 126.46, 125.99, 125.57 ppm. ^{73}Ge NMR (toluene−d_8, 13.96 MHz): δ -197.9 ($^1J(^{73}Ge-^1H)$ = 98 Hz; $\nu_{1/2}$ = 40 Hz) ppm. ATR-IR: 2061.7 cm^{-1} (Ge−H). GCMS (Method 2): t_R = 9.294 min, m/z: 201.0 ($M^{+\bullet}$ - H_3), 128.1 ($M^{+\bullet}$ - GeH_3). HRMS: Calcd. for $C_{10}H_{10}Ge$: 2003.9996, Found: 201.9940 ($M^{+\bullet}$ - 2 H).

Route B-1: 3.00 g (11.1 mmol, 1.00 eq.) benzylGeCl$_3$ were dissolved in 150 ml Et_2O at 0°C. 1.35 g (35.6 mmol, 3.2 eq.) of freshly grounded lithium aluminum hydride were slowly added as a powder at 0°C. The reaction was stirred 2 hours at 0°C and, after letting it warm up to room temperature, for another 30 minutes. The reaction was now quenched with 3% H_2SO_4 at 0°C, stirred for 10 minutes and then extracted with a saturated potassium tartrate solution. The phases were separated and the organic layer was filtered of *via* a cannula; the watery layer was washed twice with Et_2O. The organic layers were dried over Na_2SO_4. The solvent was removed under reduced pressure giving pure $RGeH_3$ as a liquid product.

benzylGeH$_3$ (**20**): Yield: 87%. ^{1}H NMR ($CDCl_3$, 300 MHz): δ 7.28-7.22 (m, 2H, ArH), 7.15-7.08 (m, 3H, ArH), 3.74 (t, 3H, Ge−H), 2.48 (q, 2H, CH_2) ppm. ^{13}C NMR ($CDCl_3$, 75.5 MHz): δ 141.55, 128.71, 127.88, 124.95, 16.76 ppm. ^{73}Ge NMR

(toluene−d_8, 13.96 MHz): δ -180 ($^1J(^{73}Ge-^1H) = 95$ Hz; $\nu_{1/2} = 12$ Hz) ppm. ATR-IR: 2060.7 cm^{-1} (Ge−H). GCMS (Method 2): t_R = 5.802 min, m/z: 166.0 ($M^{+\bullet}$), 91.1 ($M^{+\bullet}$ - GeH_3).

Route B-2: To a dispersion of 1.78 g (5.67 mmol, 1.00 eq.) $L^{CN}GeCl_3$ in 175 ml Et_2O were 0.65 g (17.0 mmol, 3 eq.) lithium aluminum hydride added at 0°C. After 30 min stirring, it was refluxed for 21 h and stirred for 4 days. The reaction was quenched with 50 ml degassed distilled water. The organic phase was dried over Na_2SO_4 and subsequently the solvent was removed. A resulting off white oil was yielded, containing $L^{CN}GeH_3$ and traces of $L^{CN}{}_2GeH_2$. The $L^{CN}GeH_3$ was condensed off, yielding pure $L^{CN}GeH_3$ as a colorless liquid.

2 −((dimethylamino)methyl)phenylGeH_3; ($L^{CN}GeH_3$) (**21**): Yield 67%. Elemental analysis (%) for $C_{10}H_{15}GeN$: C, 51.51; H, 7.20; N, 6.67. Found: C, 50.08; H, 6.63; N, 9.48. ^{1}H NMR (C_6D_6, 300 MHz): δ 7.62 (d, 1H, 6 −H, ArH), 7.16-7.06 (m, 2H, 4,5 −H, ArH), 6.99 (d, 1H, 3 −H, ArH), 4.52 (s, 3H, Ge−H), 3.17 (s, 2H, Ar−CH_2N), 1.92 (s, 6H, N(CH_3)$_2$) ppm. ^{13}C NMR (C_6D_6, 75.5 MHz): δ 144.90, 137.53, 133.25, 128.90, 128.16, 126.86, 64.48 (Ar−CH_2N), 43.29 (N(CH_3)$_2$) ppm. ^{73}Ge NMR (toluene−d_8, 13.96 MHz): δ -189.0 ($^1J(^{73}Ge-^1H) = 98$ Hz; $\nu_{1/2} = 92$ Hz) ppm. ATR-IR: 2063.1, 2009.1 cm^{-1} (Ge−H). GCMS (Method 1): t_R = 7.911 min, m/z: 211.0 ($M^{+\bullet}$), 164.9 ($M^{+\bullet}$ - C_2H_6N, - H_2), 150.9 ($M^{+\bullet}$ - C_3H_8N, - H_2), 134.1 ($M^{+\bullet}$ - GeH_3), 118.9 ($M^{+\bullet}$ - CH_3, - GeH_3), 91.0 ($M^{+\bullet}$ - C_2H_6N, - GeH_3).

4.2.2.2. Preparation of $RGeH_2$

The reaction procedure was, as previously stated, optimized only for 2,5 −xylyl$_2$GeX_2 (**11**) (Route B). Other dihydrides were gained as side products in the preparation of $RGeH_3$ (Route A); 2,5 −xylyl$_2$GeH_2 could also be gained *via* Route B. $L^{CN}{}_2GeH_2$ was prepared from the pure chloride derivative (Route C). The dihydrides with R =

2,5 −xylyl, 2,6 −xylyl and 1 −naphthyl have previously been prepared by Wolf over another reaction route but not fully characterized.[38]

Route A: From the mixture of $RGeH_3$, R_2GeH_2 and R_3GeH which was gained in the preparation of **15** - **19** were corresponding $RGeH_3$ condensed off under *vacuo* giving a colorless oily liquid or solid with R_2GeH_2 and R_3GeH present. *n*-pentane was added to the product mixture. The R_2GeH_2 dissolves preferentially and can be separated from the remaining solid R_3GeH *via* a cannula. Subsequently, the solvent is removed from the R_2GeH_2 solution under *vacuo* resulting in a colorless oily liquid or solid.

p−^{n}butylphenyl$_2$GeH$_2$ (**22**): Separation by solvatization in pentane, oily liquid; Elemental analysis (%) for $C_{20}H_{28}Ge$: C, 70.43; H, 8.28. Found: C, 68.93; H, 7.97. ^{1}H NMR ($CDCl_3$, 300 MHz): δ 7.45 (d, 4H, ArH), 7.19 (d, 4H, ArH), 5.04 (s, 2H, Ge−H), 2.61 (t, 4H, C_αH), 1.60 (p, 4H, C_βH), 1.36 (h, 4H, C_γH), 0.93 (t, 6H, C_δH) ppm. ^{13}C NMR ($CDCl_3$, 75.5 MHz): δ 144.02, 135.25, 130.90, 128.66, 35.76, 33.72, 22.53, 14.10 ppm. ^{73}Ge NMR (toluene−d_8, 13.96 MHz): δ -109.3 ($^1J(^{73}Ge-^1H) = 97$ Hz; $\nu_{1/2} = 26$ Hz) ppm. ATR-IR: 2044.2 cm^{-1} (Ge−H). GCMS (Method 2): $t_R = 13.937$ min, m/z: 341.2 ($M^{+\bullet}$), 208.0 ($M^{+\bullet}$ - *p*−^{n}butylphenyl, 180.1 ($M^{+\bullet}$ - *p*−^{n}butylphenyl, - C_2H_5), 133.1 ($M^{+\bullet}$ - GeH_2, - *p*−^{n}butylphenyl, 91.0 ($M^{+\bullet}$ - GeH_2, - *p*−^{n}butylphenyl, - C_3H_7).

3,5 −xylyl$_2$GeH$_2$ (**23**): Separation by solvatization in pentane, oily liquid; ^{1}H NMR ($CDCl_3$, 300 MHz): δ 7.19 (s, 4H, 2,6 −H, ArH), 7.04 (s, 2H, 4 −H, ArH), 5.02 (s, 2H, Ge−H), 2.33 (s, 12H, CH_3) ppm. ^{13}C NMR ($CDCl_3$, 75.5 MHz): δ 137.81, 134.01, 132.94, 130.89, 21.41 ppm. ^{73}Ge NMR (toluene−d_8, 13.96 MHz): δ -107.5 ($^1J(^{73}Ge-^1H) = 98$ Hz; $\nu_{1/2} = 35$ Hz) ppm. ATR-IR: 2044.2 cm^{-1} (Ge−H). GCMS (Method 2): $t_R = 11.765$ min, m/z: 286.0 ($M^{+\bullet}$), 180.0 ($M^{+\bullet}$ - 3,5 −xylyl), 105.1 ($M^{+\bullet}$ - GeH_2, - 3,5 −xylyl).

2,6 −xylyl$_2$GeH$_2$ (**24**): Separation by solvatization in pentane; colorless solid; M.p.: 50.7°C. Elemental analysis (%) for $C_{16}H_{20}Ge$: C, 74.08; H, 7.25. Found: C, 72.48; H,

6.99. ^{1}H NMR ($CDCl_3$, 300 MHz): δ 7.13 (t, 2H, 4 −H, ArH), 6.99 (d, 4H, 3,5 −H, ArH), 5.13 (s, 2H, Ge−H), 2.36 (s, 12H, CH_3) ppm. ^{13}C NMR ($CDCl_3$, 75.5 MHz): δ 143.85, 134.90, 129.04, 127.62, 24.00 (CH_3) ppm. ^{73}Ge NMR (toluene−d_8, 13.96 MHz): δ -185.4 ($^{1}J(^{73}Ge-^{1}H)$ = 95 Hz; $\nu_{1/2}$ = 14 Hz) ppm. ATR-IR: 2056.2 cm^{-1} (Ge−H). GCMS (Method 2): tR = 14.18 min, m/z: 286.1 ($M^{+\bullet}$), 180.0 ($M^{+\bullet}$ - 2,6 −xylyl), 165.0 ($M^{+\bullet}$ - 2,6 −xylyl, - CH_3), 151.0 ($M^{+\bullet}$ - 2,6 −xylyl, - $(CH_3)_2$), 105.1 ($M^{+\bullet}$ - 2,6 −xylyl, - GeH_2), 91.1 ($M^{+\bullet}$ - 2,6 −xylyl, - GeH_2, - CH_3), 77.1 ($M^{+\bullet}$ - 2,6 −xylyl, - GeH_2, - $(CH_3)_2$).

1 −naphthyl$_2$GeH$_2$ (25): Separation by solvatization in pentane; colorless solid; M.p.: 94.3°C. Elemental analysis (%) for $C_{20}H_{16}Ge$: C, 73.02; H, 4.90. Found: C, 74.21; H, 4.92. ^{1}H NMR ($CDCl_3$, 300 MHz): δ 8.00 (m, 2H, 8 −H, ArH), 7.89 (dd, 4H, 2,4 −H, ArH), 7.67 (d, 2H, 5 −H, ArH), 7.43 (m, 6H, 3,6,7 −H, ArH), 5.64 (s, 2H, Ge−H) ppm. ^{13}C NMR ($CDCl_3$, 75.5 MHz): δ 137.14, 135.56, 133.47, 132.90, 130.04, 128.84, 128.30, 126.36, 125.85, 125.56 ppm. ^{73}Ge NMR (toluene−d_8, 13.96 MHz): δ -127.0 ($^{1}J(^{73}Ge-^{1}H)$ = n/a; $\nu_{1/2}$ = 110 Hz) ppm. ATR-IR: 2049.5 cm^{-1} (Ge−H). GCMS (Method 2): t_R = 18.99 min, m/z: 330.1 ($M^{+\bullet}$), 252.1 ($M^{+\bullet}$ - GeH_2), 201.0 ($M^{+\bullet}$ - 1 −naphthyl), 128.0 ($M^{+\bullet}$ - 1 −naphthyl, - GeH_2).

Route B-1: To the mixture of $RGeX_3$ and R_2GeX_2 and R_3GeX (Compound **11**) Et_2O was added and freshly grounded lithium aluminum hydride was slowly added as a powder at 0°C. The reaction was stirred 2 hours at 0°C and, after letting it warm up to room temperature, for another 30 minutes. The reaction was now quenched with 3% H_2SO_4 at 0°C, stirred for 10 minutes and then extracted with a saturated potassium tartrate solution. The phases were separated and the organic layer was filtered of *via* a cannula; the watery layer was washed twice with Et_2O. The organic layers were dried over Na_2SO_4. The solvent was removed under reduced pressure giving a mixture of $RGeH_3$, R_2GeH_2 and R_3GeH. The liquid $RGeH_3$ compound was then condensed off under *vacuo* leaving a colorless solid with R_2GeH_2 and R_3GeH present. *n*-pentane was added to the product mixture. The R_2GeH_2 dissolves preferentially and can be

separated from the remaining solid R_3GeH *via* a cannula. After separation, the solvent is removed from the R_2GeH_2 solution under *vacuo* resulting in a colorless oily liquid or solid.

2,5 −xylyl$_2$GeH$_2$ (26): 62.5 mmol (1.00 eq.) 2,5 −xylyl$_{4-n}$GeX$_n$ (**11**) were suspended in 150 ml Et_2O and at 0°C. 4.28 g (112.5 mmol, 1.8 eq.) $LiAlH_4$ in 150 ml Et_2O; colorless solid; Overall yield: 81%. M.p.: 61°C. Elemental analysis (%) for $C_{16}H_{20}Ge$: C, 67.44; H, 7.07. Found: C, 67.52; H, 6.91. ^{1}H NMR ($CDCl_3$, 300 MHz): δ 7.21 (s, 2H, 6 −H, ArH), 7.08 (s, 4H, 3,4 −H, ArH), 5.03 (s, 2H, Ge−H), 2.31 (s, 6H, CH_3), 2.26 (s, 6H, CH_3) ppm. ^{13}C NMR ($CDCl_3$, 75.5 MHz): δ 140.60, 136.91, 134.96, 133.85, 130.40, 129.53, 22.48 (CH_3), 20.90 (CH_3) ppm. ^{73}Ge NMR (toluene−d_8, 13.96 MHz): δ -125.6 ($^1J(^{73}Ge-^1H)$ = 107(5) Hz; $\nu_{1/2}$ = 41 Hz) ppm. ATR-IR: 2055.2 cm^{-1} (Ge−H). GCMS (Methode2): t_R = 13.53 min, m/z: 286.1 ($M^{+\bullet}$), 180.0 ($M^{+\bullet}$ - 2,5 −xylyl), 165.0 ($M^{+\bullet}$ - 2,5 −xylyl, - CH_3), 151.0 ($M^{+\bullet}$ - 2,5 −xylyl, - $(CH_3)_2$, 105.1 ($M^{+\bullet}$ - 2,5 −xylyl, - GeH_2), 91.1 ($M^{+\bullet}$ - 2,5 −xylyl, - GeH_2, -CH_3), 77.1 ($M^{+\bullet}$ - 2,5 −xylyl, - GeH_2, - $(CH_3)_2$).

Route B-2: To a dispersion of 6.00 g (14.6 mmol, 1.00 eq.; 95% purity, 5% $L^{CN}{}_2GeCl_2{\cdot}HCl$) $L^{CN}{}_2GeCl_2$ in 175 ml Et_2O were 1.11 g (29.1 mmol, 2.00 eq.) lithium aluminum hydride added at 0°C. After 30 min stirring, it was refluxed for 24h and stirred for 7 days. The reaction was quenched with 100 ml degassed distilled water. The organic phase was dried over Na_2SO_4 and subsequently the solvent was removed. A resulting off white oil was yielded, containing $L^{CN}{}_2GeH_2$ as main product, $L^{CN}GeH_3$ and traces of $L^{CN}{}_3GeH$. The $L^{CN}GeH_3$ was condensed off, yielding pure $L^{CN}GeH_3$. The mixture of $L^{CN}{}_2GeH_2$ and $L^{CN}{}_3GeH$ was separated by recrystallization of the $L^{CN}{}_3GeH$ from toluene. The solution of $L^{CN}{}_2GeH_2$ was removed *via* a cannula and the solvent was evaporated yielding a colorless oily product.

2 −((dimethylamino)methyl)phenyl$_2$GeH$_2$; ($L^{CN}{}_2GeH_2$) (27): Yield: 84%. Elemental analysis (%) for $C_{18}H_{26}GeN_2$: C, 63.02; H, 7.64; N, 8.17. Found: C, 64.08;

H, 7.32; N, 7.97. ^{1}H NMR (C_6D_6, 300 MHz): δ 7.61 (d, 2H, 6 −H, ArH), 7.18-7.00 (m, 6H, 3,4,5 −H, ArH), 5.44 (s, 2H, Ge−H), 3.33 (s, 4H, Ar−CH_2N), 1.92 (s, 12H, N(CH_3)$_2$) ppm. ^{13}C NMR (C_6D_6, 75.5 MHz): δ 145.08, 138.01, 137.12, 128.85, 128.71, 126.96, 65.19 (Ar−CH_2N), 44.37 (N(CH_3)$_2$) ppm. ^{73}Ge NMR (toluene−d_8, 13.96 MHz): δ -118.0 ($^{1}J(^{73}\text{Ge}-^{1}\text{H})$ = n/a; $\nu_{1/2}$ = 320 Hz) ppm. ATR-IR: 2062.0, 2010.1 cm^{-1} (Ge−H). GCMS (Method 1): t_R = 14.552 min, m/z: 342.1 ($M^{+\bullet}$ - 2H), 299.1 ($M^{+\bullet}$ - C_2H_7N), 284.1 ($M^{+\bullet}$ - C_3H_8N, - H_2), 253.0 ($M^{+\bullet}$ - $(C_2H_6N)_2$, - H_2), 239,0 ($M^{+\bullet}$ - C_2H_6N, - C_3H_8N, - H_2), 208.0 ($M^{+\bullet}$ - $C_9H_{12}N$, - H_2), 191.9 ($M^{+\bullet}$ - $C_9H_{12}N$, - CH_3, - H_2), 179.1 ($M^{+\bullet}$ - $C_9H_{12}N$, - (CH_3), - H_2), 165.0 ($M^{+\bullet}$ - $C_9H_{12}N$, - C_2H_6N, - H_2), 148.9 ($M^{+\bullet}$ - $C_9H_{12}N$, - C_3H_8N, - H_2), 134.1 ($M^{+\bullet}$ - $C_9H_{12}N$, - GeH_2), 118,1 ($M^{+\bullet}$ - $C_9H_{12}N$, - GeH_2, - CH_3), 91.0 ($M^{+\bullet}$ - $C_9H_{12}N$, - GeH_2, - C_2H_6N).

4.2.3. Dehydrogenative coupling reaction of $RGeH_3$

Temperature induced (amine catalyzed) dehydrogenative coupling

Route A (reflux): A Schlenk flask with reflux condenser attached was charged with $RGeH_3$ and toluene. TMEDA was added to the stirring solution. The reaction was stirred and refluxed to achieve a color change from colorless to yellow and blurry brown. At this time, the solution was decanted and the precipitate washed with the solvent used for the reaction. The gained material was investigated using elemental analysis and/or SEM.

Ge@2,5 −xylyl$^{\text{reflux,base}}$ (**28**): 270 mg (1.34 mmol, 1.00 eq.) 2,5 −xylylGeH_3 (**17**) in 5 ml toluene, 0.17 g (1.00 eq.) TMEDA added. Stirred for 24h; refluxed for 80h. Yield: $<$ 10 mg of brown solids. SEM/EDX analysis.

Route B (thermal decomposition): A Schlenk flask with reflux condenser attached was charged with $RGeH_3$ and DME. If stated, TMEDA was added to the stirring solution. The reaction was refluxed. Since the conversion did not occur after 68h

reflux, thermal decomposition was used by letting the solvent evaporate at elevated temperature affording a color change and the formation of a brown solid at *circa* 220 °C which was collected and washed with pentane to remove cleaved naphthalene. The filtrate was analyzed with GC-MS. The solid product is disperseable in THF and was investigated by EA, SEM, SAXS (and GPC).

Ge@1 −naphthyl^{T,base} (**29**): 500 mg (2.346 mmol, 1.00 eq.) 1 −naphthylGeH$_3$ (**19**) in 5 ml DME, 286 mg (1.00 eq.) TMEDA added. Refluxed for 68h; thermal decomposition at *circa* 220 °C. Yield: $>$ 200 mg of brown solids. Elemental analysis (%): C, 39.49; H, 2.52; N, 0.11.

Ge@1 −naphthyl^{T} (**30**): 500 mg (2.346 mmol, 1.00 eq.) 1 −naphthylGeH$_3$ (**19**) in 5 ml DME. Refluxed for 68h; thermal decomposition at *circa* 220 °C. Yield: $>$ 200 mg of brown solids. Elemental analysis (%): C, 40.57; H, 2.51; N, 0.10.

Microwave induced (amine catalyzed) dehydrogenative coupling

A microwave vial was charged with RGeH$_3$ and DME. If stated, TMEDA was added to the reaction mixture. The reaction was placed in the microwave and the mixture was reacted at corresponding temperatures. The afforded polymeric material was collected by centrifugation or evaporation of the solvent and washed with pentane. The filtrate was analyzed with GC-MS. The solid product was investigated by EA, SEM, SAXS and if disperseable in THF also with MALDI-TOF and GPC.

Ge@1 −naphthyl$^{micro,base,250°}$ (**31**): 1.00 g (4.97 mmol, 1.00 eq.) 1 −naphthylGeH$_3$ (**19**) in 4 ml DME, 578 mg (1.00 eq.) TMEDA added. Orange precipitate is yielded: $>$ 200 mg. Elemental analysis (%): C, 43.36; H, 3.28; N, 0.30.

Ge@2,5 −xylyl$^{micro,base,250°,10min}$ (**32**): 210 mg (1.16 mmol, 1.00 eq.) 2,5 −xylylGeH$_3$ (**17**) in 2,5 ml DME, 116 mg (1.00 eq.) TMEDA added. Orange precipitate is yielded. Elemental analysis (%): C, 23.00; H, 3.23; N, 0.93.

Ge@1 −naphthyl$^{micro,base,210^\circ,10min}$ (**33**): 280 mg (1.39 mmol, 1.00 eq.) 1 −naphthylGeH$_3$ (**19**) in 2,5 ml DME, 162 mg (1.00 eq.) TMEDA added. Orange not dispersable precipitate is yielded. Elemental analysis (%): C, 24.98; H, 1.42; N, 0.39.

Ge@1 −naphthyl$^{micro,250^\circ,5min}$ (**34**): 298 mg (1.48 mmol, 1.00 eq.) 1 −naphthylGeH$_3$ (**19**) in 2,5 ml DME. Orange precipitate is yielded. Elemental analysis (%): C, 35.63; H, 3.45; N, 0.35.

Ge@1 −naphthyl$^{micro,250^\circ,3x5min}$ (**35**): 305 mg (1.51 mmol, 1.00 eq.) 1 −naphthylGeH$_3$ (**19**) in 2,5 ml DME. Orange precipitate is yielded. Elemental analysis (%): C, 23.48; H, 2.75; N, 0.35.

Ge@benzyl$^{micro,base,250^\circ,3x5min}$ (**36**): 240 mg (1.44 mmol, 1.00 eq.) benzylGeH$_3$ (**20**) in 2,5 ml DME, 167 mg (1.00 eq.) TMEDA added. Orange solution is yielded. The polymeric material was gained by evaporation of the solvents under reduced pressure and washed with pentane: orange solids. Elemental analysis (%): C, 39.76; H, 3.77; N, 0.31.

Ge@benzyl$^{micro,250^\circ,3x5min}$ (**37**): 292 mg (1.75 mmol, 1.00 eq.) benzylGeH$_3$ (**20**) in 3 ml DME. Color change, but no product could be isolated.

4.3. Synthesis of Ge(ap)$_2$ complexes towards organogermanium monohalides

2,4–di–*tert*–butyl–6–(*tert*–butylamino)phenol (apH$_2$) (**38**): In a 100 ml three-neck-flask 5.00 g (22.5 mmol, 1.00 eq.) 3,5 −di−*tert*−butylcatechol were dissolved in 30 ml acetonitrile and placed over 3 Å molecular sieves. 2,4 ml (22.5 mmol, 1.00 eq.) of *t*−BuNH$_2$ and 0.57 g (2.25 mmol, 0.10 eq.) were added to the brown solution, which turned dark green upon addition. The reaction mixture was refluxed for two hours. As

soon as the reaction mixture was cooled down, it was filtered using a cannula and the solids were washed thrice with each time 50 ml Et_2O. To the combined dark green organic solutions, 80 ml saturated $Na_2S_2O_4$ solution was added and the color turned to brown. The organic layer was dried over $MgSO_4$ and subsequently the solvents were evaporated under *vacuo*. apH_2 was collected by recrystallization from acetonitrile as off white crystalline solid.

Yield: 52%. ^{1}H NMR ($CDCl_3$, 400 MHz): δ 7.82 (b, 1H, OH), 7.12 (d, 1H, H_5), 6.93 (d, 1H, H_4), 2.35 (b, 1H, NH), 1.40 (s, 9H, H_1), 1.28 (s, 9H, H_2), 1.17 (s, 9H, H_3) ppm. ^{13}C NMR ($CDCl_3$, 100 MHz): δ 140.00, 137.15, 134.55, 130.96, 130.30, 129.14, 22.31 (CH_3), 20.41 (CH_3) ppm

Ge(ap)$_2$ (**39**): 487 mg (1.75 mmol, 2.00 eq.) of apH_2 were dissolved in 10 ml THF. To this solution a solution of 600 mg (3.60 mmol, 4.10 eq.) LiN(TMS) in 4 ml THF was added dropwise while stirring and the solution changed to a slight green color. The mixture was stirred for 60 minutes. Subsequently, $GeCl_4$ was added dropwise to the reaction mixture and it turned deep dark blue. The addition was continued until this color dissipated to a slight yellow solution (233 mg, 1.20 eq.). The reaction was left to stir for 30 minutes at which point the solvent was evaporated to yield an off white slurry. To this residue pentane or hexanes were added and the alkane phase was collected by centrifugation. DCM was added to the solids and the DCM phase was collected as well. Pure $Ge(ap)_2$ was obtained by evaporation of the solvent of the DCM phase and by cooling the alkane phase as white powder.

Yield: 61%. ^{1}H NMR ($CDCl_3$, 400 MHz): δ 7.04 (d, 1H, H_5), 6.81 (d, 1H, H_4), 1.56 (s, 18H, H_3), 1.40 (s, 18H, H_2), 1.36 (s, 18H, H_1) ppm. ^{13}C NMR ($CDCl_3$, 100 MHz): δ 142.29 ($C_{12/10}$), 141.62 (C_{11}), 134.92 ($C_{10/12}$), 134.50 (C_9), 112.51 (C_8), 108.87 (C_7), 54.28 (C_6), 34.92 (C_5), 34.85 (C_4), 32.01 (C_3), 30.23 (C_2), 29.66 (C_1) ppm. HRMS: Calcd. for $C_{36}H_{58}N_2O_2Na^{70}Ge$: 643.36330, Found: 643.36385 ($M{\cdot}Na^+$).

Conversion using Grignard reagents: 250 mg $Ge(ap)_2$ (0.40 mmol, 1.00 eq.) was

dissolved in 7 ml THF and 4 ml of respective Grignard reagent solution 2M in THF (8 mmol, 20.0 eq.) were added. The reaction was refluxed for 24 hours. 15ml hexanes, 10 ml water and 10 ml 1 M HCl were added. The organic layer was collected as a suspension and was filtered to give apH_2·HCl as solid product. The solvent of the filtrate was removed using a rotary evaporator, and the gained mixture was dissolved in a small amount of DCM. The mixture was purified using preparatory TLC on a 2 mm x 20 cm x 20 cm silica gel plate using hexanes as eluent. The bands were identified and the solid phase was extracted with 50 ml chloroform overnight. Liquids were collected by filtration and the solids were washed with 30 ml of chloroform. The products were collected by evaporation of the solvent using the rotary evaporator.

apH_2·HCl: ^{1}H NMR ($CDCl_3$, 400 MHz): δ 10.39 (s, 2H, NH_3^+), 7.91 (s, 1H, OH), 7.33 (d, 1H, Ar-H), 7.27 (d, 1H, Ar-H), 1.39 (s, 9H, *t*-bu), 1.34 (s, 9H, *t*-bu), 1.28 (s, 9H, *t*-bu) ppm. ^{13}C NMR ($CDCl_3$, 100 MHz): δ 147.30, 143.70, 141.89, 125.10, 122.08, 121.62, 63.49, 35.64, 34.58, 31.48, 29.87, 26.24 ppm.

$GeBu_4$: BuGeCl was used as Grignard reagent, reflux for 24 hours. Yield: no conversion; 43% apH_2·HCl recovered.

$GePh_4$: PhGeCl was used as Grignard reagent, reflux for 24 hours. Yield: no full conversion; main product Ph_3GeCl; 65% apH_2·HCl recovered.

Appendix A.

Appendix

Numbering of compounds

Table A.1.: Numbering of compounds within this thesis.

	Compound	no.
$\mathbf{RGeX_3}$	$p-^n$butylphenylGeX_3	**1**
	3,5 $-$xylylGeX_3	**2**
	2,5 $-$xylylGeX_3	**3**
	2,6 $-$xylylGeX_3	**4**
	1 $-$naphthylGeX_3	**5**
$\mathbf{RGeCl_3}$	$p-^n$butylphenylGeCl_3	**6**
	3,5 $-$xylylGeCl_3	**7**
	2,5 $-$xylylGeCl_3	**8**
	2,6 $-$xylylGeCl_3	**9**
	1 $-$naphthylGeCl_3	**10**
$\mathbf{R_2GeX_2}$	2,5 $-$xylyl$_2$GeX_2	**11**
$\mathbf{R_2GeCl_2}$	2,5 $-$xylyl$_2$GeCl_2	**12**
	2,6 $-$xylyl$_2$GeCl_2	**13**
	1 $-$naphthyl$_2$GeCl_2	**14**
$\mathbf{RGeH_3}$	$p-^n$butylphenylGeH_3	**15**
	3,5 $-$xylylGeH_3	**16**
	2,5 $-$xylylGeH_3	**17**
	2,6 $-$xylylGeH_3	**18**
	1 $-$naphthylGeH_3	**19**

	benzylGeH$_3$	**20**
	2 −((dimethylamino)methyl)phenylGeH$_3$; (L^{CN}GeH$_3$)	**21**
R$_2$GeH$_2$	$p-^n$butylphenyl$_2$GeH$_2$	**22**
	3,5 −xylyl$_2$GeH$_2$	**23**
	2,6 −xylyl$_2$GeH$_2$	**24**
	1 −naphthyl$_2$GeH$_2$	**25**
	2,5 −xylyl$_2$GeH$_2$	**26**
	2 −((dimethylamino)methyl)phenyl$_2$GeH$_2$; (L$^{CN}{}_2$GeH$_2$)	**27**
Ge@R	Ge@2,5 −xylyl^{reflux,base}	**28**
	Ge@1 −naphthyl^{T,base}	**29**
	Ge@1 −naphthyl^{T}	**30**
	Ge@1 −naphthyl$^{micro,base,250°}$	**31**
	Ge@2,5 −xylyl$^{micro,base,250°,10min}$	**32**
	Ge@1 −naphthyl$^{micro,base,210°,10min}$	**33**
	Ge@1 −naphthyl$^{micro,250°,5min}$	**34**
	Ge@1 −naphthyl$^{micro,250°,3x5min}$	**35**
	Ge@benzyl$^{micro,base,250°,3x5min}$	**36**
	Ge@benzyl$^{micro,250°,3x5min}$	**37**
	2,4–di–***tert***–butyl–6–(***tert***–butylamino)phenol (apH$_2$)	**38**
	germanium–bis–2,4–di–*tert*–butyl–6–(*tert*–butylamino)phenolate (Ge(ap)$_2$)	**39**

GCMS methods

Table A.2.: GCMS method 1.

	Rate [°**C/min**]	**Value** [°**C**]	**Hold time** [**min**]
Initial		40	2
Ramp 1	20	100	0
Ramp 2	16	200	0
Ramp 3	12	320	20

Table A.3.: GCMS method 2.

	Rate [°**C/min**]	**Value** [°**C**]	**Hold time** [**min**]
Initial		40	2
Ramp 1	20	300	10

Table A.4.: Crystallographic data and details of measurements for compounds **8**, **9**, **10**, **12**, **13** and **14**; Mo Kα (λ=0.71073 Å). R1 = $\Sigma/|F_o| - |F_c|/|\Sigma|F_d|$; wR2 = $[\Sigma_w(F_o^2 - F_2^2)^2/\Sigma_w(F_o^2)^2]^{1/2}$

Compound	**2,5−xylyl$_2$GeCl$_2$ (12)**	**2,6−xylyl$_2$GeCl$_2$ (13)**	**1-naphthyl$_2$GeCl$_2$ (14)**	**2,5−xylylGeCl$_3$ (8)**	**2,6−xylylGeCl$_3$ (9)**	**1-naphthylGeCl$_3$ (10)**
Formula	$C_{16}H_{18}Cl_2Ge$	$C_{16}H_{18}Cl_2Ge$	$C_{20}H_{14}Cl_2Ge$	$C_8H_9Cl_3Ge$	$C_8H_9Cl_3Ge$	$C_{10}H_7Cl_3Ge$
Fw (g mol^{-1})	353.79	353.79	397.82	284.09	284.09	306.10
a (Å)	9.3391(4)	8.597(2)	15.1757(9)	9.0113(16)	17.4763(7)	10.0721(8)
b (Å)	15.5032(6)	8.629(3)	7.3251(5)	7.1970(13)	7.1344(3)	12.2163(9)
c (Å)	11.4915(5)	10.759(3)	15.9134(10)	9.1579(16)	8.3358(3)	36.758(3)
α (°)	90	80.361(10)	90	90	90	90
β (°)	110.358(1)	82.891(11)	110.992(2)	117.056(4)	90	90
γ (°)	90	82.295(10)	90	90	90	90
V (Å^3)	1559.88(11)	775.5(4)	1651.58(18)	528.93(16)	1039.33(7)	4522.9(6)
Z	4	2	4	2	4	16
Crystal size (mm)	0.12 × 0.10 × 0.09	2.30	0.05 × 0.05 × 0.05	0.15 × 0.14 × 0.09	0.31 × 0.26 × 0.10	0.05 × 0.03 × 0.01
Crystal habit	Block, colorless	Block, colorless	Block, colorless	Block, colorless	Block, colorless	Plate, colorless
Crystal system	Monoclinic	Triclinic	Monoclinic	Monoclinic	Orthorhombic	Orthorhombic
Space group	$P2_1/c$	P-1	$P2_1/n$	$P2_1/m$	Pnma	Pbca
d_{calc} (mg/m^3)	1.506	1.515	1.600	1.784	1.816	1.798
μ (mm^{-1})	2.29	2.30	2.17	3.60	3.66	3.37
T (K)	100(2)	100(2)	100(2)	100(2)	100(2)	100(2)
2Θ range (°)	2.3–33.2	2.4–33.0	2.3–32.8	2.5–33.2	2.3–30.7	2.7–26.0
F(000)	720	360	800	280	560	2400
R_{int}	0.049	0.096	0.083	0.048	0.091	0.151
independent reflns	5932	5912	6268	2163	2091	4211
No. of params	176	176	264	70	72	253
R1, wR2 (all data)	R1 = 0.0236 wR2 = 0.0552	R1 = 0.0546 wR2 = 0.1196	R1 = 0.0313 wR2 = 0.0667	R1 = 0.0193 wR2 = 0.0460	R1 = 0.0426 wR2 = 0.0910	R1 = 0.1086 wR2 = 0.1989
R1, wR2 (>2σ)	R1 = 0.0201 wR2 = 0.0537	R1 = 0.0456 wR2 = 0.1150	R1 = 0.0248 wR2 = 0.0636	R1 = 0.0172 wR2 = 0.0448	R1 = 0.0347 wR2 = 0.0865	R1 = 0.0844 wR2 = 0.1873

List of Figures

List of Figures

List of Tables

Bibliography

[1] C. Winkler, *Ber. Dtsch. Chem. Ges.* **1886**, 19, 210

[2] A. F. Hollemann; E. Wiberg; N. Wiberg, *Lehrbuch der anorganischen Chemie*, Berlin, Boston: De Gruyter, **2007**

[3] C. Winkler, *Chem. Ber.* **1887**, 667

[4] G. Morgan; H. Drew, *J. Chem. Soc.* **1925**, 127, 1760

[5] D. Tabern; W. Orndorff; L. Dennis, *J. Am. Chem. Soc.* **1925**, 47, 2039

[6] B. Gribov; G. Domrachev; B. Zhuk; A. Bo; B. Ba; C. Bu, *Deposition of Films and Coatings by Decomposition of Organometallic Compounds*, Moscow: Nauka, **1981**

[7] E. Lukevics; L. Ignatovich, "Biological Activity of Germanium Compounds", *PATAI'S Chemistry of Functional Groups*, New York: John Wiley & Sons, Ltd, **2009**

[8] G. Razuvaev; B. Gribov; G. Domrachev; B. Salamatin, *Organometallic Compounds in Electronics*, Moscow: Science, **1972**

[9] R. Miller; R. Sooriyakumaran, *J. Polym. Sci. Part A Polym. Chem.* **1987**, 25, 111

[10] K. Mochida; S. Nagano, *Inorg. Chem. Commun.* **1998**, 1, 289

[11] S. Tomoda; M. Shimoda; Y. Takeuchi; Y. Kajii; K. Obi; I. Tanaka; K. Honda, *J. Chem. Soc., Chem. Commun.* **1988**, 910

[12] C. Elschenbroich, *Organometallchemie*, Wiesbaden: B. G. Teubner Verlag, **2008**

[13] K. Oshima, *Sci. Synth.* **2003**, 5, 9

[14] C. Kraus; L. Foster, *J. Am. Chem. Soc.* **1927**, 49, 457

[15] J. Simons; E. Wagner; J. Müller, *J. Am. Chem. Soc.* **1933**, 55, 3705

[16] G. Cerveau; C. Chuit; R. Corriu; C. Reye, *Organometallics* **1988**, 7, 786

[17] G. Cerveau; C. Chuit; R. Corriu; C. Reye, *Organometallics* **1991**, 10, 1510

Bibliography

[18] M. Glavinovic; M. Krause; L. Yang; J. McLeod; L. Liu; K. Baines; T. Friscic; J. Lumb, *Sci. Adv.* **2017**, 3, e1700149

[19] M. Krause, *Doctoral Thesis, University of Western Ontrio, London (ON), Canada* **2017**

[20] J. Cooke; C. Dixon; M. Netherton; G. Kollegger; K. Baines, *Synth. React. Inorg. Met.-Org. Chem.* **1996**, 26, 1205

[21] C. Samanamu; C. Anderson; J. Golen; C. Moore; A. Rheingold; C. Weinert, *J. Organomet. Chem.* **2011**, 696, 2993

[22] S. Komanduri; A. Shumaker; K. Roewe; M. Wolf; F. Uhlig; C. Moore; A. Rheingold; C. Weinert, *Organometallics* **2016**, 35, 3240

[23] M. Chaubon; B. Dittrich; J. Escudie; H. Ramdane; H. Ranaivonjatovo; J. Satge, *Synth. React. Inorg. Met.-Org. Chem.* **1997**, 27, 519

[24] M. Amadoruge; E. Short; C. Moore; A. Rheingold; C. Weinert, *J. Organomet. Chem.* **2010**, 695, 1813

[25] M. Wolf; A. Falk; M. Flock; A. Torvisco; F. Uhlig, *J. Organomet. Chem.* **2017**, 851, 143

[26] K. Kocheshkov, *Ber. Dtsch. Chem. Ges.* **1933**, 66, 1661

[27] W. Neumann; G. Burkhardt, *Justus Liebigs Ann. Chem.* **1963**, 663, 11

[28] F. Rijkens; G. van der Kerk, *Recl. Trav. Chim. Pays-Bas.* **1964**, 83, 723

[29] K. Kuehlein; W. Neumann, *Justus Liebigs Ann. Chem.* **1967**, 702, 17

[30] R. Laurent; A. Laporterie; J. Dubac; J. Berlan, *Organometallics* **1994**, 13, 2493

[31] V. Zhun; I. Sbitneva; E. Chernyshev, *Russ. J. Gen. Chem.* **2005**, 75, 867

[32] V. Zhun; I. Sbitneva; A. Polivanov; E. Chernyshev, *Russ. J. Gen. Chem.* **2006**, 76, 1564

[33] R. Kultyshev; S. Prakash; G. Olah; J. Faller; J. Parr, *Organometallics* **2004**, 23, 3184

[34] J. Faller; R. Kultyshev; J. Parr, *J. Organomet. Chem.* **2004**, 689, 2565

[35] S. Bhattacharya; P. Raj; R. Srivastava, *J. Organomet. Chem.* **1976**, 105, 45

[36] J. Satge; P. Riviere, *Bull. Soc. Chim. Fr.* **1966**, 1773

[37] J. Park; S. Batcheller; S. Masamune, *J. Organomet. Chem.* **1989**, 367, 39

[38] M. Wolf, *Doctoral Thesis, Graz University of Technology, Graz, Austria* **2017**

[39] F. Riedmiller; G. Wegner; A. Jockisch; H. Schmidbaur, *Organometallics* **1999**, 18, 4317

[40] M. Okamoto; T. Asano; E. Suzuki, *Organometallics* **2001**, 20, 5583

[41] J. Ohshita; Y. Toyoshima; A. Iwata; H. Tang; A. Kunai, *Chem. Lett.* **2001**, 886

[42] K. Zaitsev; A. Kapranov; Y. Oprunenko; A. Churakov; J. Howard; B. Tarasevich; S. Karlov; G. Zaitseva, *J. Organomet. Chem.* **2012**, 700, 207

[43] M. Voronkov; A. Egorochkin, *The Chemistry of Organic Germanium, Tin and Lead Compounds*, New York: John Wiley & Sons, **2003**, 131

[44] E. Voegelen, *Z. Anorg. Chem* **1902**, 30, 325

[45] H. Gilman; C. Gerow, *J. Am. Chem. Soc.* **1955**, 77, 5509

[46] C. Tamborski; F. Ford; W. Lehn; G. Moore; E. Soloski, *J. Org. Chem.* **1962**, 27, 619

[47] O. Johnson; D. Harris, *J. Am. Chem- Soc.* **1950**, 72, 5566

[48] M. Dakkouri; H. Kehrer, *Chem. Ber.* **1983**, 116, 2041

[49] M. Kamitani; K. Fukumoto; R. Tada; M. Itazaki; H. Nakazawa, *Organometallics* **2012**, 31, 2957

[50] D. Nieder; L. Klemmer; Y. Kaiser; V. Huch; D. Scheschkewitz, *Organometallics* **2017**, 37, 632

[51] T. Gar; O. Chernysheva; A. Kisin; V. Mironov, *Zh. Obshch. Khim.* **1985**, 55, 1057

[52] F. Cosledan; A. Castel; P. Riviere; J. Satge; M. Veith; V. Huch, *Organometallics* **1998**, 17, 2222

[53] U. Masafumi; K. Yuuki; M. Hideyuki, *Heteroat. Chem.* **2001**, 12, 238

[54] G. Spikes; J. Fettinger; P. Power, *J. Am. Chem. Soc.* **2005**, 127, 12232

[55] M. Hill, *Struct. Bond.* **2010**, 136, 189

[56] K. Zaitsev; A. Kapranov; A. Churakov; O. Poleshchuk; Y. Oprunenko; B. Tarasevich; G. Zaitseva; S. Karlov, *Organometallics* **2013**, 32, 6500

[57] D. Gerion; N. Zaitseva; C. Saw; M. Casula; S. Fakra; T. Van Buuren; G. Galli, *Nano Lett.* **2004**, 4, 597

[58] C. Zeppek; A. Torvisco; M. Flock; C. Guglieri; H. Amenitsch; F. F. Uhlig, **in prep.**

[59] I. Manners, *Angew. Chem., Int. Ed.* **1996**, 35, 1602

[60] C. Carraher; C. Pittman; M. Zeldin; A. Abd-El-Aziz, *Macromol. Containing Met. Met.-Like Elem.* **2005**, 4, 225

[61] D. Foucher, *Catenated Germanium and Tin Oligomers and Polymers. In Main Group Strategies towards Fundtional Hybrid Materials* **2018**, Wiley, 209

[62] J. Hlina; R. Zitz; H. Wagner; F. Stella; J. Baumgartner; C. Marschner, *Inorg. Chim. Acta* **2014**, 422, 120

[63] A. Fukazawa; H. Tsuji; K. Tamao, *J. Am. Chem. Soc.* **2006**, 128, 6800

[64] K. Tamao; H. Tsuji; M. Terada; M. Asahara; S. Yamaguchi; A. Toshimitsu, *Angew. Chem., Int. Ed.* **2000**, 39, 3287

[65] H. Tsuji; M. Terada; A.Toshimitsu; K Tamao, *J. Am. Chem. Soc.* **2003**, 125, 7486

[66] V. Balaji; J. Michl, *Polyhedron* **1991**, 10, 1265

[67] C. Weinert, *Dalton Trans.* **2009**, 10, 1691

[68] W. Metlesics; H. Zeiss, *J. Am. Chem. Soc.* **1960**, 82, 3321

[69] M. Brown; G. Fowles, *J. Chem. Soc.* **1958**, 2811

[70] O. Johnson, *Chem. Rev.* **2019**, 48, 259

[71] W. Neumann; K. Kuehlein, *Justus Liebigs Ann. Chem.* **1965**, 683, 1

[72] S. Roller; D. Simon; M. Draeger, *J. Organomet. Chem.* **1986**, 301, 27

[73] S. Roller; M. Draeger, *J. Organomet. Chem.* **1986**, 316, 57

[74] A. Castel; P. Riviere; B. Saint-Roch; J. Satge; J. Malrieu, *J. Organomet. Chem.* **1983**, 247, 149

[75] F. Glockling; K. Hooton, *J. Chem. Soc.* **1962**, 3509

[76] M. Draeger; D. Simon, *J. Organomet. Chem.* **1986**, 306, 183

[77] F. Glockling; K. Hooton, *J. Chem. Soc.* **1963**, 1849

[78] K. Zaitsev; E. Lermontova; A. Churakov; V. Tafeenko; B. Tarasevich; O. Poleshchuk; A. Kharcheva; T. Magdesieva; O. Nikitin; G. Zaitseva; S. Karlov, *Organometallics* **2015**, 34, 2765

[79] S. Kobayashi; S. Cao, *Chem. Lett.* **1993**, 1385

[80] S. Kashimura; M. Ishifune; N. Yamashita; H. Bu; M. Takebayashi; S. Kitajima; D. Yoshiwara; Y. Kataoka; R. Nishida; S. Kawasaki; H. Murase; T. Shono, *The Journal of Organic Chemistry* **1999**, 64, 6615

[81] M. Okano; K. Takeda; T. Toriumi; H. Hamano, *Electrochim. Acta* **1998**, 44, 659

[82] Y. Yokoyama; M. Hayakawa; T. Azemi; K. Mochida, *J. Chem. Soc., Chem. Commun.* **1995**

[83] T. Azemi; Y. Yokoyama; K. Mochida, *J. Organomet. Chem.* **2005**, 690, 1588

[84] C. Aitken; J. Harrod; A. Malek; E. Samuel, *J. Organomet. Chem.* **1988**, 349, 285

[85] D. Wang; Y. Chang; Q. Wang; J. Cao; D. Farmer; R. Gordon; H. Dai, *J. Am. Chem. Soc.* **2004**, 126, 11602

[86] T. Hanrath; B. Korgel, *J. Am. Chem. Soc.* **2002**, 124, 1424

[87] C. Fang; H. Föll; J. Carstensen, *Nano Lett.* **2006**, 6, 1578

[88] D. Talapin; J. Lee; M. Kovalenko; E. Shevchenko, *Chem. Rev.* **2010**, 110, 389

[89] E. Henderson; C. Hessel; J. Veinot, *J. Am. Chem. Soc.* **2008**, 130, 3624

[90] H. Chiu; S. Kauzlarich, *Chem. Mater.* **2006**, 18, 1023

[91] H. Chiu; C. Chervin; S. Kauzlarich, *Chem. Mater.* **2005**, 17, 4858

[92] E. Fok; M. Shih; A. Meldrum; J. Veinot, *Chem. Commun.* **2004**, 386

[93] H. Wu; J. Liu; Y. Wang; Y. Zeng; J. Jiang, *Mater. Lett.* **2006**, 60, 986

[94] X. Lu; K. Ziegler; A. Ghezelbash; K. Johnston; B. Korgel, *Nano Lett.* **2004**, 4, 969

[95] N. Chou; K. Oyler; N. Motl; R. Schaak, *Chem. Mater.* **2009**, 21, 4105

[96] S. Guha; M. Wall; L. Chase, *Nuclear Instruments and Methods in Physics Research B* **1999**, 147, 367

[97] A. Kornowski; M. Giersig; R. Vogel, *Adv. Mater.* **1993**, 5, 634

[98] X. Ma; F. Wu; S. Kauzlarich, *Journal of Solid and State Chemistry* **2008**, 181, 1628

[99] B. Taylor; S. Kauzlarich; G. Delgado; H. Lee, *Chem. Mater.* **1999**, 11, 2493

[100] D. VaughnII; R. Schaak, *Chem. Soc. Rev.* **2013**, 42, 2861

[101] D. Xue; J. Wang; Y. Wang; S. Xin; Y. Guo; L. Wan, *Adv. Mater.* **2011**, 23, 3704

[102] N. Choi; M. Tanaka, *J. Organomet. Chem.* **1998**, 564, 81

[103] C. Zeppek, *Doctoral Thesis, Graz University of Technology, Graz, Austria* **2015**

[104] S. Reischauer, *Master Thesis, Graz University of Technology, Graz, Austria* **2018**

[105] P. Bruce; B. Scrosati; J. Tarascon, *Angew. Chem. Int. Ed.* **2008**, 47, 2930

[106] H. Kim; Y. Son; C. Park; J. Cho; H. Choi, *Angew. Chem. Int. Ed.* **2013**, 52, 5997

[107] G. Jo; I. Choi; H. Ahn; M. Park, *Chem. Commun.* **2012**, 48, 3987

[108] C. Park; J. Kim; H. Kim; H. Sohn, *Chem. Soc. Rev.* **2010**, 39, 3115

[109] S. Yoon; C. Park; H. Sohn, *Electrochem. Solid-State Lett.* **2008**, 11, A42

[110] M. Park; Y. Cho; K. Kim; J. Kim; M. Liu; J. Cho, *Angew. Chem. Int. Ed.* **2011**, 50, 9647

[111] S. Jin; N. Li; H. Cui; C. Wang, *ACS Appl. Mater. Interfaces* **2014**, 6, 19397

[112] A. Piskunov; I. Aivazyan; A. Poddelsky; G. Fukin; E. Baranov; V. Cherkasov; G. Abakumov, *Eur. J. Inorg. Chem.* **2008**, 1435

[113] K. Blackmore; J. Ziller; A. Heyduk, *Inorg. Chem.* **2005**, 44, 5559

[114] M. Chegerev; A. Piskunov; A. Starikova; S. Kubrin; G. Fukin; V. Cherkasov; G. Abakumov, *Eur. J. Inorg. Chem.* **2018**, 1087

[115] A. Piskunov; I. Aivazyan; G. Abakumov; V. Cherkasov; O. Kuznetsova; G. Fukin; E. Baranov, *Russ. Chem. Bull., Int. Ed.* **2007**, 56, 261

[116] K. Tsys; M. Chegerev; G. Fukin; A. Piskunov, *Mendeleev Commun.* **2018**, 28, 527

[117] D. Harris; W. Nebergall; O. Johnson, *Inorg. Synth.* **1957**, 5, 72

[118] M. Lechner; M. Trummer; I. Bräunlich; P. Smith; W. Caseri; F. Uhlig, *Appl. Organomet. Chem.* **2011**, 25, 769

[119] C. Breliere; F. Carre; R. Corriu; G. Royo, *Organometallics* **1988**, 7, 1006

[120] H. Schmidbaur, *Chem. Ber.* **1964**, 97, 1639

[121] B. Clark; D. Griller, *Organometallics* **1991**, 10, 746

[122] Y. Takeuchi; H. Yamamoto; K. Tanaka; K. Ogawa J. Harada; T. Iwamoto; H. Yuge, *Tetrahedron* **1998**, 54, 9811

[123] P. Riviere; M. Riviere-Baudet; A. Castel; J. Satge; A.. Lavabre, *Synth. React. Inorg. Met.-Org. Chem.* **1987**, 17, 539

[124] A. Castel; P. Riviere; J. Satge; H. Ko, *Organometallics* **1990**, 9, 205

[125] T. Birchall; I. Drummond, *J. Chem. Soc. A* **1970**, 1401

[126] M. Unno; Y. Kawai; H. Matsumoto, *Heteroat. Chem.* **2001**, 12, 238

[127] J. Pola; J. Parsons; R. Taylor, *J. Mater. Chem.* **1992**, 2, 1289

[128] E. Liepins; I. Zicmane; E. Lukevics, *J. Organomet. Chem.* **1988**, 341, 315

[129] C. Weinert, *ISRN Spectroscopy* **2012**, 2012, 1

[130] R. Thomson; A. Wilkins; K. Mackay, *Phosphorus, Sulfur, and Silicon and the Related Elements* **1999**, 150, 319

[131] K. Mackay; P. Watkinson; A. Wilkins, *J. Chem. Soc. Dalton and Trens.* **1984**, 133

[132] R. Kidd; H. Spinney, *J. Am. Chem. Soc.* **1973**, 95, 88

[133] J. Kaufmann; W. Sahn; A. Schwenk, *Z. Naturforsch.* **1971**, 26A, 1384

[134] Y. Takeuchi; K. Tanaka; S. Aoyagi; H. Yamamoto, *Magn. Reson. Chem.* **2002**, 40, 241

[135] A. Sutrisno; M. Hanson; P. Rupar; V. Terskikh; K. Baines; Y. Huang, *Chem. Commun.* **2010**, 46, 2817

[136] M. Hanson; A. Sutrisno; V. Terskikh; K. Baines; Y. Huang, *Chemistry - A European Journal* **2012**, 18, 13770

[137] A. Wilkins; P. Watkinson; K. Mackay, *J. Chem. Soc. Dalton Trans.* **1987**, 2365

[138] Y. Takeuchi; T. Takayama, *Annu. Rep. NMR Spectrosc.* **2005**, 54, 155

[139] E. Liepins; I. Zicmane; L. Ignatovich; E. Lukevics, *J. Organomet. Chem.* **1990**, 389, 23

[140] E. Meyer; R. Castellano; F. Diederich, *Angew. Chem., Int. Ed.* **2003**, 42, 1210

[141] S. Nayak; R. Sathishkumar; T. Row, *CrystEngComm* **2010**, 12, 3112

[142] C. Janiak 2000, *J. Chem. Soc., Dalton Trans.* **2000**, 3885

[143] C. Hunter; J. Sanders, *J. Am. Chem. Soc.* **1990**, 112, 5525

[144] S. Alvarez, *Dalton Trans.* **2013**, 42, 8617

[145] P. Johnson; S. Almstätter; F. Dielmannand M. Bodensteiner; M. Scheer, *Z. Anorg. Allg. Chem.* **2010**, 636, 1275

[146] K. Nakamoto, *Applications in Organometallic Chemistry, in Infrared and Raman Spectra of Inorganic and Coordination Compounds: Part B: Applications in Coordination, Organometallic, and Bioinorganic Chemistry*, New York: John Wiley & Sons, **2006**, 292

[147] F. Glockling; J. Light, *J. Chem. Soc. (A)* **1968**, 717

[148] Bruker, "APEX2 and SAINT. Bruker AXS Inc.: Madison, Wisconsin, USA", **2012**

[149] R. Blessing, *Acta Crystallogr., Sect. A* **1995**, 51, 33

[150] G. Sheldrick, *Acta Crystallogr., Sect. A* **1990**, 46. 467

[151] G. Sheldrick 2008, *Acta Crystallogr., Sect. A* **2008**, 64, 112

[152] G. Sheldrick 2015, *Acta Crystallogr., Sect. A: Found. Adv.* **2015**, 71, 3

[153] A. Spek, *J. Appl. Crystallogr.* **2003**, 36, 7

[154] A. Spek, *Acta Crystallographica Section D* **2009**, 65, 148

[155] Y. Nelyubina; M. Antipin; K. Lyssenko, *J. Phys. Chem. A* **2007**, 111, 1091

[156] R. Willett; B. Twamley; W. Montfrooij; G. Granroth; S. Nagler; D. Hall; J. Park; B. Watson; M. Meisel; D. Talham, *Inorg. Chem.* **2006**, 45, 7689

[157] F. Allen, *Acta Crystallogr., Sect. B* **2002**, B58, 380

[158] C. Macrae; I. Bruno; J. Chisholm; P. Edgington; P. McCabe; E. Pidcock; L. Rodriguez-Monge; R. Taylor; J. van de Streek; P. Wood, *J. Appl. Crystallogr.* **2008**, 41, 466

[159] H. Putz; K. Brandenburg, "Diamond - Crystal and Molecular Structure Visualization. 3.2i ed.; Crystal Impact: Bonn, Germany."